DEPARTMENT OF ELECTRONIC AND ELECTRICAL ENGINEERING
LOUGHBOROUGH UNIVERSITY OF TECHNOLOGY

COMPUTER SIMULATION IN FISH ABUNDANCE MEASUREMENT

BY

GUO LIANXI, B.Sc

A master's thesis
submitted in partial fulfilment of the requirements for the award of
master of philosophy of the loughborough university of technology

September 1988

Supervisor: Professor J.W.R.Griffiths, B.Sc.(ENG)
Ph.D., C.Eng., F.I.E.E., F.I.E.R.E.
Department of Electronic and Electrical Engineering

ACKNOWLEDGEMENT

I would like to express my sincere thanks to my supervisor Professor J. W. R. Griffiths for his help, guidance and invaluable suggestions, as well as criticism throughout the course of this research. In addition, I would like to thank him for providing financial assistance during the last two months in order that this thesis could be completed.

My thanks go to my colleagues in the Systems Research Laboratory and the Signal Processing Research Laboratory for their friendship and kind help on a number of occassions during my time here, particularly, Mr.J.W.Goodge, Mr.G.Lu and Dr.L.A.A.Warnes, for their useful discussions and assistance relating to my experiments. The work of Mr.A.M.Easom in correcting the English of this thesis is also appreciated.

I would like to acknowledge financial support of the Dalian Fisheries College of CHINA for my study in United Kingdom.

Finally, but by no means of least importance, I wish to express my special appreciation to my mother and my wife for their patience, understanding and moral encouragement throughout my education.

SYNOPSIS

This thesis describes the computer modelling of an echo-sounder system used in fish abundance measurement. Some years ago, Griffiths and Smith established a computer model of a typical sonar system which was used to try to evaluate the accuracy with which the number of targets could be estimated using the integrated energy from the output of the system. However, the model was fairly simple and did not take into account some important factors such as fish behaviour which may have a significant effect on the estimates. This project has taken these factors into account and has attempted to extend the earlier computer model.

The target strength of fish is the most important factor in the measurement of fish abundance. It will not in general be constant in the practical measurement because of the variability of many factors which contribute to its magnitude. One of the major factors is the variability in the fish's tilt angle which is due to the movement of the fish itself. The effect of the tilt angle on average target strength was examined including, the range of the tilt angle, the mean tilt angle, the standard deviation of the tilt angle distribution, and the frequency of the acoustical signal. The average target strength was calculated for these different conditions.

Some functions for the variation of the target strength with tilt angle have been assumed and used in the model. The probability distributions for the variation of the target strength were then obtained using these functions with two assumed tilt angle distributions (uniform and normal). It was found that the probability density distribution of the target strength was not symmetrical and does not obey a Gaussian distribution like the earlier modelling work assumed. This required a modification in the method of generating the target strength in

the simulation. The results obtained from the modified model have shown qualitative agreement with measured distributions.

Practical experiments were carried out to measure the target strengths for different kind of spheres. The results obtained from the experiments are promising and basically consistent with those expected.

CONTENTS

1. INTRODUCTION

Acoustic estimates of fish stock size are at present one of the fisheries management's objectives. They can be used directly or in conjunction with other estimation methods to provide management information. Estimates of fish abundance in fisheries research have been made using sonar systems for some years, and various techniques have been developed to extract the information concerning fish abundance using these systems. The output signals from a sonar system depend on many factors such as the target strength of the fish being surveyed, the influence of the medium such as the propagation losses, the sensitivity of the receiver and the beam directivity both on transmission and reception etc..

Due to the rapid development in high speed digital electronics, sonar systems for the estimation of fish abundance measurement have been advanced and digitised considerably over the past few years. They have been developed with very much more power, higher resolution in range and angle, and much improved form of display [1]. Particularly, the systems have been enhanced by the application of computer systems [2]. Provided that the target strength of fish is well known, the measurement system could provide accurate information about fish abundance in the surveying area.

However, due to the internal and external geometry of a fish, its target strength can vary widely with its size, the insonifying frequency, and the insonified aspect. It is difficult to derive a function of such factors as fish size, insonifying frequency and fish orientation, from which the target strength of fish could be calculated exactly and yet it is found [3] that these factors have a

significant effect on the estimates. Fortunately, some information about fish behaviour is available [4-20], and this encourages examination of the effect of these factors about fish behaviour on the measurement of fish abundance in order to improve the accuracy of the acoustic estimates of fish stock size.

Some years ago, Griffiths and Smith [21] modelled an echo- sounder system for fish abundance measurement as a linear system with which the number of targets could be estimated from the integrated energy. It may be the first use of computer modelling attempting to determine the accuracy of the estimation of biomass using acoustic measurement. Later, Griffiths and Chan [22] extended the model to simulate an electronically scanned sonar system for the same application. Abundance estimates obtained from the computer models in references [21] and [22] proved satisfactory. However, some important factors such as the directivity of the target strength of fish etc., which may have a significant effect on the estimates, were not considered in these models.

The work described in this thesis attempts to extend the work done by Griffiths *et al.* to take into account these further factors about fish behaviour in the computer model for estimating fish abundance. A computer simulation was carried out in which the effects of fish behaviour on the estimation were considered and some typical results are presented.

This thesis is divided into the following:

(1) Review of basic principle on the estimates of fish stocks;

(2) Introduction of the computer model of an echo-sounder system for fish abundance measurements;

(3) Consideration of the effects of some known factors on the fish abundance measurement;

(4) Simulation of a sonar system which takes into account some information of fish behaviour in fish abundance measurement.

The thesis consists of 8 chapters with 1 appendix. Brief outlines of the contents of each chapter are given below:

Chapter 2 reviews the theory of the echo integration technique of estimating fish abundance. The echo-sounder system is described in relation to its use in the measurement of fish abundance, and two important instruments, the echo counter and the echo integrator, are discussed. Measurements of the echo signals are used in the echo integrator and the echo counter to derive quantitative information about the targets.

Computer simulation techniques have been used to simulate some practical system in order to study the performances of these systems. Chapter 3 describes a computer model for a simple echo-sounder system used for fish abundance measurement. The computer model represents the behaviour of the echo-sounder system as a linear system having an impulse response corresponding to the shape of the transmitted pulse and which has as an input a series of impulses. The strength of these individual impulses depends on the target strength of the fish, the propagation losses of signals, the sensitivity of the receiver and the directivity both on transmission and reception. The target strength of the fish depends strongly on its orientation, its size and its species.

Chapter 4 investigates some factors which might affect the accuracy of an estimation of the number of targets insonified. The magnitudes of the signals reflected by fish are not constant from pulse to pulse because of the variability of the many factors which contribute towards the echo amplitude. One of the major factors causing variability is the movement of the fish itself which includes tilt, roll and pitch. However, when the fish is viewed in the dorsal aspect it has been shown that the significant factor is the tilt angle [20, 33] and that the distribution of the tilt angle is close to normal [4, 19].

To make an estimation of the number of targets insonified using the integrated energy from the output of the echo-sounder system, the mean square value (MSV) of the target strength for the species of fish under observation must be first evaluated. Therefore, the influence of the tilt angle distribution on the MSV was investigated.

Moreover, based on representing a fish by its swimbladder and assuming the tilt angle distribution, the probability distribution for the variation of the target strength could be estimated. It is found from the results that the distribution of target strength was not symmetrical and is certainly not a Gaussian distribution as was assumed in the earlier modelling work. When the mean angle of tilt of the fish is not zero then the possibility of a double moded distribution arises. This finding would be important for the present or further work and this led a modification in the method of generating target strength.

Chapter 5 brings together the concepts discussed in chapter 3 and chapter 4 to develop the sonar model for fish abundance measurement. A series of targets of random strength are generated with the knowledge of fish behaviour, such as

assumed tilt angle distribution and fish length distribution. Fish reaction to a surveying vessel is also considered in the computer simulation. Olsen *et al.* proposed a mathematical model [11] for representing the avoidance reaction pattern which might influence fish behaviour, and the mean tilt angles at different depths are obtained from this model. This random series representing the expected target strength of the fish could be used in the simulated echo-sounder system, and estimates of fish abundance could be made using its output. The estimated number of targets could be evaluated and compared with the known value which had been generated.

Based on the sonar modelling discussed in chapter 5, chapter 6 presents some typical results of the computer simulation in the form of regression graphs. The variance and the correlation coefficient are calculated in order to compare the accuracy of the estimates under different conditions.

In chapter 7, a practical experiment is described in which a number of table tennis balls of about 37 mm diameter, a copper sphere of 30 mm diameter as well as a tungsten sphere of 40 mm diameter were used as the targets for the practical experiment. The experiments were carried out in a large tank in the department and a frequency of 3 MHz was adopted since some equipment operating at this frequency was available. With a high operating frequency, i.e., if the wavelength is much shorter than the dimensions of the targets, then the theory of scattering becomes more complicated and diffraction phenomena occurring at the surface of the targets become more significant [25]. Moreover, acoustic energy lost through water is greater. Although the frequency used in these experiments is not of course used in practical fisheries work, it enables work to be carried out in the tank where the targets are necessary at very short

ranges. The data collected from the experimental apparatus were processed by regression analysis and the target strengths of these spheres were obtained by using graphic solution.

Conclusions and suggestions for further work are given in chapter 8.

2. REVIEW THE USE OF THE ECHO SOUNDER IN FISH ABUNDANCE MEASUREMENT

2.1 INTRODUCTION

The echo sounder is the earliest form of sonar equipment and has been used in fisheries for some 50 years [1]. To understand the theory of the echo sounder and to try to extend its uses, this chapter gives a brief description of the echo sounder system used in fish abundance measurement.

2.2 BASIC PRINCIPLE

There are two main kinds of sonar systems, the active sonar and the passive sonar. The former itself generates and transmits acoustic signals. When a target is insonified, part of the signal energy will be reflected and return as sonar echoes to the source. The echoes are then received by the receiver of the system and processed in various ways.

The passive or listening sonar is only used to detect sounds produced by the targets under investigation. As the sounds generated by the fish are very weak, it has seldom been applied in fisheries [1].

Echo sounders are one kind of the active sonar system and are used in fisheries work and other applications. A functional block diagram of a typical echo sounder system is shown in Fig.2.1. A short burst, or pulse, of an acoustic wave is transmitted at regular intervals in the vertical direction, and it spreads out into the water in the form of an expanding spherical cap of acoustic energy

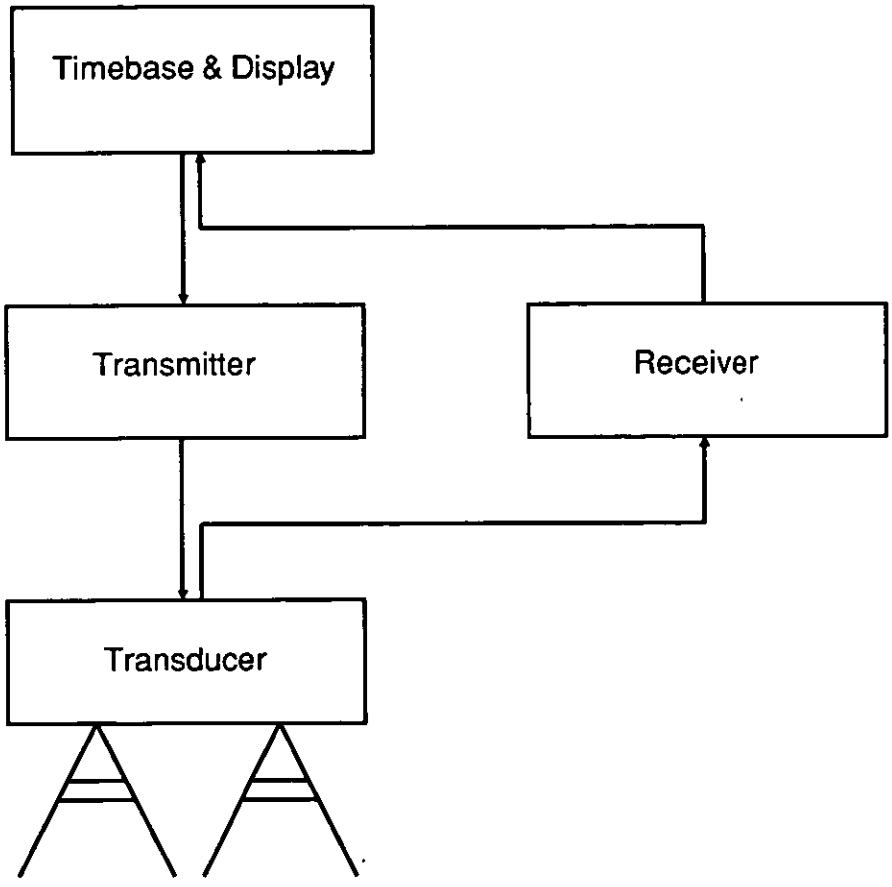

Fig. 2.1 Block diagram of an echo sounder

which is contained within the beamwidth of the transmission. The beamwidth is usually defined as the angular width between the -3dB points of the main lobe. Of course, an acoustic beam is not a cone with well defined boundaries; it is a concentration of acoustic energy which is usually greatest on the central axis of the beam and diminishes as the angle from the axis increases until eventually there is zero intensity. After that there are usually some smaller or minor side-lobes. The transmitted pulses travel at a very slow speed compared with that of light, but considerably faster than sound in air. The propagation speed of the sound pulses in the water is about 1500 m/s and depends on the depth, temperature and salinity of the water medium. If some objects, e.g., fish, lie in its path, the acoustic energy would be reflected and spread out from the objects. Some of this reaches the receiver of the system and is detected. It should be noted that the received acoustic energy includes some of that scattered by marine organisms, gas bubbles, and other inhomogeneities. The signals with the expected information are then processed with the help of the sonar equipment doing such tasks as signal converting, detecting, amplifying etc. and finally being presented in a visual or audible form.

It is known that the echo sounder system can provide two kinds of useful information. One is the range from the echo sounder to the target insonified. It is easy to calculate using the formula $R = ct/2$, where, c is the velocity of sound, and t is the time that has elapsed between the transmission of the pulse and the reception of the echo. The other kind is the target strength which is quite difficult to predict and is more complicated.

In order to derive the quantity which describes the target itself by means of an echo-sounder, it is necessary to correct the received echo for the effects of the

wave spreading, the absorption loss, and the uncertain bearing of the target within the transmitted beam [1]. The correction for spreading and absorption losses is normally done by applying time varied gain (TVG) to the receiving amplifier. The last of these corrections can be done through a statistical interpretation of many echoes based on assumptions about the target distribution or by the split-beam or dual-beam techniques [16,26]. The accuracy of the quantity also depends on the stability of amplifier gains and the transducer efficiency.

2.3 DEVELOPMENT OF THE ECHO SOUNDER

Original uses of the echo sounder were to measure the depth of the water and to trace the profile of the sea-bottom. Later it was used to indicate the presence of fish in the water [23]. Although the equipment available was of rather poor quality and the results obtained by using them could not be expected to be accurate, they were believed to be effective tools for detecting fish underwater. For example, under favourable conditions, i.e., when single fish traces could be distinguished, the number of fish echoes could be counted.

With the growth in the world population, people begin to turn their attention toward to the sea as a major source of food. The size of this natural resource is limited and its harvesting must be tightly controlled if it is to be preserved. This gives fishery officials an important task, that is, monitoring the abundance of various fish species. In the past this monitoring was done by sampling the population with net catches, a technique which has been proved to be both costly and inaccurate. It has long been recognized that acoustics can provide this information. Reference [26] describes an echo sounder which has been modified and used in the estimation of fish

abundance. For this particular purpose two important applications of the echo sounder system are echo counting and echo integration techniques.

2.4 APPLICATIONS OF THE ECHO SOUNDER IN FISH ABUNDANCE MEASUREMENT

Two important applications of the echo-sounder mentioned here are echo integration and echo counting in which the measurements of the echo signals are used to derive quantitative information about the biomass. Both methods depend on the assumption that the targets will be randomly distributed in the cross section of the transmitted beam. The data from many echoes are combined to produce one result which is an average property of the target ensemble. This statistical treatment overcomes a fundamental limitation of the single-beam echo sounder, namely, the uncertainty about the position of a particular target within the beam. A block diagram of both echo counting system and echo integration system which are joined together is shown in Fig.2.2.

2.4.1 The Echo Counter

The basic principle of an echo counting system is quite simple. An acoustic pulse is transmitted into the water. The individual scatterers in the volume insonified reflect part of this energy back to the transducer. If the spatial density of the scatterers do not overlap then the total number of scatterers insonified could be determined by simply counting the number of echoes out of the receiver. The scattering density is then determined by dividing the number of counts by the volume sampled.

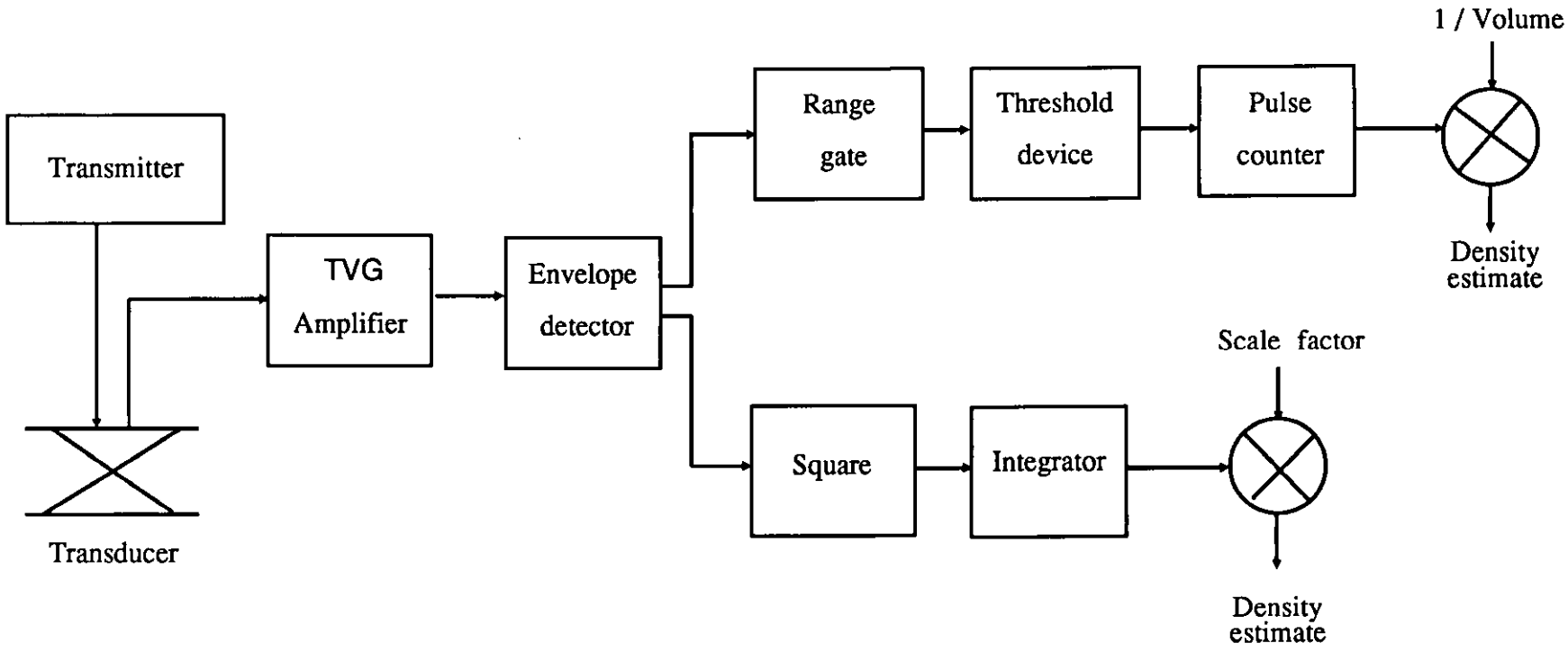

Fig.2.2 Block diagram of both echo counter and echo integrator

In order to resolve the echo from one fish, the target must be separated from others by a minimum increment of range. This minimum resolvable distance is c(Tp+t)/2 [1], where, Tp, is the pulse length, and t is proportional to the rise time of a single target echo. t is normally less than Tp and it is inversely proportional to the bandwidth [1]. If the spatial density of the targets becomes too high, the echoes from individual scatterers begin to overlap and the spatial density estimate becomes biased low.

The transmitter and the receiver compose a basic echo sounder system. The TVG (Time-Varied Gain) amplifier is used to equalize the signals received from fish at different depths. The envelope detector removes the carrier from the signal. The range gate is used to control the depth interval. The threshold device eliminates the low level noise and amplitude variations from the signal. The pulse counter is used to count the number of echoes. The principle of the echo counter system is roughly described here. More details about the system could be found in the references [26]-[29].

2.4.2 The Echo Integrator

In addition to the echo counting method, there is a common method which is used for quantifying the number of scatterers insonified by an acoustic echo sounder system. The system is called echo integration which, unlike echo counting, can provide more accurate estimates of fish abundance in dense populations and the accuracy of the measurement tends to improve with increasing fish density [26].

The echo integration method of processing is based on the assumptions that the echoes from the individual scatterers add incoherently and that the effects of multiple scattering and shadowing can be neglected. Under these assumptions, it can be easily shown that the average integrated intensity of the received echoes is proportional to the number of scatterers insonified [24]. This proportionality holds for both low density populations of scatterers where the individual echoes do not overlap and higher density populations where the received signals at any time are composed of a large number of overlapping echoes (provided that multiple scattering and shadowing can be neglected). Therefore, if the mean target strength of a single target could be accurately estimated, an unbiased estimate of scattering density could be obtained by properly scaling the output of the integrator.

The TVG amplifier, as in the echo counting system, is used to compensate for all losses due to spreading and absorption. The envelope detector is used for removing the carrier and produces a signal proportional to the envelope of the amplified signal. In the echo integrator, the signals are squared to produce an output which is proportional to intensity.

As was previously stated the echo counting and echo integration techniques are based on the assumptions that the echoes from the individual scatterers, i.e., fish, are incoherent and that the effect of multiple scattering and shadowing are small enough to be neglected. It is also assumed that the distribution of fish in the region surveyed is random and obeys some probability density functions. In practice, it is difficult to know the exact distribution of fish underwater.

It is shown in references [21, 22] that the mathematical models used for estimating fish abundance are quite complicated and that it is difficult to make them represent practical systems. However, the echo sounder system modelled could be simulated on a computer so as to allow a greater interaction between the user and the modelled system. Moreover, the accuracy of the estimation can be improved in view of the general lack of information on the spatial distributions and behavior of fish. More details about the mathematical models are described in the reference [29].

3. A COMPUTER MODEL OF AN ECHO SOUNDER SYSTEM

3.1 INTRODUCTION

In the preceeding chapter the basic principles of echo counting and echo integration were introduced. The models have been developed over the past years such ways as to derive a bound for the variance of estimates and analytical measurement of target strength etc. [18-23]. But such models are frequently complex and difficult to comprehend without an advanced knowledge of mathematics. Moreover, most of the physical meaning of the system modelled can be lost.

A computer model which is the same as the mathematical one in principle compensates for some of the disadvantages of the mathematical model. It is easy to form and process on a computer, it also simplifies the analysis and calculation of the system to an extent, without loss of the original physical meaning. Moreover, it would be easy to use for demonstrating the physical meaning of the system by means of visual displays or graphics.

3.2 BASIC MODEL

The establishment of a computer model is at first dependent on the basic principle of an echo sounder system in operation. For this model, the basic geometry for an echo sounder system is shown in Fig.3.1. Any target far from a certain distance in the system is assumed to be a point target and is randomly located at a position (R_i, θ_i, ϕ_i) relative to the transmitter/receiver of the echo sounder system. Let the acoustic pulse transmitted in the direction of the acoustic

axis be $X(t)\cos(\omega t)$, where the $X(t)$ is the pulse envelope and $\cos(\omega t)$ the carrier. The carrier angular frequency ω is given by $2\pi f$ such that f is the frequency at which the echo sounder is operating. The transmitted pulse signal propagates through the water medium and reaches the target at the position R_i, θ_i and ϕ_i. Due to the finite acoustic velocity in the water, the signal reaching the target will be delayed in time. The delayed time is R_i/c, where c is the velocity of sound. In addition, the carrier amplitude, $X(t)$, will also be changed with the angular position of the target relative to the acoustic axis, square law spreading and the attenuation of the acoustic wave in the medium. A proportion of the incident signal will be reflected by the target and this strength (and phase) of the reflected signal will depend on

a) the size, shape and construction of the target;

b) the insonified orientation of the target.

This pulse signal will then be subject to the same losses and delay on the return path as on the forward path.

Thus, the signal received from a single point target at a position R_i, θ_i and ϕ_i relative to the transmitter/receiver of the echo sounder system can be represented by the following expression:

$$V_i = A_i.\beta(\theta_i, \phi_i).X(t - \frac{2R_i}{c}).\cos(\omega(t - \frac{2R_i}{c})) \qquad \text{..... (3 - 1)}$$

where A_i is a random variable which depends on the target strength and other factors, such as the spreading and absorption losses of propagation, the influence of the medium and the sensitivity of the receiver. $\beta(\theta_i, \phi_i)$ takes into account the beam directivity both on transmission and reception.

As time t can be expressed in terms of range R, that is,

$$R = \frac{c.t}{2} \qquad \text{..... (3 - 2)}$$

equation (3 - 1) can be conveniently expressed in terms of range rather than time. Substituting (3 - 2) into (3 - 1), an alternative equation can be easily obtained, i.e.,

$$V_i = A_i.\beta(\theta_i, \phi_i).X(\frac{2}{c}(R - R_i)).\cos(\frac{2\omega}{c}(R - R_i)) \qquad \text{..... (3 - 3)}$$

If $$h(R) = X(\frac{2R}{c}).\cos(\frac{2\omega R}{c})$$

and $$T_i.\delta(R - R_i) = A_i.\beta(\theta_i, \phi_i).\delta(R - R_i) \qquad \text{..... (3 - 4)}$$

where $\delta(R - Ri)$ is delta function. Thus, the equation (3 - 3) mentioned above can then be expressed as the convolution of two functions

$$V_i = h(R) * T_i\, \delta(R - R_i)$$

When a number of targets were considered

$$V = \Sigma V_i = h(R) * \Sigma T_i.\delta(R - R_i)$$

This equation represents the linear relationship of the system having an impulse response h(R) corresponding to the shape of the transmitted pulse, and which has as an input a series of impulses of strength Ti occurring at ranges Ri. Such a representation is shown in Fig.3.2.

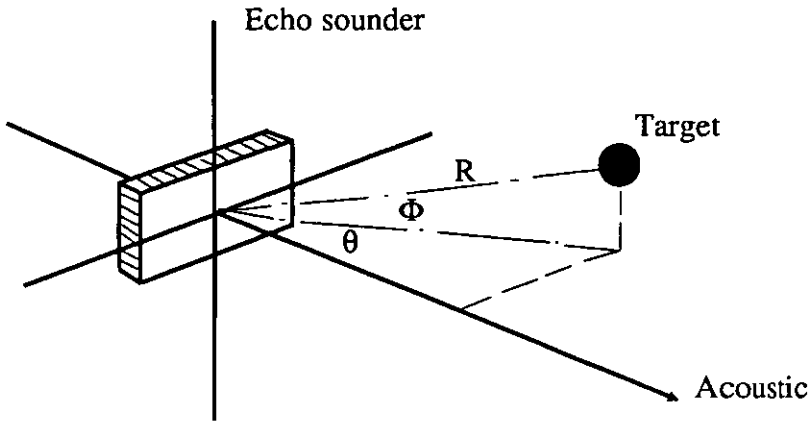

Fig. 3.1 Showing the axes of measurement

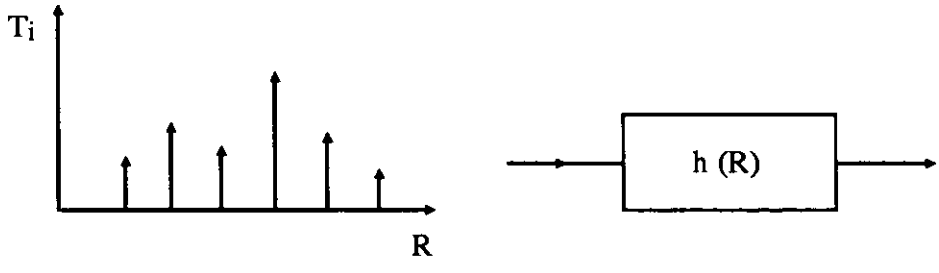

$$h(R) = X(2R/c).\cos(2\omega R/c)$$

Fig. 3.2 Representation as linear system

If the unit of range as well as the angular frequency were normalised such that $2/c = 1$ and $\omega = 1$ respectively, these decisions will only affect the range scale of the final output.

In the model, the transmitted pulse shape adopted in term of the normalised range unit was given by

$$X(R) = \frac{1}{2}(1 - \cos(\frac{2\pi R}{\Delta})) \qquad 0 < R < \Delta$$

$$= 0. \qquad \text{elsewhere}$$

Here Δ represents the pulse length in range units. The X(R) is a typical received sonar waveform from a single target, but could be changed and replaced by some other expressions if so required.

The beam directivity $\beta(\theta_i, \phi_i)$ in the model was assumed that

$$\beta(\theta_i, \phi_i) = e^{-a\theta_i^2} \cdot e^{-b\phi_i^2} \qquad \ldots\ldots (3 - 5)$$

where a and b are constants that determine the beamwidth at the -3dB point (or half power point) in both the θ and ϕ domains. This beam pattern was chosen because it is mathematically simple, and convenient to use, and a fairly close representation to the practical situation. The natural beam pattern, of course, can be simulated in the model if required.

As for the choice of the pulse shape X(R) and the assumption of the beam pattern $\beta(\theta, \phi)$ etc., more detailed description of which is given in the references [21 - 22].

A computer programme simulating the model was written in BASIC to be run on a BBC computer. Some typical outputs from the computer model with a particular set of parameters were illustrated in Fig.3.3 and Fig.3.4. Fig.3.3a shows the waveform of the signal returned fom a single target at receiver. Fig.3.3b shows the envelope of the signal after being envelope detected. The envelope detector in the model is set to be "perfect" one which is equivalent to the square root of a complex number. With reference to equations (3 - 3) and (3 - 4), if let Vi be the real component of the complex and Vi' the imaginary component, where

$$V_i = T_i.X(R - R_i).\cos(R - R_i) \qquad .....(3 - 6)$$

and $$V_i' = T_i.X(R - R_i).\sin(R - R_i) \qquad .....(3 - 7)$$

then

$$\sqrt{(V_i)^2 + (V_i')^2} = T_i.X(R - R_i)$$

which is the "perfect" envelope of the signal waveform. Of course, the method of obtaining the envelope here was only artificially used in the computer model because it is mathematically simple and is easy to generate on the computer. This process of obtaining the envelope has already been discussed in reference [22]. It should be noted that the method would be still used in the model in chapter 5, even though it is not realistic for obtaining so "perfect" an envelope waveform.

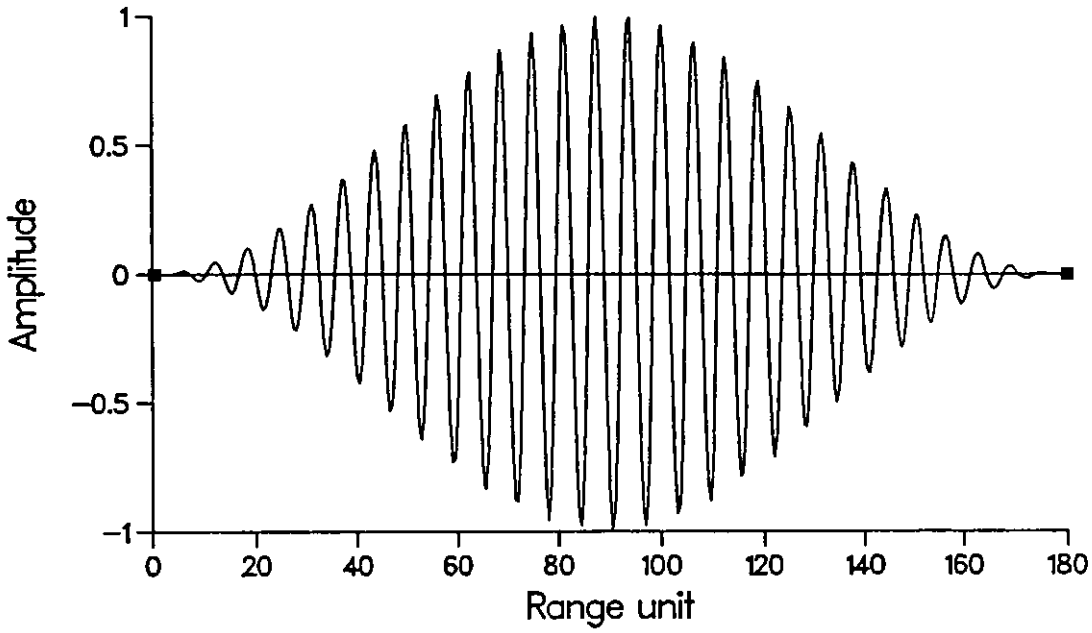

Fig.3.3a Single target output.

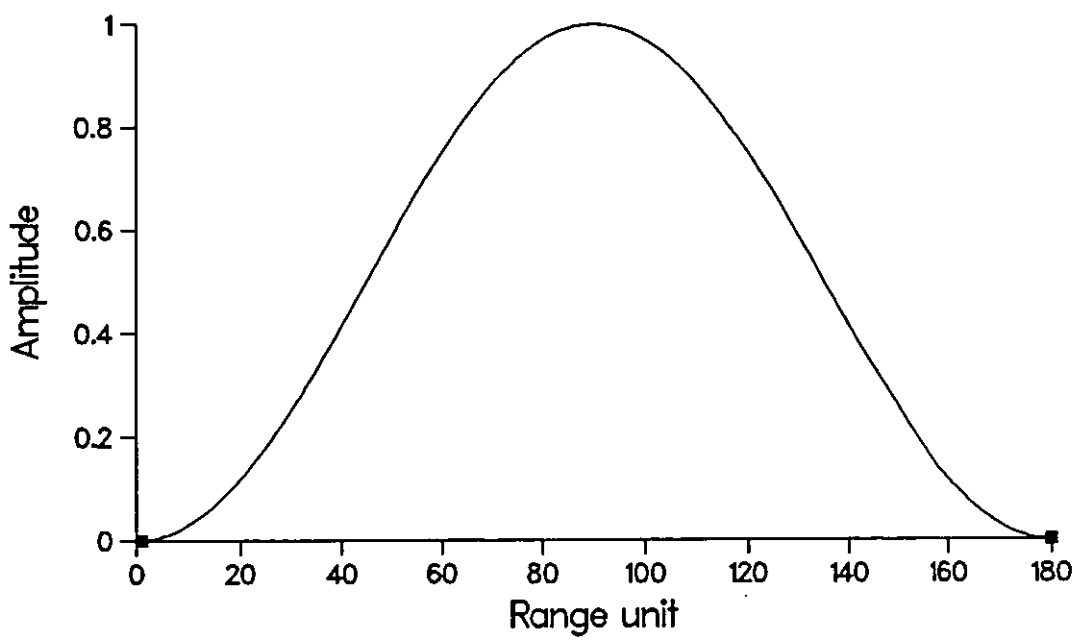

Fig.3.3b Envelope of the output.

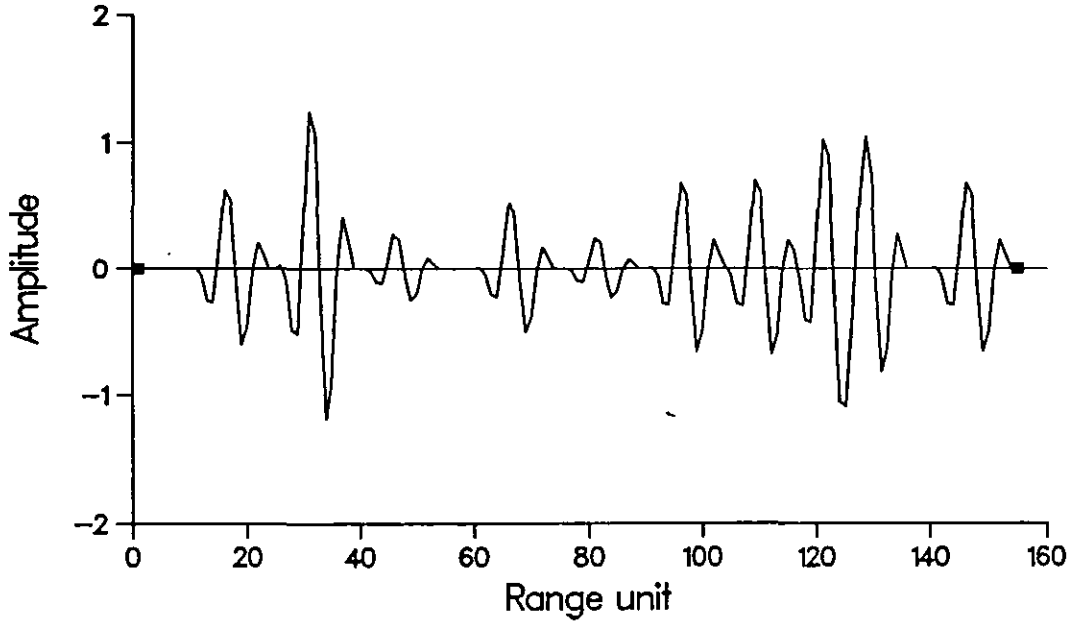

Fig.3.4a Multiple target output.

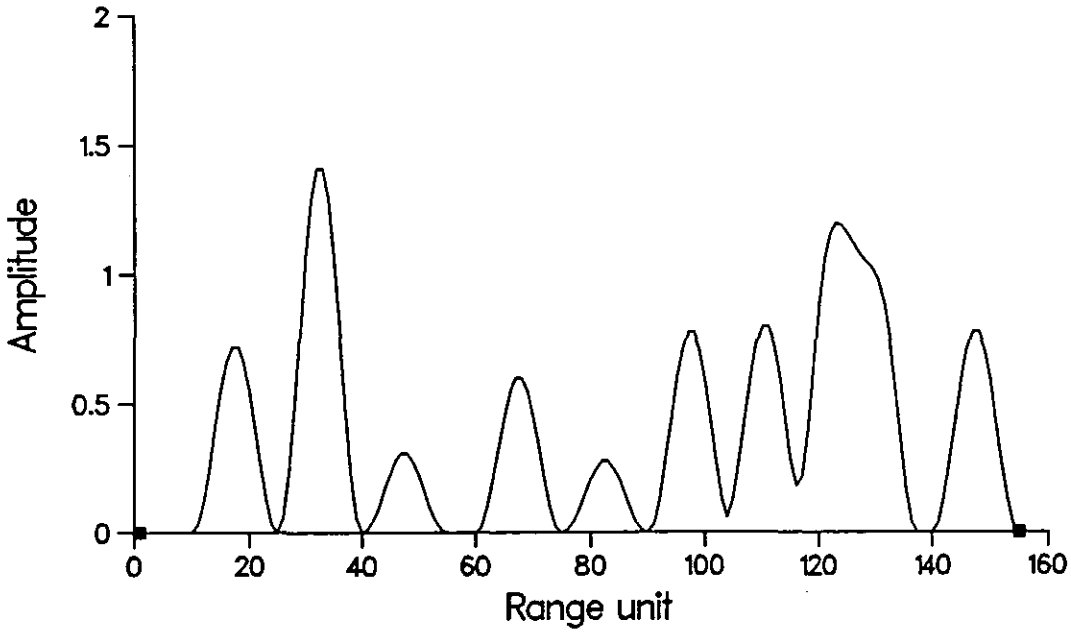

Fig.3.4b Envelope of the output.

4. STUDY OF FACTORS AFFECTING FISH ABUNDANCE MEASUREMENT

4.1 INTRODUCTION

It is well known that an important task of the acoustic calibration technique for integrator-abundance estimates is to predict the proportionality between the echo energy and the target strength, and further to find out the proportionality constant between the fish density and the integrated signal output [11].

For some years estimates of fish abundance have been made using the output of a sonar system. By considering the integrated energy of the echo of the species of fish involved, an estimate of the biomass can be made. The integrated echo energy from the output of the sonar system depends on many factors which include propagation losses, the target strength of fish, the sensitivity of the receiver, the position of a target in the beam, the distribution density of fish and the species of fish involved etc.. Pope [34] set out the goals for fishery management in terms of the overall accuracy for different situations.

The target strength is, in practice, very important and is not in general constant due to the behaviour of fish. Many published papers have shown that the target strength of a fish depends strongly on the orientation of the fish as well as on its size and on the frequency of the acoustic signal. The orientation includes tilt, roll and pitch, but when the fish is viewed in the dorsal aspect it has been shown that the significant factor is the tilt angle [20,33].

It is indicated in reference [31] that the observed target strength will depend on the parameters of the sonar system. Therefore, under the conditions of different observations and measurements, different target strengths are obtained from the same target measured. For the studying of the target strength of fish, some mathematical models of target strength were established [29] and it is shown that there is a basic agreement between the measured results and the computed results obtained from these models. A similar model of target strength will be introduced in section 4.2. Of course, it does not mean that this model is superior to the others. It is only another trial to the assumption of the swimbladder being simplified as a finite cylinder. The results obtained from the model are in general satisfactory and have shown some agreement with the others within certain limits.

Due to the fish tilt angle strongly affecting the target strength or backscattering cross section, it is respectively discussed that the target strength is affected by several parameters such as the mean tilt, the range of tilt angle, the deviation of the tilt angle distribution and the frequency of the acoustic signal. In order to simplify the analysis of the effect of the parameters on the target strength, some functions representing the variation for the target strength with tilt angle are assumed. The curves derived from these functions are in general close to the measured ones. Moreover, using the knowledge of both the distribution of tilt angle of the fish and the function of its target strength with tilt angle, the probability distribution for the variation of the target strength can be predicted.

In the measurements of target strength care has to be taken to avoid scaring the fish. The presence of the vessel may substantially influence the behaviour of fish in its vicinity. The avoidance behaviour displayed by the fish

may lead to considerable changes in both spatial and swimming orientation and this will affect the recorded target strength. Therefore, such effects on the target strength under real surveying conditions should be incorporated in the model.

Fish density and its size will be finally discussed in section 4.6. Even though the spatial position of the fish do not distribute randomly in the water [17], it is difficult to predict or accurately calculate the fish position and density. The nearest neighbour distance of the fish is affected by their size and the fish do not approach closer than a certain distance from one another. This valuable information provides that the highest fish density does not exceed a certain level. Therefore, understanding the positions of individual fish within fish schools as well as their internal structure has significant implications for fish abundance estimates.

4.2 SONAR SCATTERING BY A SWIMBLADDER

4.2.1 Introduction

The backscattering cross section, or target strength, of fish is an important quantity of interest in fish abundance measurement which strongly demands detailed knowledge about it. For this reason, numerous and diverse studies have been done for this purpose. There have *in situ* measurement, controlled measurement on tethered or encaged fish and modelling in which some simple geometric shapes of swimbladder are assumed. Of course, established models based on these assumptions are inadequate, but it is a way to approach the practical situations and it also makes it possible to give a quantitative estimation of the backscattering cross section of fish.

Experimental studies of the reflectivity of fish have shown that the propensity of an insonified target to reflect sound is principally dependent on its size, internal composition, geometry and orientation [25]. In theory, the target strength of a fish can be computed from the knowledge of these factors. In practice, the calculation is rarely, if ever performed because of its complexity. Fortunately, the experimental measurements have confirmed that for commercial fish of small and middle size and with low frequency, namely, to the fish finding equipment operation at around 38 KHz, the primary contributor to the value of the acoustic section, or to the echo energy is the swimbladder. When the frequency (if the size of fish keeps constant) increases, the total echo signal is formed by flesh, bone, and bladder signals. With still higher frequency, the swimbladder signal becomes lower than that from flesh and bones [25]. Therefore, at the intermediate frequencies of the present study, there is good reason to believe that the swimbladder is the preeminent scattering organ of fish. A mean contribution of from 90 to 95 percent to the echo energy is expected [33].

For the purposes of modelling or understanding echo formation by fish, two observable quantities are generally considered, orientation and degree of swimming movement. It is shown that the swimming movement does not significantly affect the dorsal target strength [3]. While the data on the orientation distribution of fish is important to acoustical methods of estimating fish abundance, the tilt angle, one of the factors affected by the orientation distribution, is of primary importance, and the roll angle dependence of that is slight, so is neglected [32]. Therefore, only the effect of the tilt angle on the target strength of fish is considered for the present study.

The Kirchhoff approximation is used to compute the backscattering cross section, or target strength in the present work. It has had notable success in both acoustics and optics [25], and is generally worth trying at an early stage in model scatterings.

4.2.2 Model

The quantitative characteristics of the reflectivity of a single object are determined by the target strength or acoustic scattering cross section of the object. The target strength is normally defined in the traditional mannar

$$TS = 10 \log(Ir/Ii) \qquad \text{.....(4 - 1)}$$

where Ir is the intensity of return at 1 metre and Ii the incident intensity. The acoustic scattering cross section of the object is a standard area that produces an ideal all-directional reflection similar to that which would be produced by the real object in a given direction. The acoustic scattering cross section of the object, σ, is given as reference [25]

$$\sigma = \frac{4\pi r^2 Ir}{Ii}$$

where r is the distance from the target. According to the definition of target strength (i.e. r = 1), the equation (4 - 1) can be expressed as follows

$$TS = 10 \log(\frac{\sigma}{4\pi}) \qquad \text{..... (4 - 2)}$$

A swimbladdered fish may be represented entirely by its swimbladder, which is assumed to be a finite cylinder. The sonar or backscattering cross section of the swimbladder can be determined by the physical optics method or Kirchhoff method. It is known that the sonar or backscattering cross section of any fish is

$$\sigma = 4\pi \mid f(\theta = \pi) \mid^2$$

where the $f(\theta)$ is a scattering function in the backscattering direction.

Kirchhoff showed that, in three-dimensions, the Rayleigh-Kirchhoff integrals can be approximated by the expression [35]

$$f(\pi) = \pm\frac{i}{\lambda}\int\int_S (\hat{k}\cdot\hat{n})\exp(2i\vec{k}\cdot\vec{r}')dA' \qquad \text{..... (4 - 3)}$$

where the s is the insonified portion of the scatterer's surface. the outward normal is $\hat{n}$, the surface element is dA', $\hat{k} = \frac{\vec{k}}{k}$, r' is the position vector of the surface element with infinitesimal area dA' , and the upper (lower) signs correspond to rigid (soft) scatterers. In addition, $i = \sqrt{-1}$ and $\lambda = 2\pi/k$ = the acoustic wavelength of the radiation in the incident beam.

The solution of the backscattering cross section may be achieved by the equation (4 - 3). Let the cylinder's length be 2b, a its radius, and k the wavenumber of the incident wave. The contributions from the curved side and the top flat surface of the cylinder are given (4 - 4) and (4 - 5) respectively by

$$f_1(\pi) = ikab\cos\theta' j_0(2kb\sin\theta')\left\{\left(\frac{2}{\pi} - H_1(2ka\cos\theta')\right) - iJ_1(2ka\cos\theta)\right\} \qquad \text{..... (4 - 4)}$$

$$f_2(\pi) = ika\left\{\frac{a}{2}\sin\theta'\exp(-i2kb\sin\theta')\frac{J_1(2ka\cos\theta')}{ka\cos\theta'}\right\} \qquad \text{..... (4 - 5)}$$

The complete answer, in closed form, taking into account the top and side contributions, respectively, is given by the sum of the two results given in (4-4) and (4-5), namely,

$$TS = 10 \log| f_1(\pi) + f_2(\pi) |^2 \qquad \text{..... (4 - 6)}$$

A brief derivations of equations (4 - 4) and (4 - 5) are given in the appendix 1. From equation (4 - 6), it follows that the pattern of scattering depends on the orientation of the fish in the acoustic field and on the fish size/wavelength ratio.

4.2.3 Swimbladder

In locating fish, of most interest is the quantitative characteristics of backscattering, which are expressed most frequently as acoustic backscattering cross sections or acoustic sections of fish.

It is known that fish swimbladders have different shapes and relative dimensions. For most fish it can be roughly assumed that the swimbladder is close to a cylinder of 0.05 fish length in diameter and 0.25 fish length in length [25]. If the sound energy reflected by the other parts of the fish body is ignored, the task of accounting for the sound scattered by the fish may be simplified to determine the acoustic characteristics of a cylindrical swimbladder insonified from an arbitrary direction which can be expressed by the corresponding tilt angles.

Thus, replacing the fish with a cylinder of the same size as the swimbladder makes it possible to obtain the quantitative analysis describing the acoustic characteristics backscattered by fish.

4.2.4 Insonified Angle

Of practical interest is the dependence of the value of backscattering on the insonification angle. Some experiments showed that the axis of the swimbladder in many commercial fish is inclined about the longitudinal axis of the fish body. For example, in herring the mean angle of inclination (α_b) is about 5^o. This phenomena is most prominent in cod whose swimbladder is located at $\alpha_b = 7^o$ to 10^o about the axis of the fish body [25]. In all species, the horizontal position of the swimbladder corresponds to the head-downward inclination of the fish. This is why the maximum target strength appears at around tilt angle of -5^o.

The tilt angle here is defined as the angle made by the centerline, or imaginary line running from the root of the tail to the tip of the upper jaw, with the horizontal plane. The sign convention is that positive angles denote head-up orientation; negative angles, head-down orientation.

4.2.5 Examination of the Models

The fundamental computation quantity is the backscattering cross section, or target strength, as a function of the insonification conditions and fish orientation. Expression (4-3) makes it possible to determine the dependence of the reflectivity of the fish on its orientation in the incident acoustical field.

For an excellent approximation in applications of vertical echo sounders, the orientation can be represented entirely by the tilt angle. In fact, the significant orientation is indeed the tilt angle.

Examples of the basic computations performed for each fish are shown in Fig.4.1 for fish length of 11.5 cm at different frequencies. All the figures showed that maximum backscattering cross section, or target strength occured with insonification directed perpendicularly to the axis of the swimbladder. In other words, the maximum backscattering cross section is shifted about a perpendicular plane to the axis of the fish body by the value of the inclination angle of the swimbladder. This is confirmed by these figures.

To test the model, predictions of target strengths based on assumed swimbladders of gadoids of lengths from 11.5 cm to 40 cm are compared with conventional target strength measurements of the same size fish. A comparison of from Figs.4.1 to 4.4 showed that the theoretical diagram is in general very similar to the experimental one.

From the Fig.4.1 to Fig.4.4 it follows that the diagrams of scattering for larger fish or higher frequency have more abrupt changes from maximum to minimum, a greater number of lobes, and consenquently narrower lobe width.

In addition to considering the magnitude of the backscattering cross section, or target strength, this function was compared with a simple mathematical model, which is just a beam pattern from a transducer. In this stage, the relationship between the scattering function $f(\pi)$ and tilt angle θ' is drawn to compare it with the simple beam pattern $\beta(\theta)$ of the transducer. It should be noted that since the magnitude of the scattering function $f(\pi)$ changes with frequency and tilt angle, both the maximum magnitude and the wavelength of the scattering function $f(\pi)$ are normalized to be unity. This decision will only affect the magnitudes of the

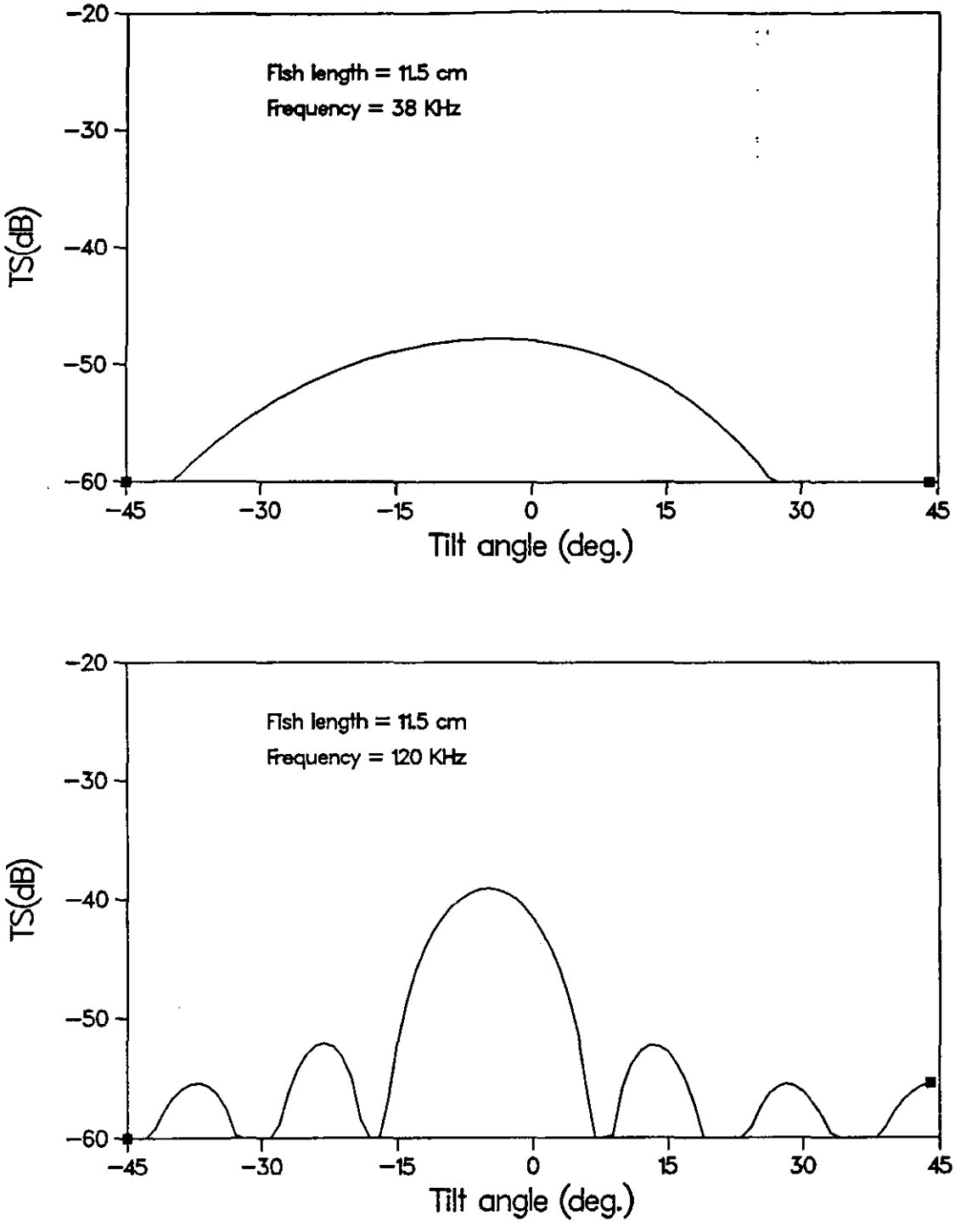

Fig.4.1 Dorsal aspect target strength functions of the same length of a fish at different frequencies.

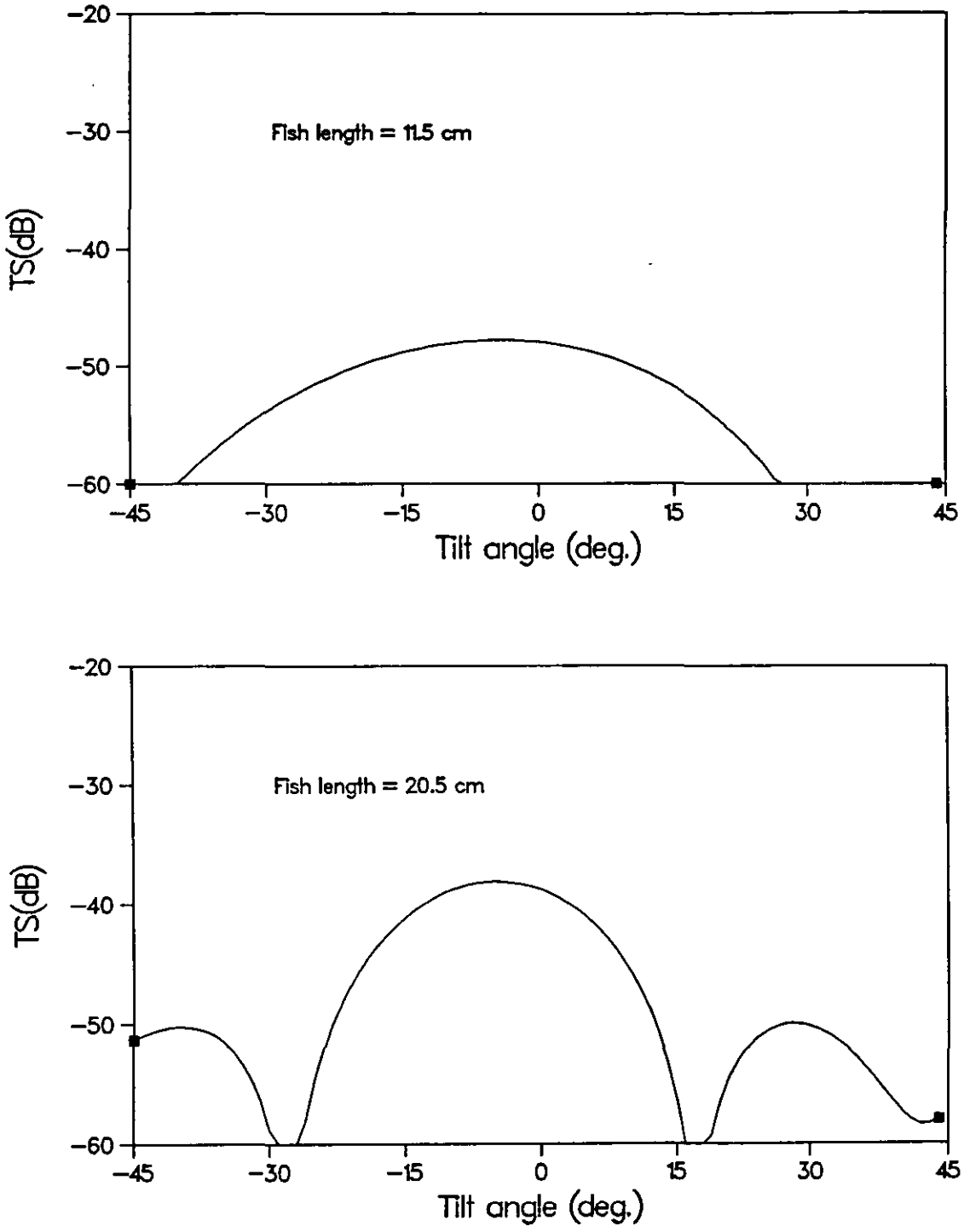

Fig.4.2a Dorsal aspect target strength functions of different length of a fish at 38 kHz.

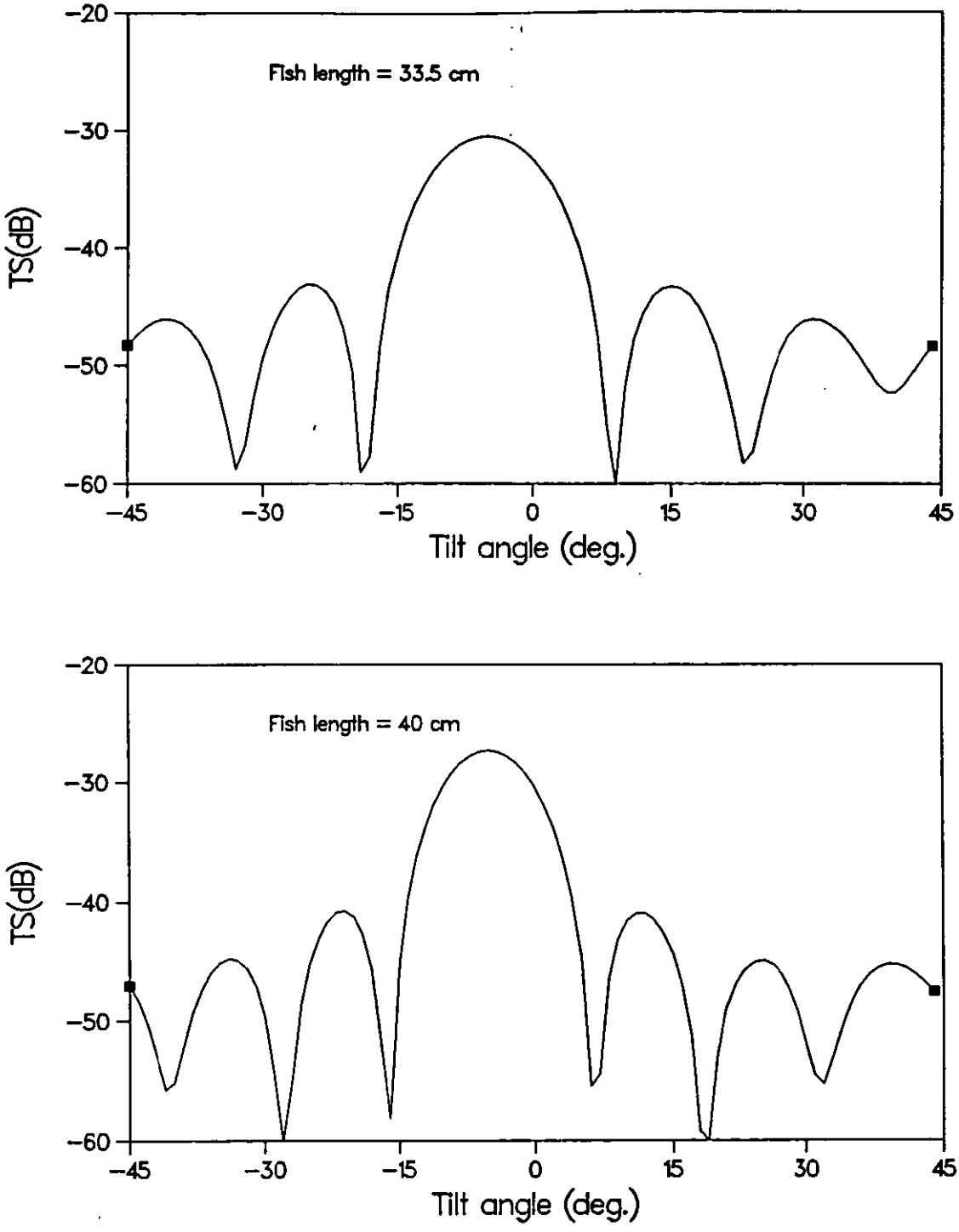

Fig.4.2b Dorsal aspect target strength functions of different length of a fish at 38 kHz.

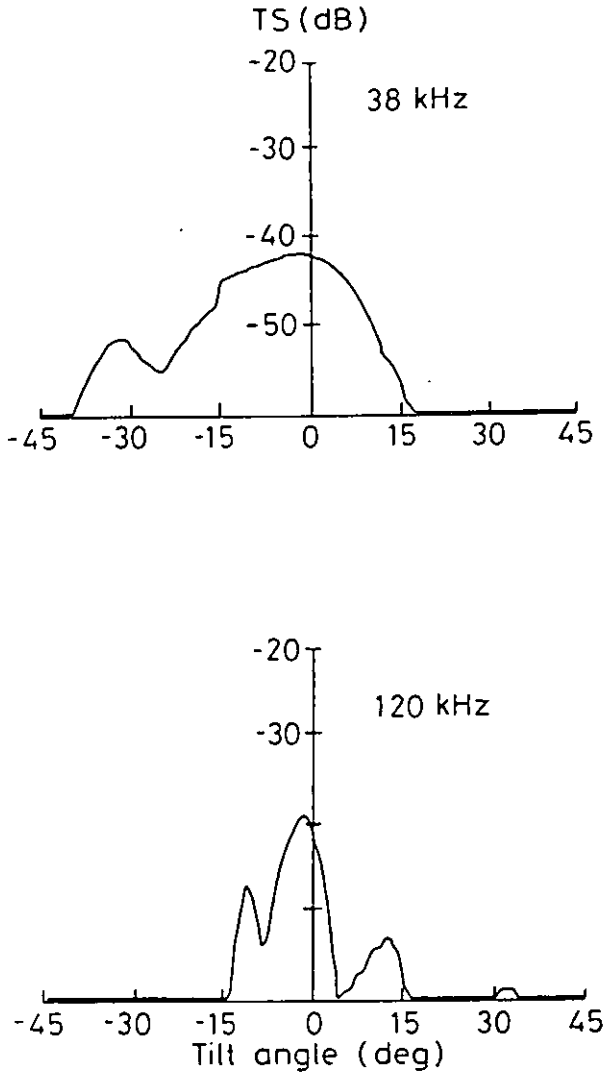

Fig.4.3 Comparison of dorsal aspect target strength functions of an 11.2 cm cod at 38 and 120 KHz. (After Foote, K.G.)

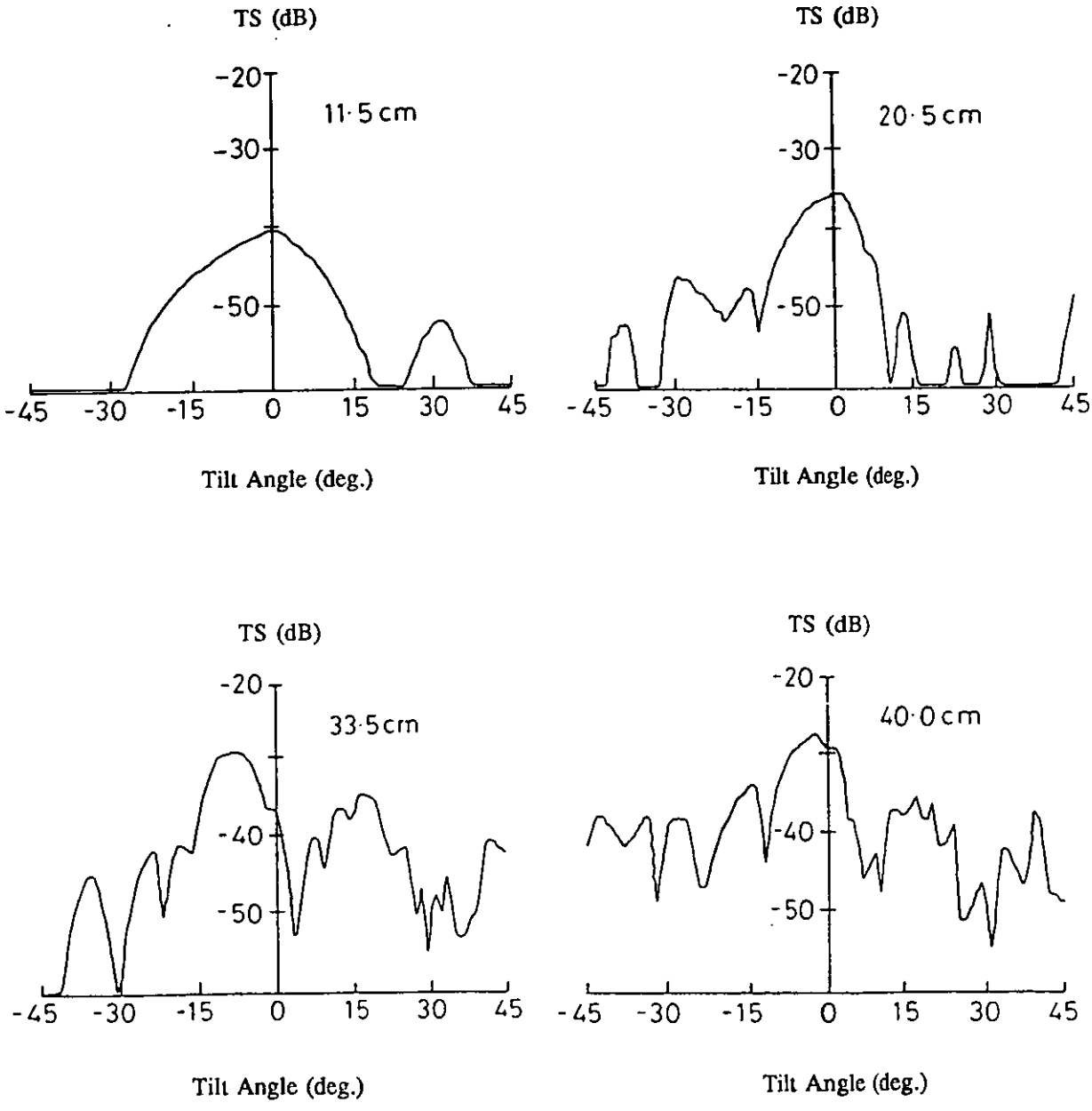

Fig.4.4 Comparison of dorsal aspect target strength functions of four cod, arranged by length, at 38 KHz. (After Foote, K.G.)

$f(\pi)$ and $\beta(\theta)$, while the shapes, or forms of these characteristic curves are all similar. The reason why they are done so will be given in the next section.

It can also be seen from equations (4-4) and (4 - 5) that the proposed model is quite complicated when compared with a transducer's beam pattern. But strange to say, the shapes, or forms of both of them against tilt angle are very similar under the conditions of the maximum amplitude and wavelength being normalized to unity. This is demonstrated in Figs.4.5 and 4.6. It is found that if the number of wavelengths of the simple mathematical model is twice that of the complicated one, the curves derived from the two models seem to be very similar. This finding could give an important idea on which the complicated model might be replaced by the simple one, or a transducer's beam pattern. It is obvious that what would only be modified is that the wavenumber, n, of the simple model would be twice that , k, of the complicated one. In this case the magnitudes of the beam pattern should correspond to the practical ones which are obtained from the *in situ* measurements under the conditions of the corresponding tilt angles, frequencies, fish sizes and species.

Due to the complicated configuration of fish and the movement of itself, the incident wave insonifies its different sections at different times and at differnt angles. Therefore, the target strength for the same size of the fish in the same species is different at different times. This is because the target strength is affected by the tilt angle.

It is well known that if the dimensions of fish in the direction of the incident acoustic energy considerably exceed the wavelength, the theory of scattering

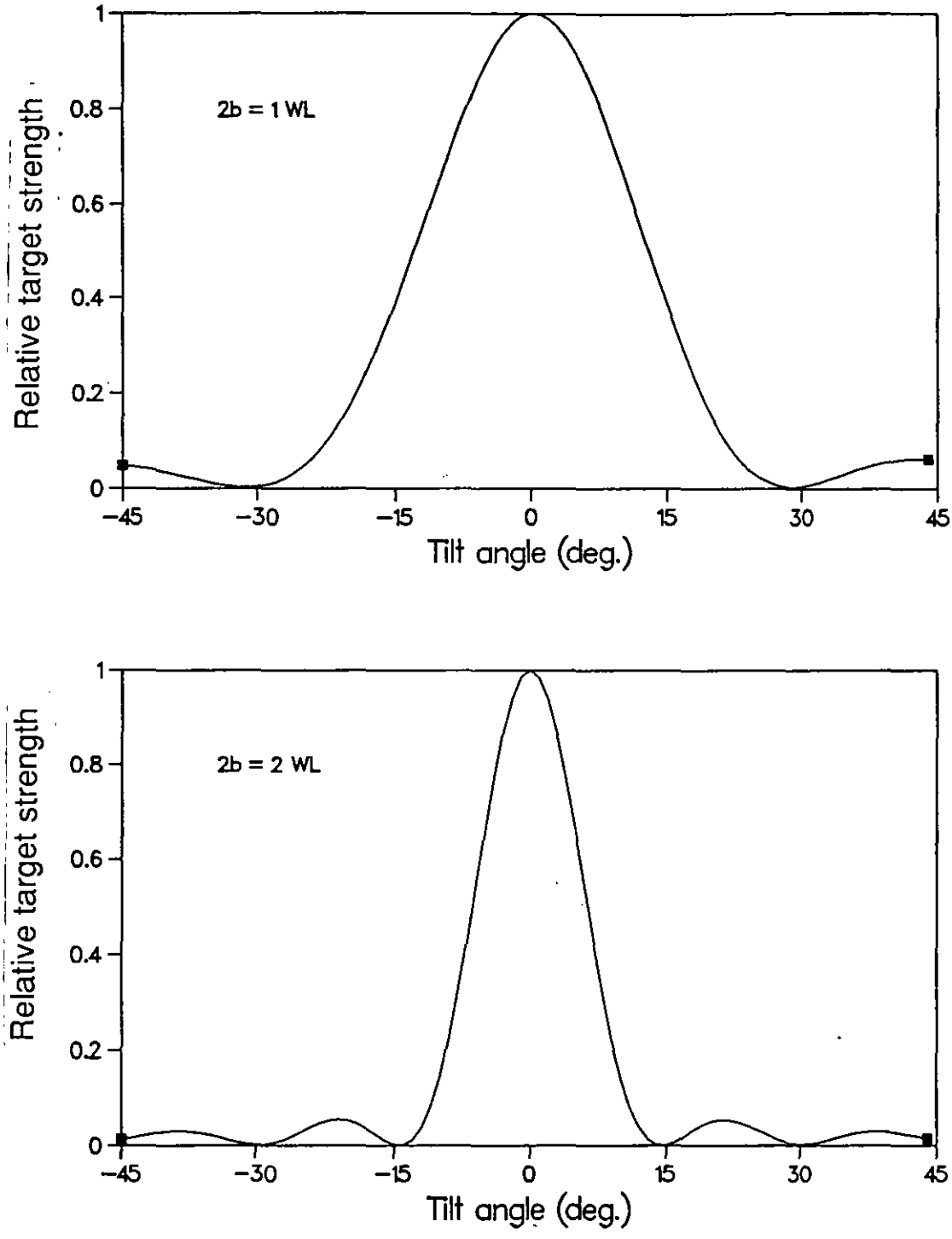

Fig.4.5a Dorsal aspect target strength functions normalised both in amplitude and wavelength.

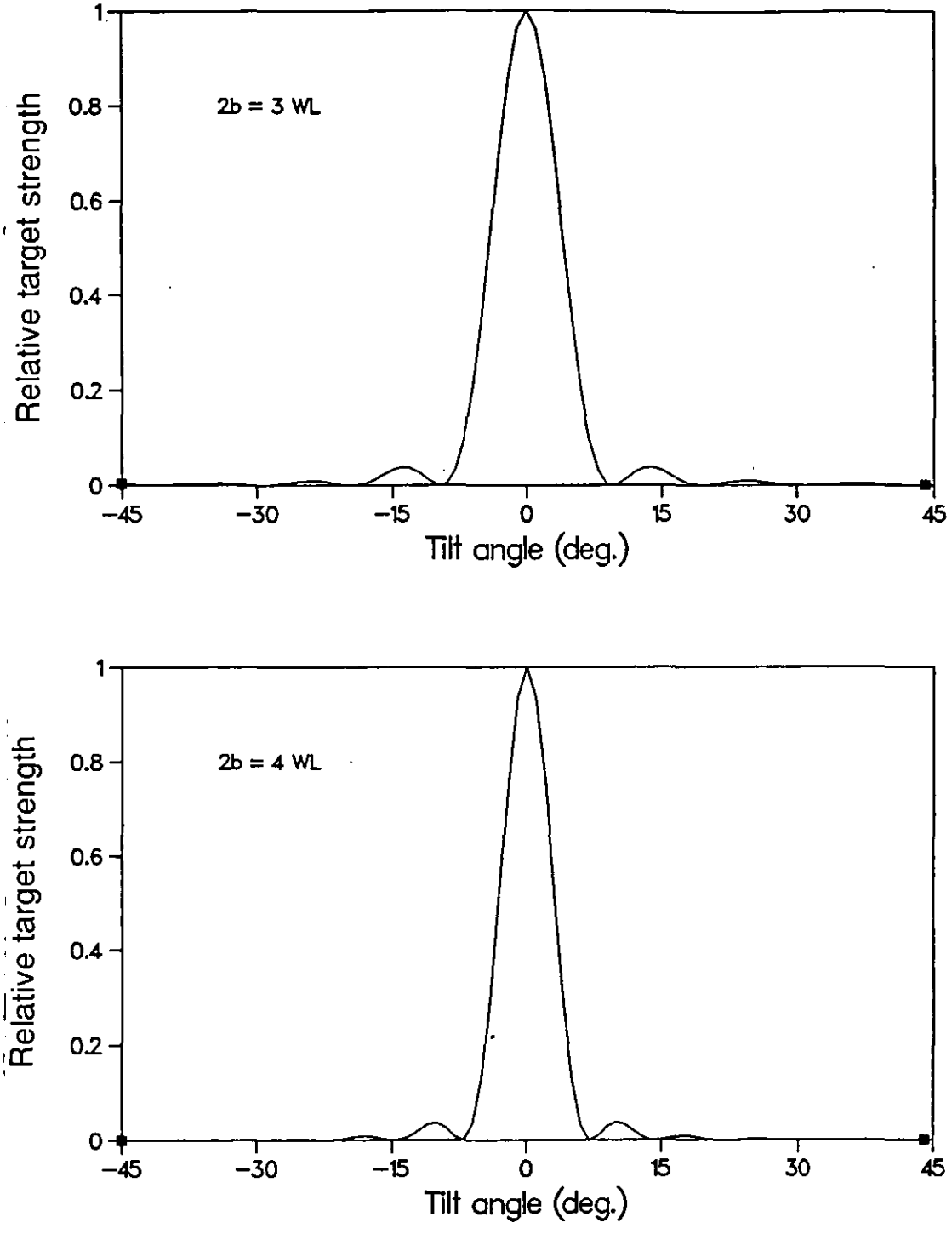

Fig.4.5b Dorsal aspect target strength functions. normalised both in amplitude and wavelength.

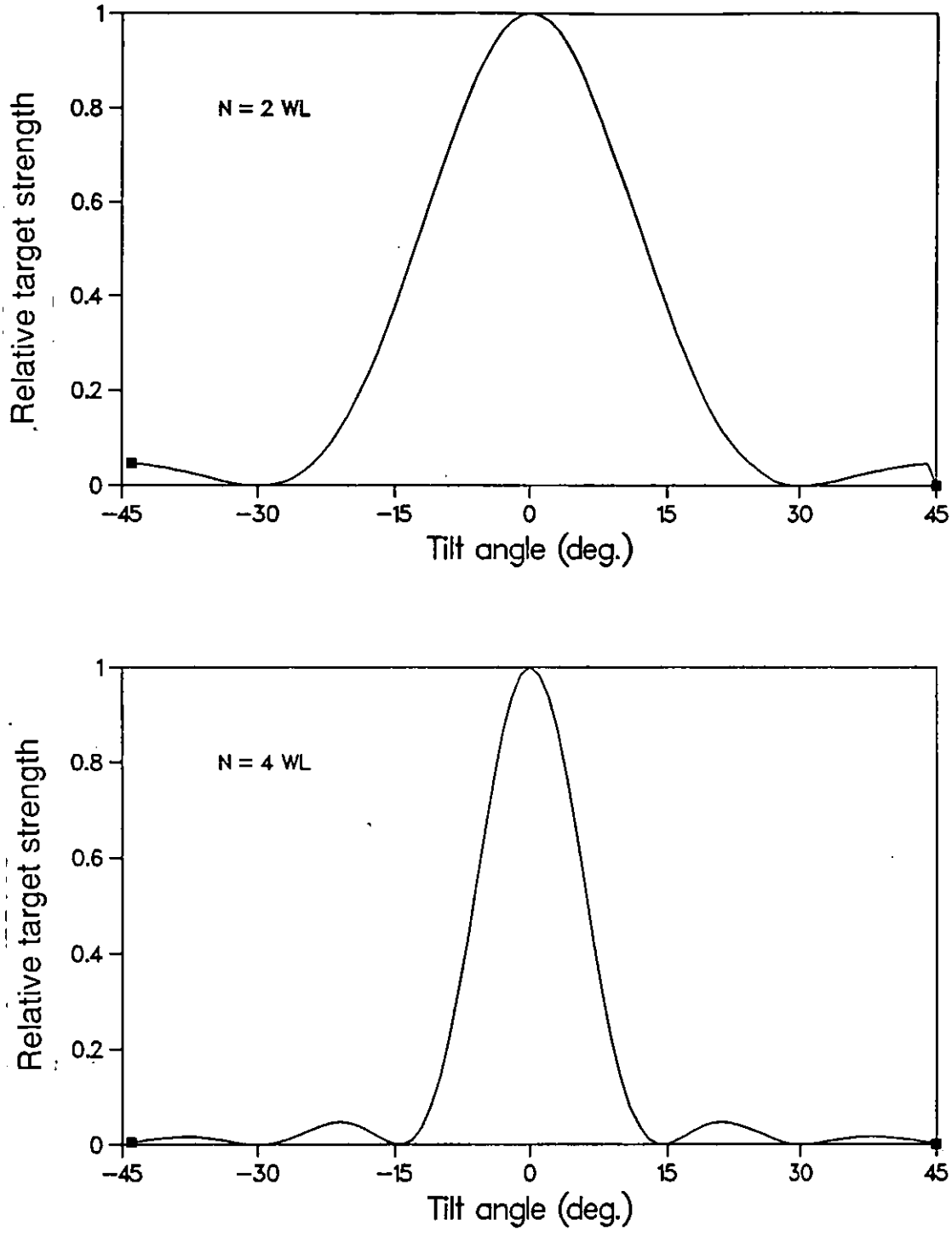

Fig.4.6a Beam pattern funcions of a transducer.

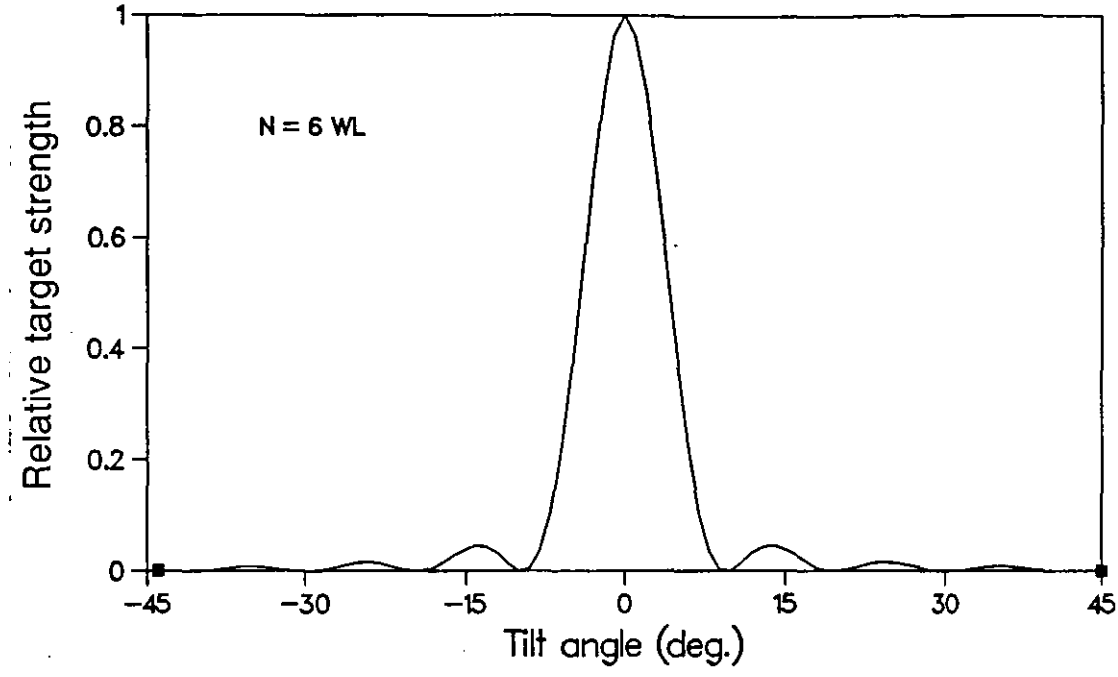

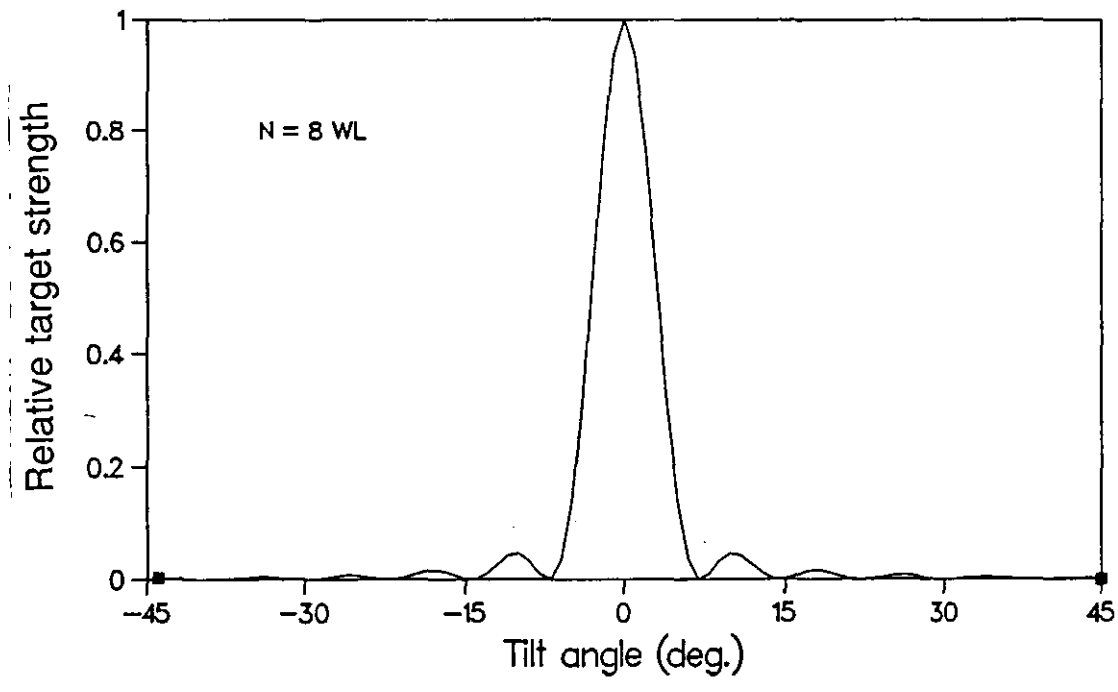

Fig.4.6b Beam pattern funcions of a transducer.

becomes more complicated, diffraction phenomena occurring at the surface of fish are then involved.

It should be noted that some of the premises supporting the analytical method of determining the acoustic characteristics of swimbladdered fish require further experimental confirmation, and the range of application of the premises needs to be defined more precisely. In particular, these problems include: determination of the amount of acoustic energy scattered by the swimbladder; correctness of the approximation of the form of the swimbladder to a cylinder etc..

4.3 EFFECT OF THE PDF OF TILT ANGLE ON THE MSV ESTIMATION OF TARGET STRENGTH

4.3.1 Introduction

It is known that the accuracy of the fish abundance estimation is dependent on the average target strength. Due to the internal and external geometry of fish, its target strength can vary widely with its size, the insonifying frequency, and the insonified aspect. Thus, a reasonably effective and simple approximation of the mean-squared backscattering cross sections or the mean square target strength is required by fisheries research and management groups. In the previous work [22], the mean square value of the target strength was used in determining the expected average energy of a single pulse in order to estimate the number of targets. The approximation can then be applied to some models in order to statistically estimate the fish abundance.

4.3.2 Model

Some similar equations are represented in references [32] and [33], which could be used to determine the average target strength. These equations account for the influences of the tilt angle distribution of fish and beam patterns on observations of target strength. For the purpose of modelling and understanding, it is reasonable to assume that the effect of the distribution of the tilt angle and the sonar beam pattern on the MSV are independent of each other [22]. The two important factors in the measurement of the fish abundance are the mean target strength and the mean square target strength defined as

$$\overline{TS} = \int TS(\theta) g(\theta) d\theta$$

and

$$\overline{TS^2} = \int TS^2(\theta) g(\theta) d\theta \qquad \text{..... (4 – 7)}$$

where g(θ) is the PDF of tilt angle. The mean square fluctuation determines the scattter of the results and is thus an very important parameter.

To make an estimate of the effect of the dependence of tilt angle on the average target strength, for simplicity, the two functions shown in Fig.4.7 for the variation of target strength with tilt angle were assumed. These expressions are as follows,

$$T_1(\theta) = 20\log(b \cdot \exp(-c\theta^2)) \qquad \text{..... (4 - 8)}$$

$$T_2(\theta) = 20\log\left\{a \cdot \left|\frac{\sin(k\sin(\theta))}{k\sin(\theta)}\right|\right\} \qquad \text{..... (4 - 9)}$$

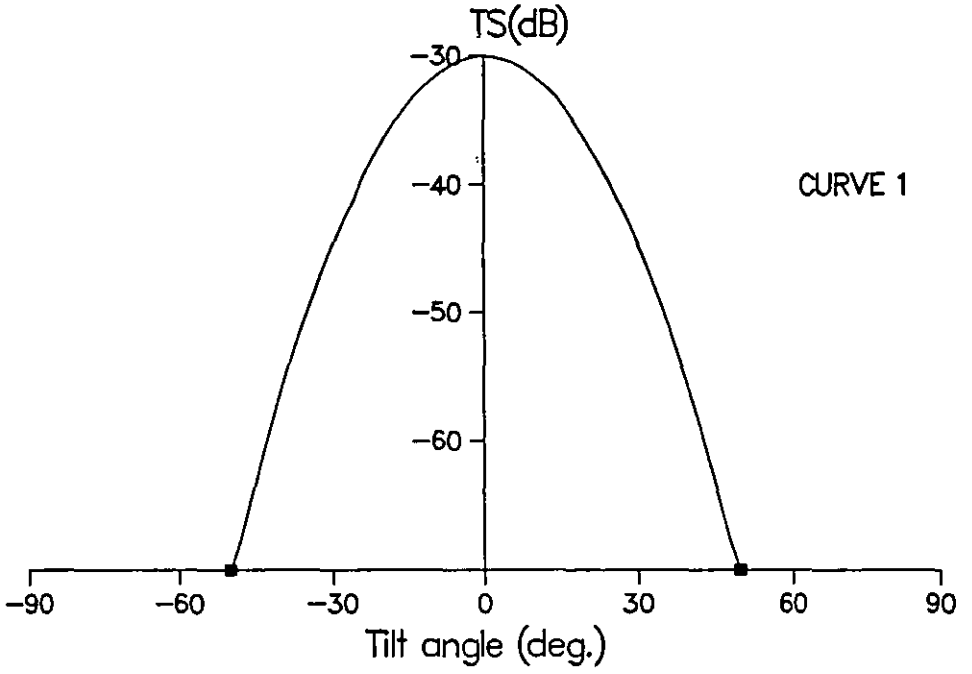

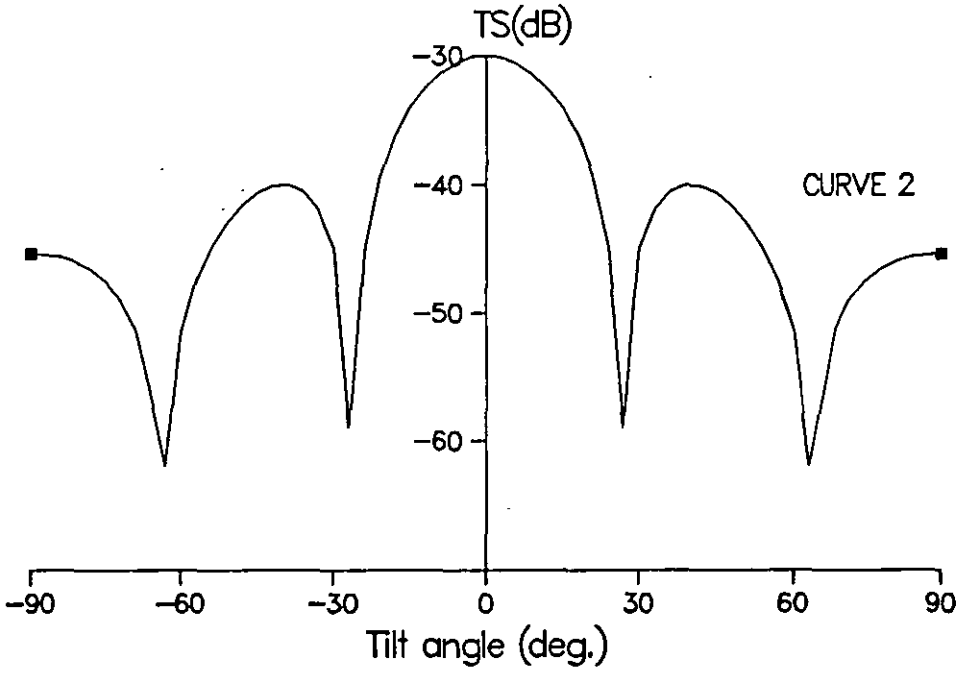

Fig.4.7 Distributions of target strength versus angle assumed in model.

where a, b, c and k are factors which depends on the length of fish, the insonifying frequency and other biological characteristics of fish.

It is shown in references [30] and [32] that the PDF of the tilt angle is characterized by a truncated Gaussian distribution in the tilt angle and used for calculating the MSV of the backscattering cross section of a fish. A uniform distribution for the probability distribution of tilt angle was also assumed aiming to replace the normal distribution since it was not only simple but probably has, to some extent, the same effect as the normal distribution on the average target strength.

4.3.3 Examination of Effects

(1). The effect of the range of tilt angle, θ_r, on the MSV of target strength

In this stage, the standard deviation S_q was constant and the range of tilt angle, θ_r, was varied. It was found in Fig.4.8a and Fig.4.8b that the results were not much different using truncation at $\pm 1.5S_q$ and $\pm 3S_q$ when the standard deviation was 5. If the standard deviation S_q exceeds 15, the results shown in Fig.4.8b become worse and incomparable.

(2). The effect of the standard deviation S_q on the MSV of target strength

Some typical results were obtained by varying S_q from 5 to 25 at the respective ranges of the tilt angle, θ_r, such as 60^o and 90^o. It was observed from Fig.4.9a and Fig.4.9b that when S_q was increased, the MSV decreased and approached the results obtained using the uniform distribution instead of the

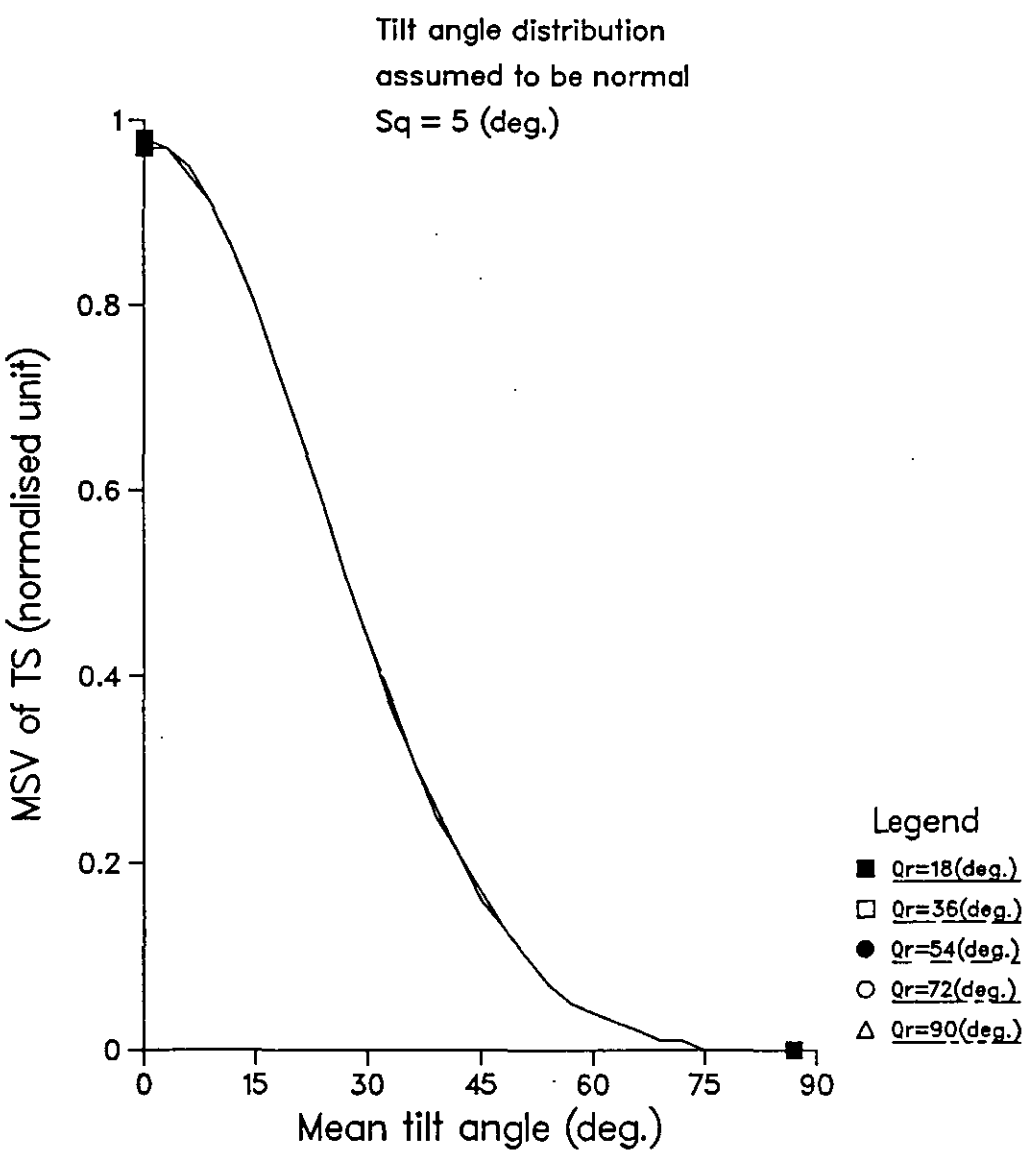

Fig.4.8a The effect of range of tilt angle, Qr, on mean square value of target strength.

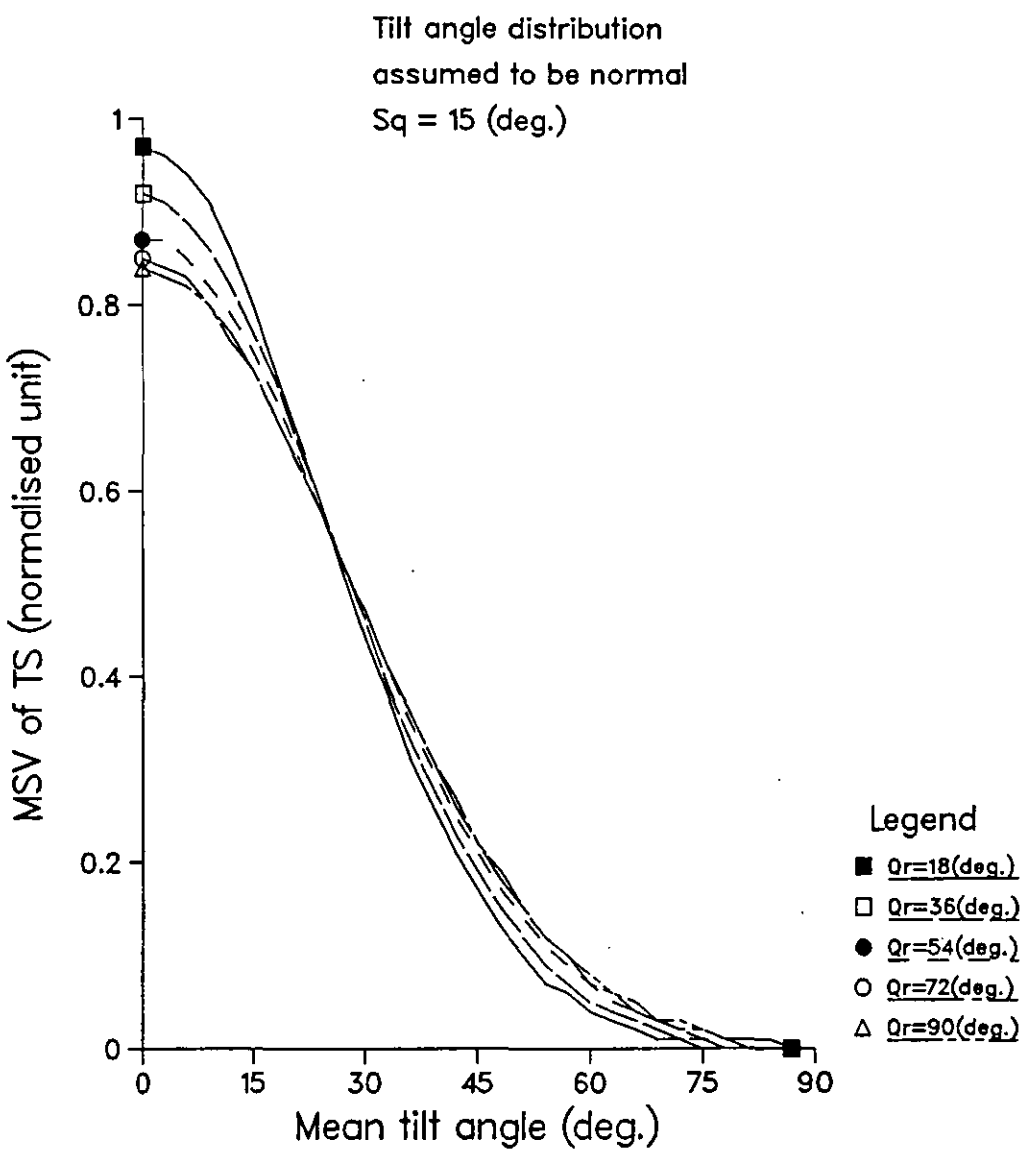

Fig.4.8b The effect of range of tilt angle, Qr, on mean square value of target strength.

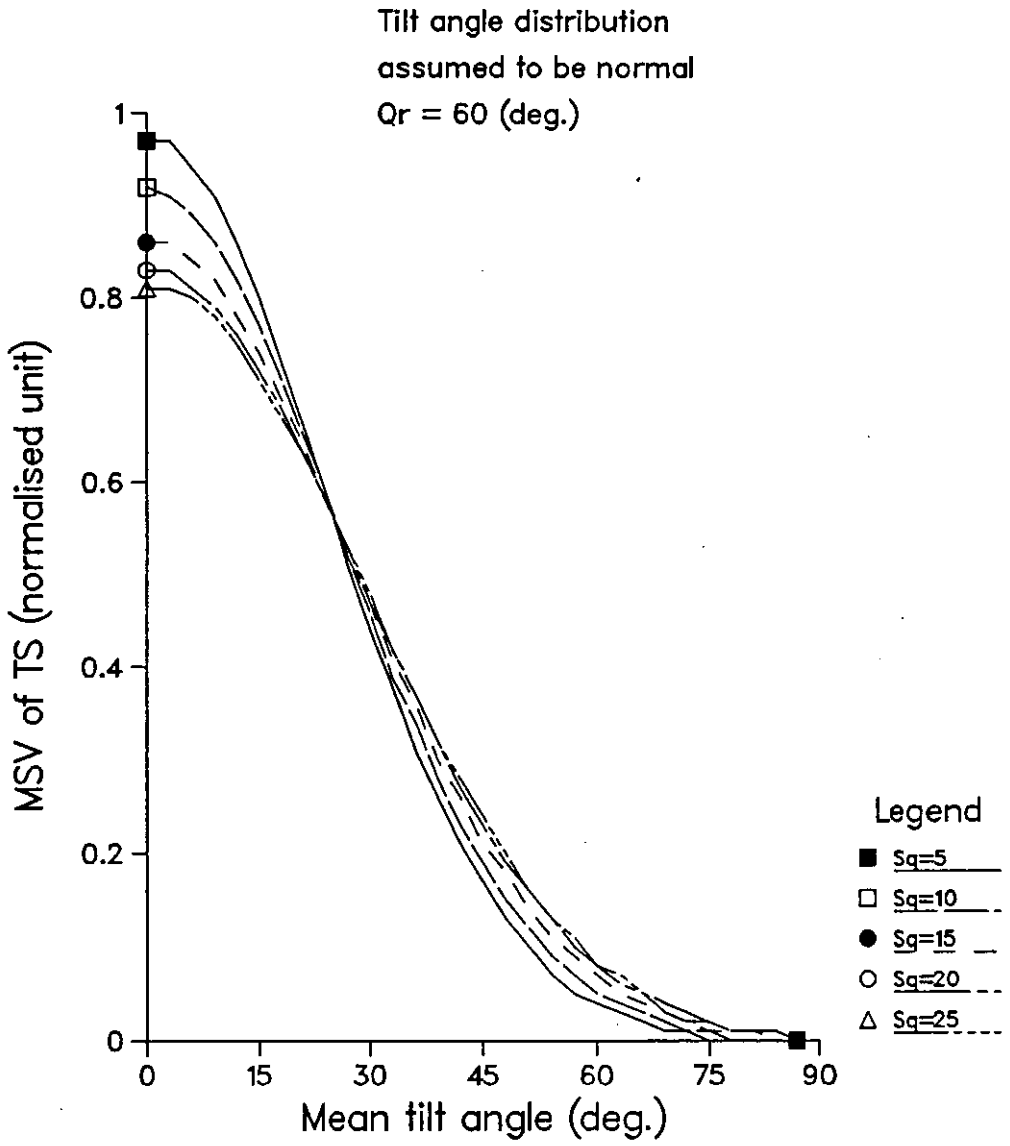

Fig.4.9a The effect of standard deviation, Sq, on mean square value of target strength.

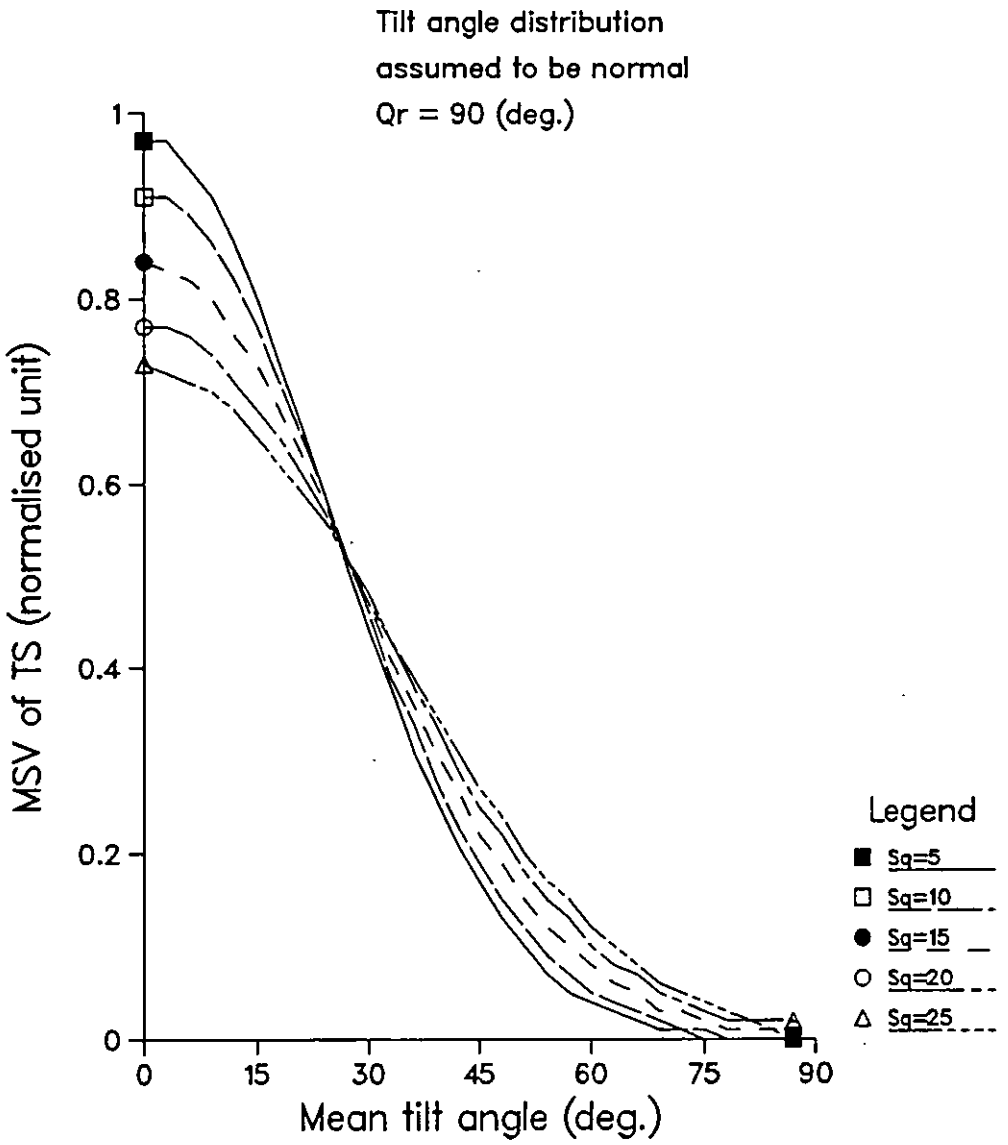

Fig.4.9b The effect of standard deviation, Sq, on mean square value of target strength.

Gaussian one with tilt angle θ as shown in Fig.4.9c. If the range of tilt angle is smaller, then the results obtained from the Gaussian distribution are similar to those from the uniform one.

(3). The effect of the target strength function of fish with tilt angle θ on the MSV of target strength

It is known that the reflection direction pattern or target strength function of fish varies with aspects. i.e. the tilt angle and length of fish as well as the frequency of the acoustic signal. Of course, the biological characteristics of a fish also affect the function. It is observed that the patterns of these functions are similar to the measured ones as shown from Figs.4.1 to 4.4. When the frequency or the length of a fish is increased, the main lobe and sublobe of the reflection direction pattern become narrower and narrower. In the case of the narrower lobe, bigger standard deviation S_q or wider range of tilt angle, θ_r, will seriously affect the MSV of target strength. It is also observed that the results obtained by using the uniform and normal models for the tilt angle distribution are similar. This is confirmed in Fig.4.10.

(4). The effect of the mean tilt angle θ_m on the MSV of target strength

It was observed from all the graphs in the section that the MSV of target strength decreased with the increase of the mean tilt angle θ_m. But it remained almost constant when the mean tilt angle was less than 10. After that the MSV dropped very quickly.

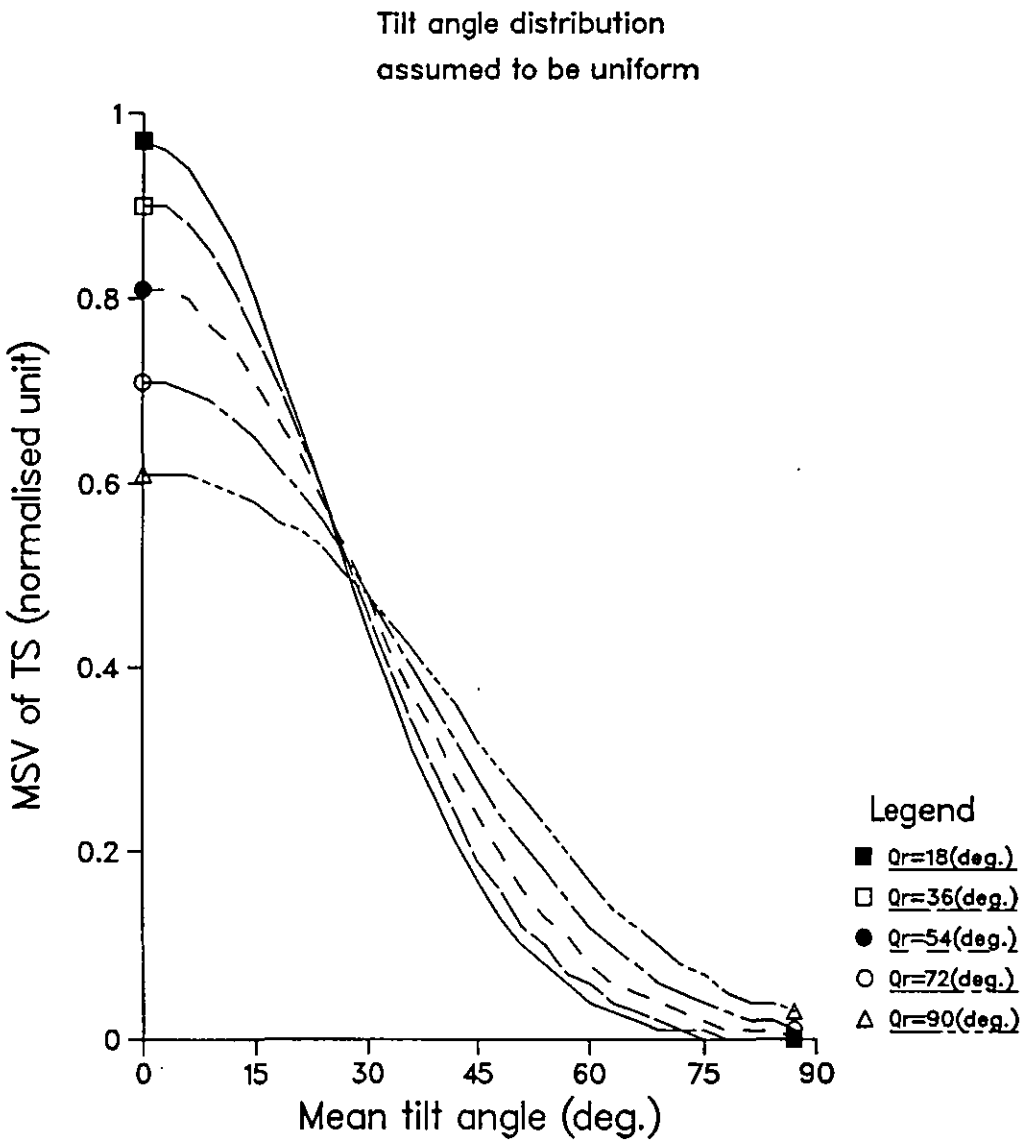

Fig.4.9c The effect of range of tilt angle, Qr, on mean square value of target strength.

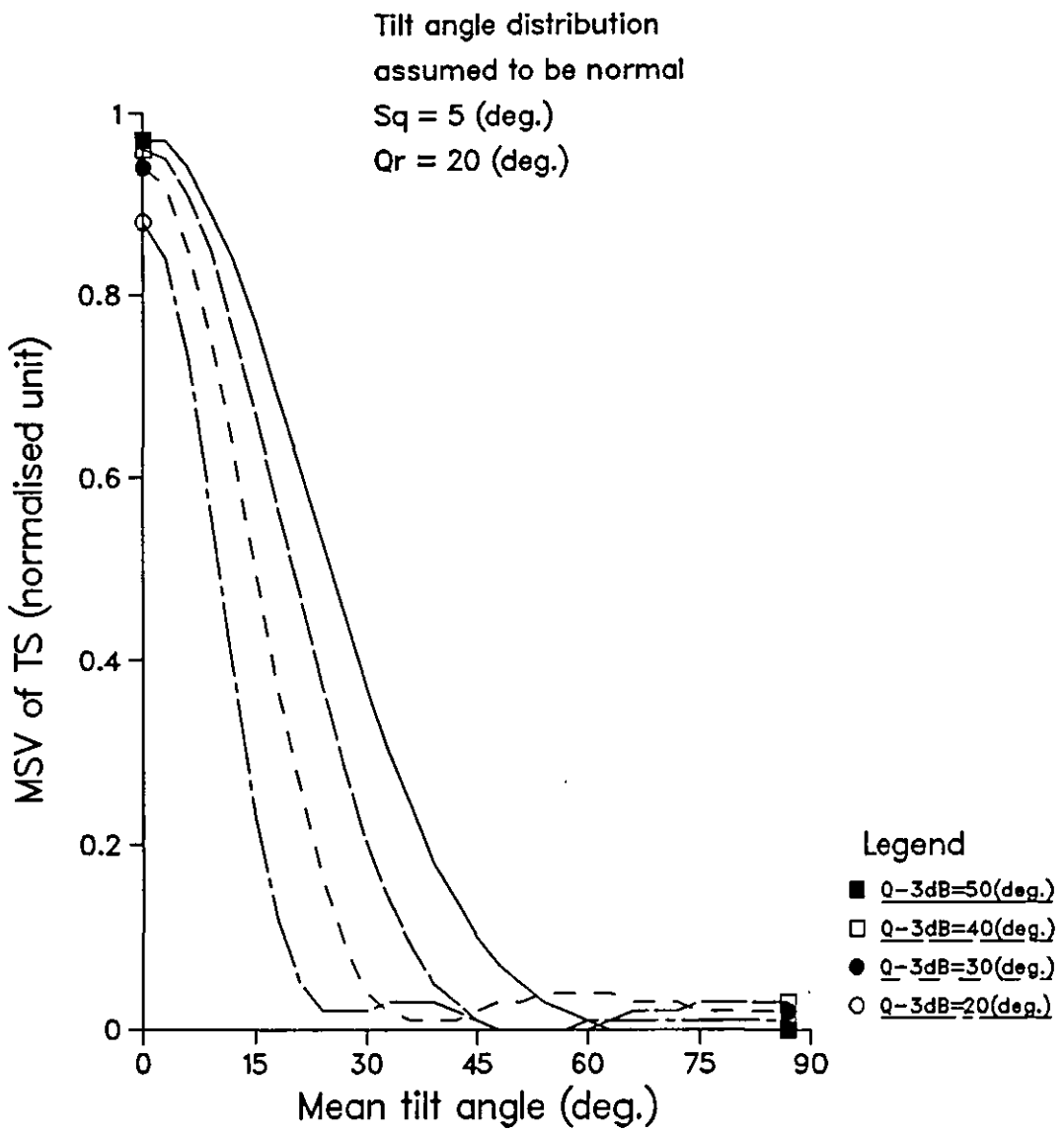

Fig.4.10a The effect of TS functions with tilt on mean square value of target strength.

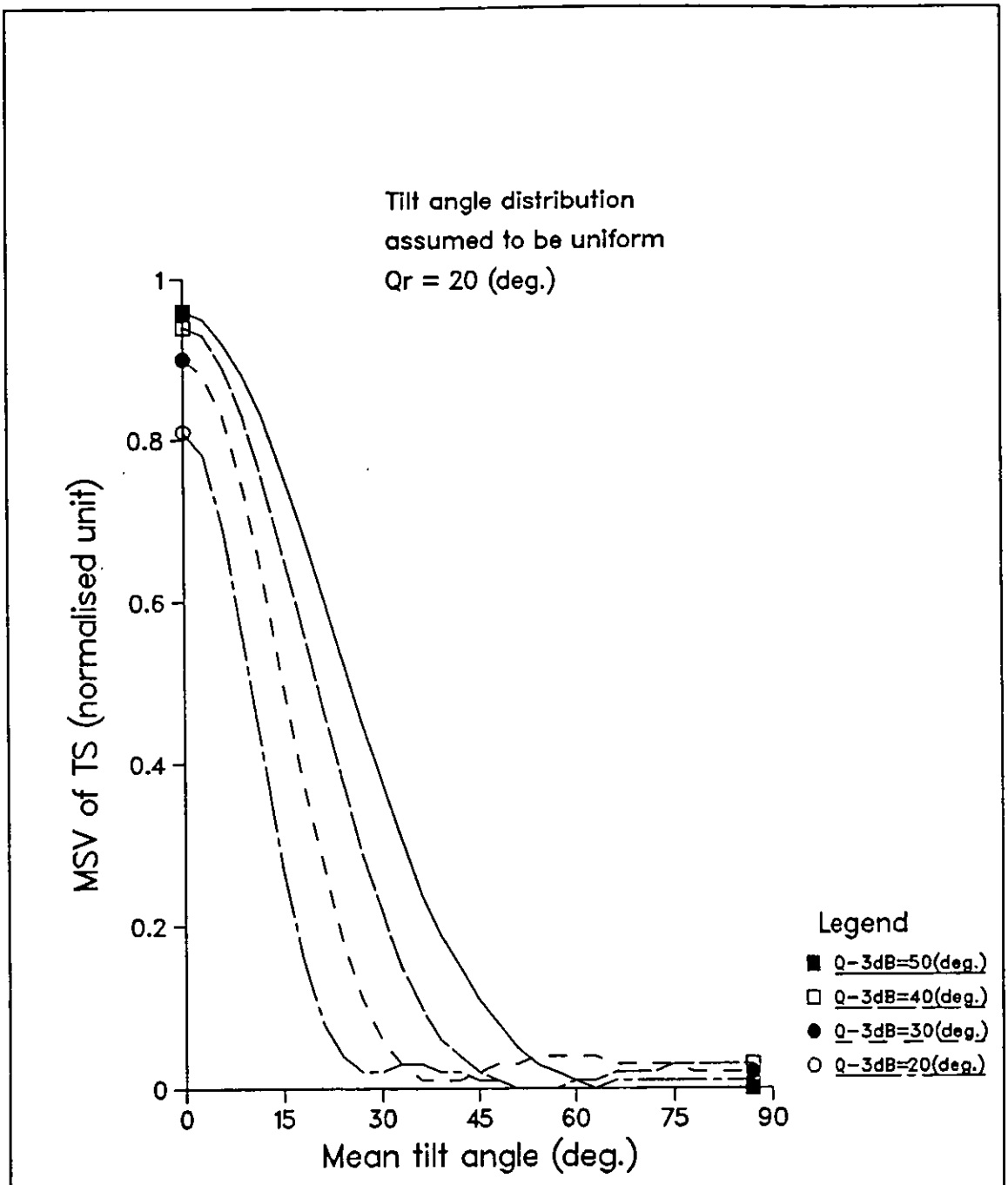

Fig.4.10b The effect of TS functions with tilt on mean square value of target strength.

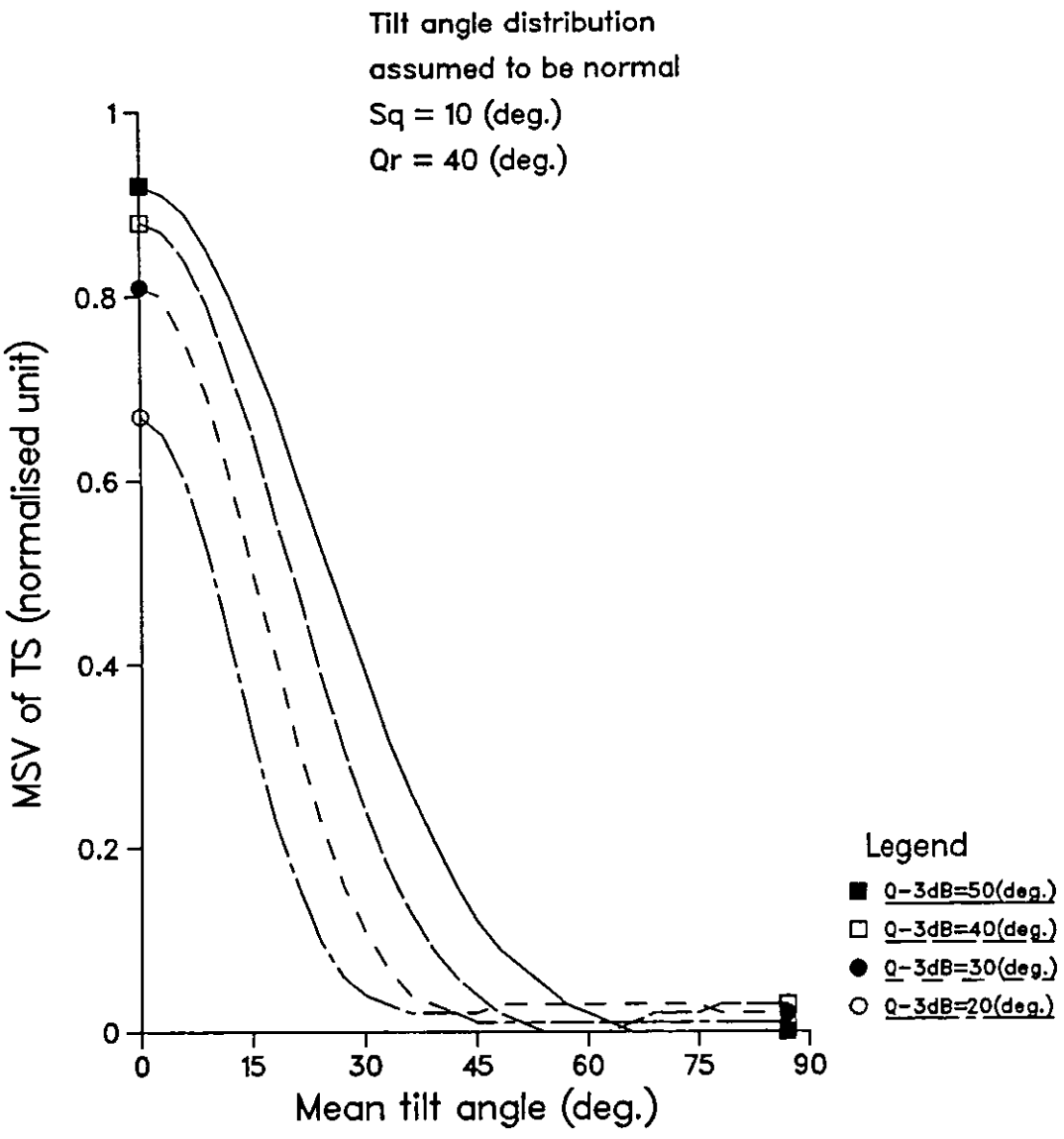

Fig.4.10c The effect of TS functions with tilt on mean square value of target strength.

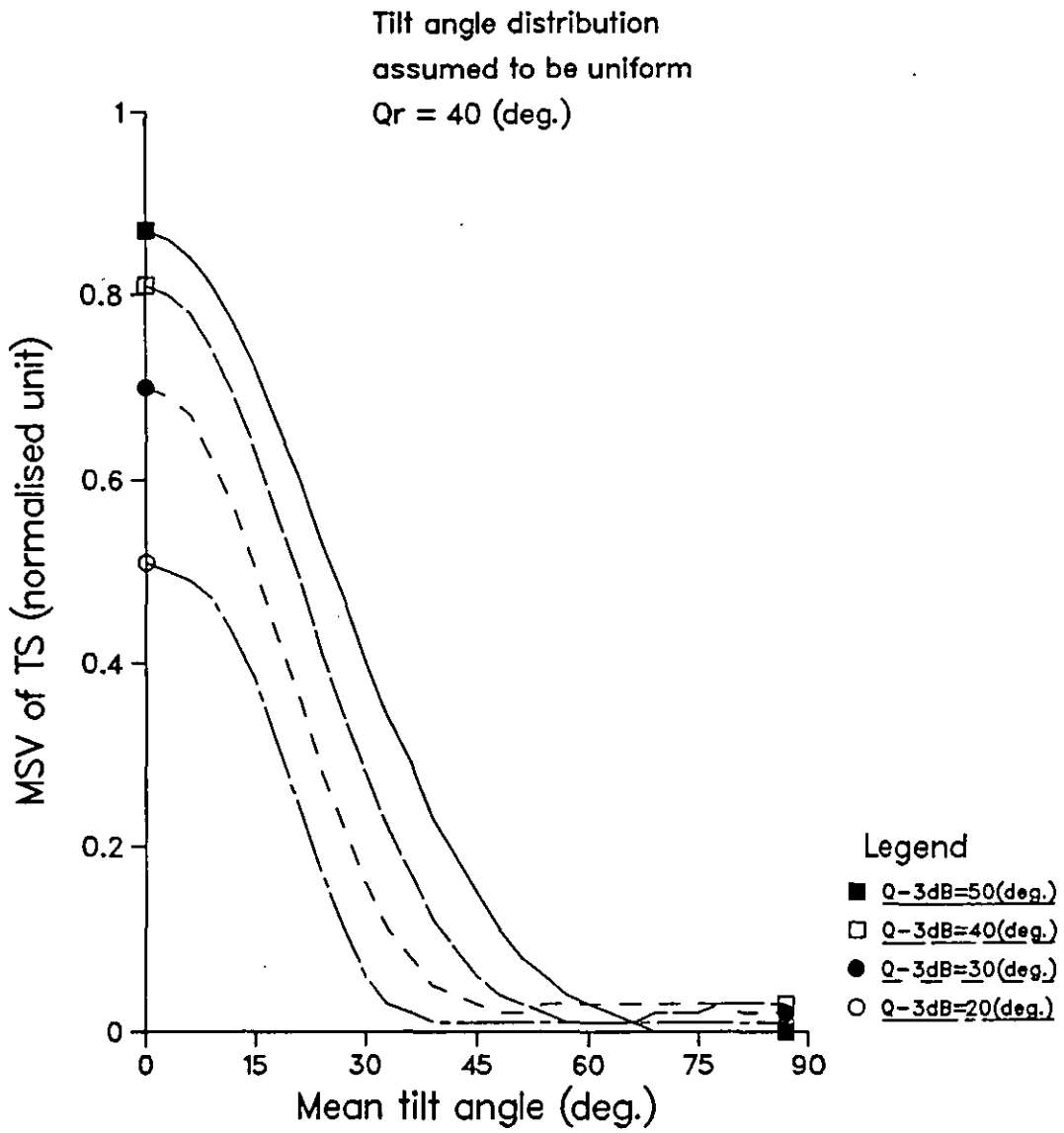

Fig.4.10d The effect of TS functions with tilt on mean square value of target strength.

4.4 PROBABILITY DISTRIBUTION FOR THE VARIATION OF TARGET STRENGTH

In the earlier modelling work in references [21] and [22], it was assumed that target strength of fish varied according to an arbitrary probability distribution and for simplicity the Gaussian distribution was chosen.

As mentioned before, the target strength of a fish depends strongly on the orientation of the fish, particularly, on the variation of its tilt angle. The distribution of the target strength of fish against tilt angle for a particular fish was obtained by measurement in reference [3] and it was found that the shape of this curve varies considerably with species. But, as might be expected, there is a strong inverse correlation between the width of this function and the length of the fish.

To make an estimate of the effect of the dependence of target strength on angle on the probability distribution of target strength, it is necessary also to know or to assume the probability distribution that represents the way in which the tilt angle will vary in practice. In reference [4] and [19] measurements are reported on different species and it is shown that this distribution is close to normal. Using these two functions it is then possible to predict the probability distribution for the variation of target strength and hence to calculate the effect of this probability distribution on the estimation of biomass.

For simplicity again, either a uniform or normal distribution for the probability distribution of tilt angle was assumed, and functions of target strength,

$T_1(\theta)$ and $T_2(\theta)$, were also used. The probability distribution for the variation of the target strength can then be obtained by using the following equation,

$$P(TS) = P(\theta)/T'(\theta) \qquad \text{..... (4 - 10)}$$

where $P(\theta)$ is the probability distribution of tilt angle of fish and $T'(\theta)$ the first derivative of the function of target strength with tilt angle.

Alternatively, it can be also solved by statistics. In this method, random variable numbers were generated from the probability distribution function of tilt angle and using these random values ,1000 samples could be obtained from the function of target strength. Each sample was represented by a number which gives information about the quantity being determined. These samples were grouped into 15 class intervals from -30dB to -60dB and the values within each was assumed to be equal. Thus a group frequency distribution may be represented by histogram. This graphical representation of the empirical distribution gives an important feature of the problem to be studied. It is fairly clear from the nature of this problem that the distribution of target strength of the fish obtained from the statistics or from the equation (4 - 10) will not be symmetrical, and this can be seen from Fig.4.11 to Fig.4.18. This shows a set of distributions calculated using simulation for each of the four conditions discussed above, and for four different angles of tilt in each case. It is observed from these figures that when the mean tilt angle of the fish is not zero then the possibility of a double moded distribution arises.

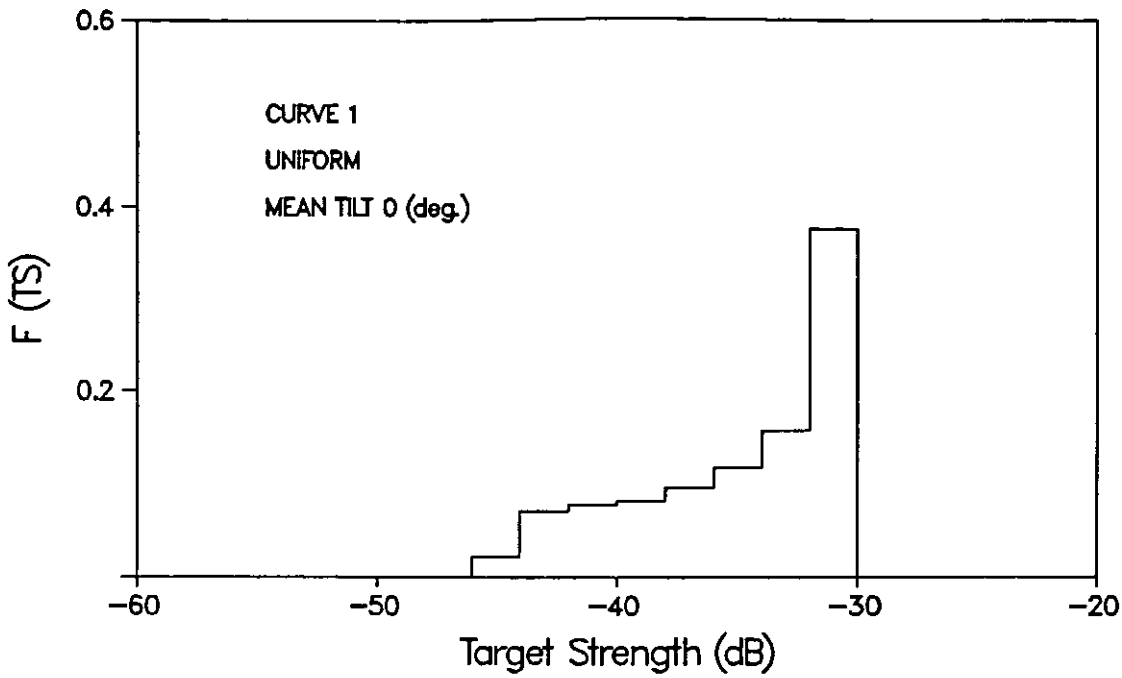

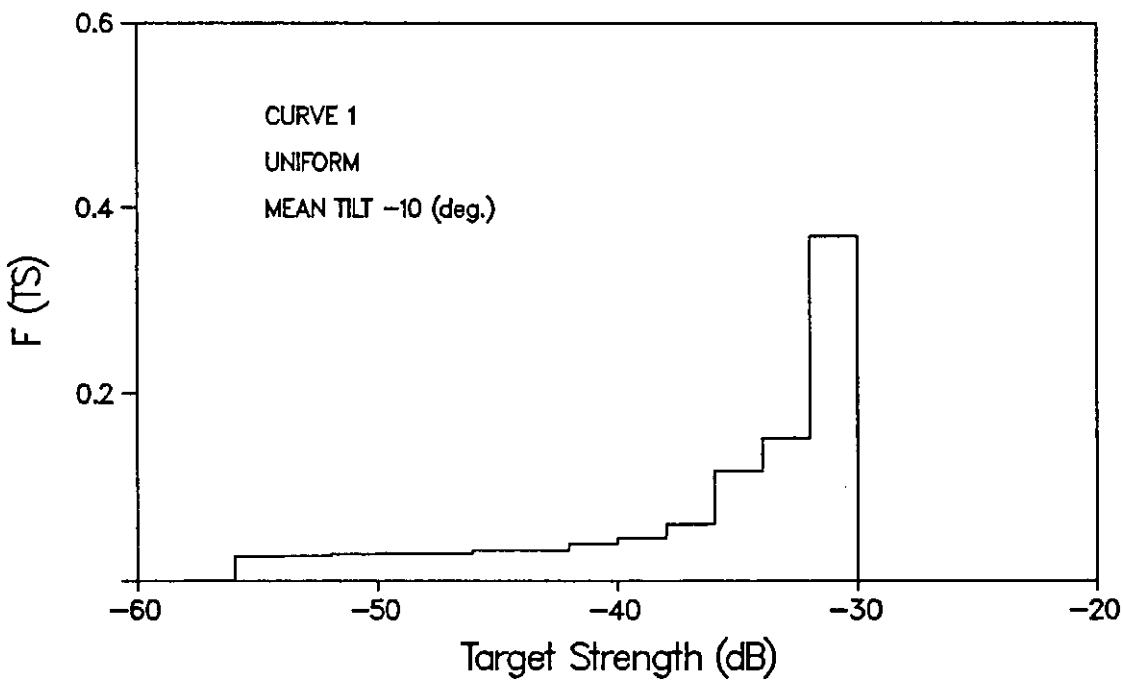

Fig.4.11 Probability distributions for the target strength of the fish obtained from the model with various assumptions.

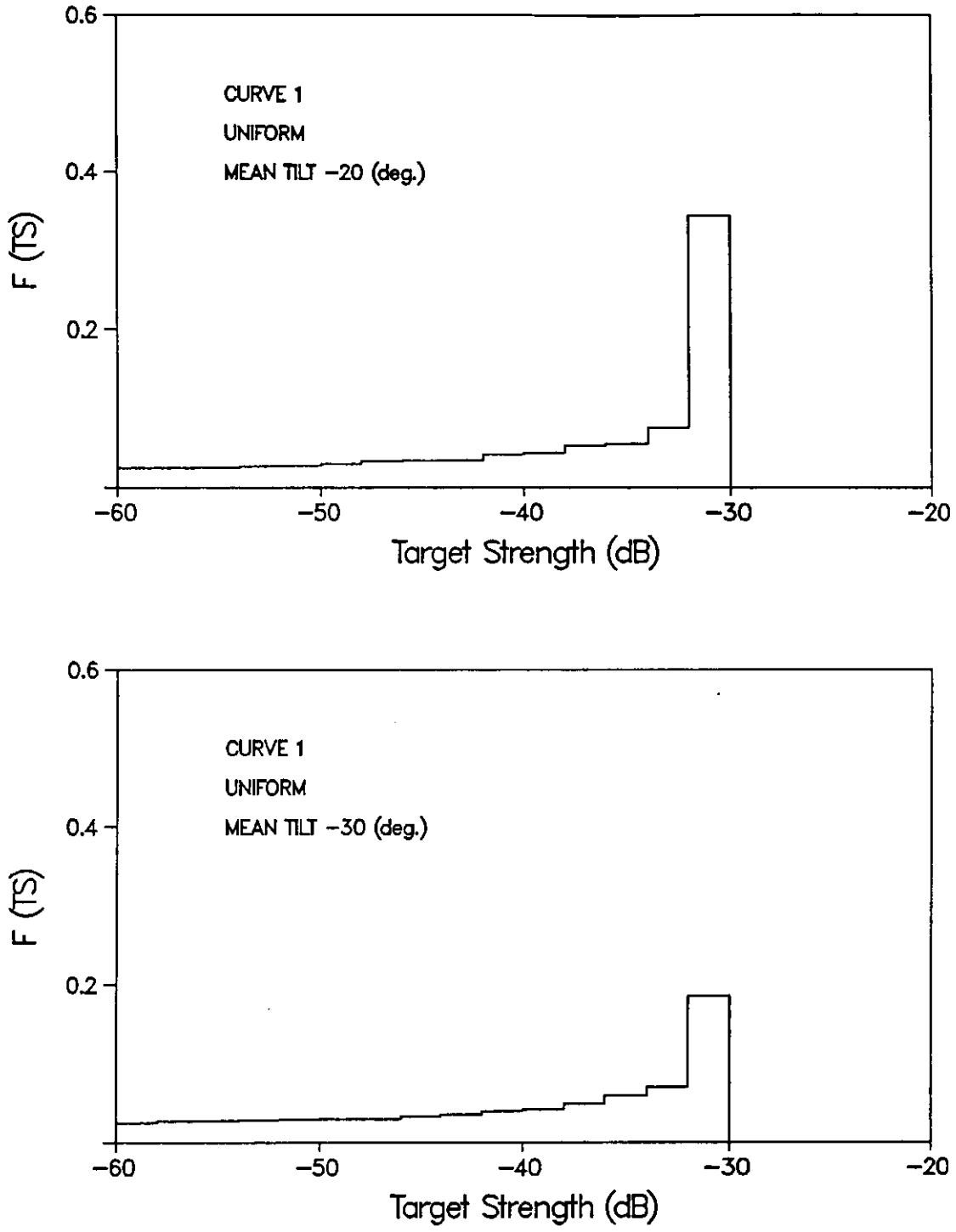

Fig.4.12 Probability distributions for the target strength of the fish obtained from the model with various assumptions.

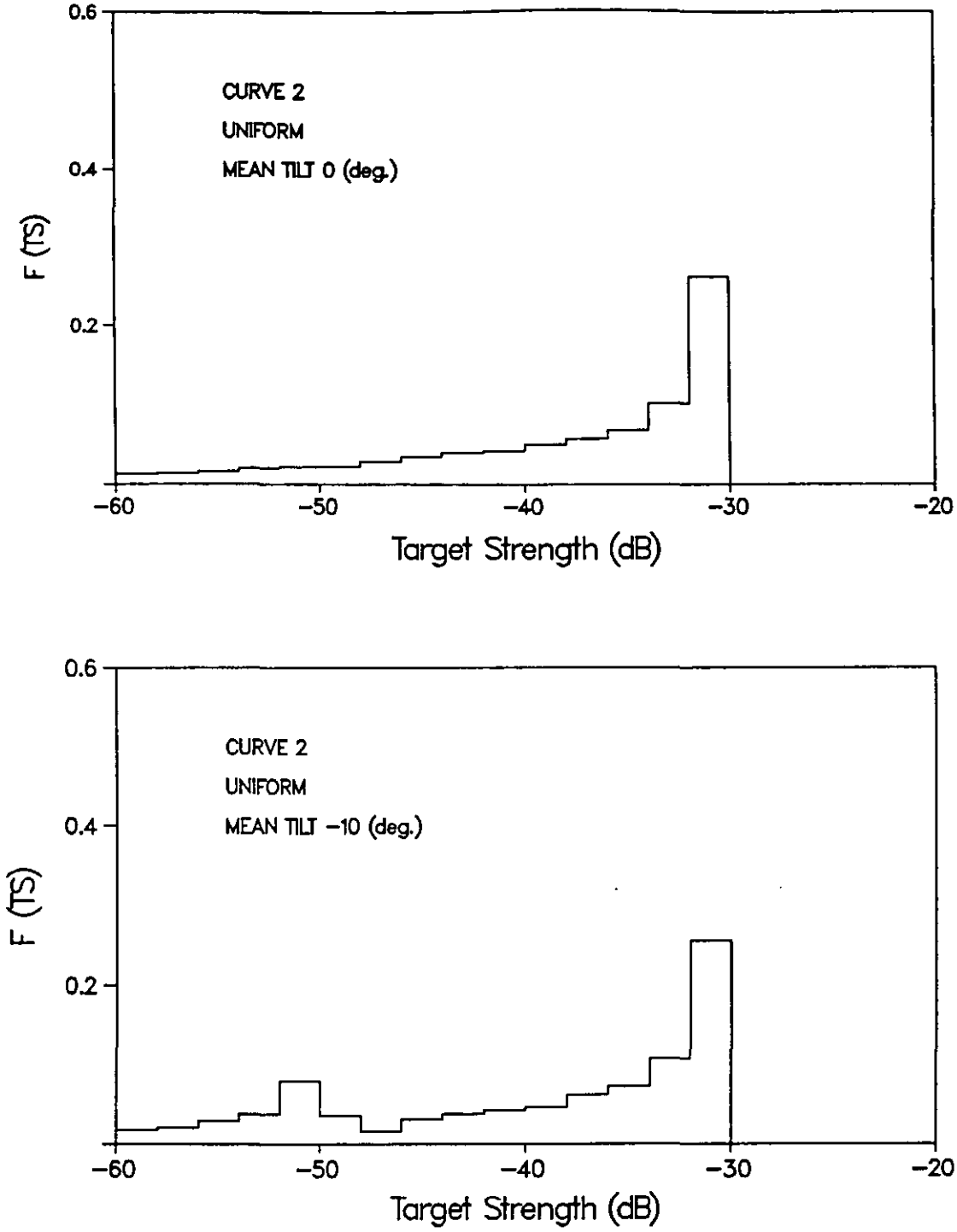

Fig.4.13 Probability distributions for the target strength of the fish obtained from the model with various assumptions.

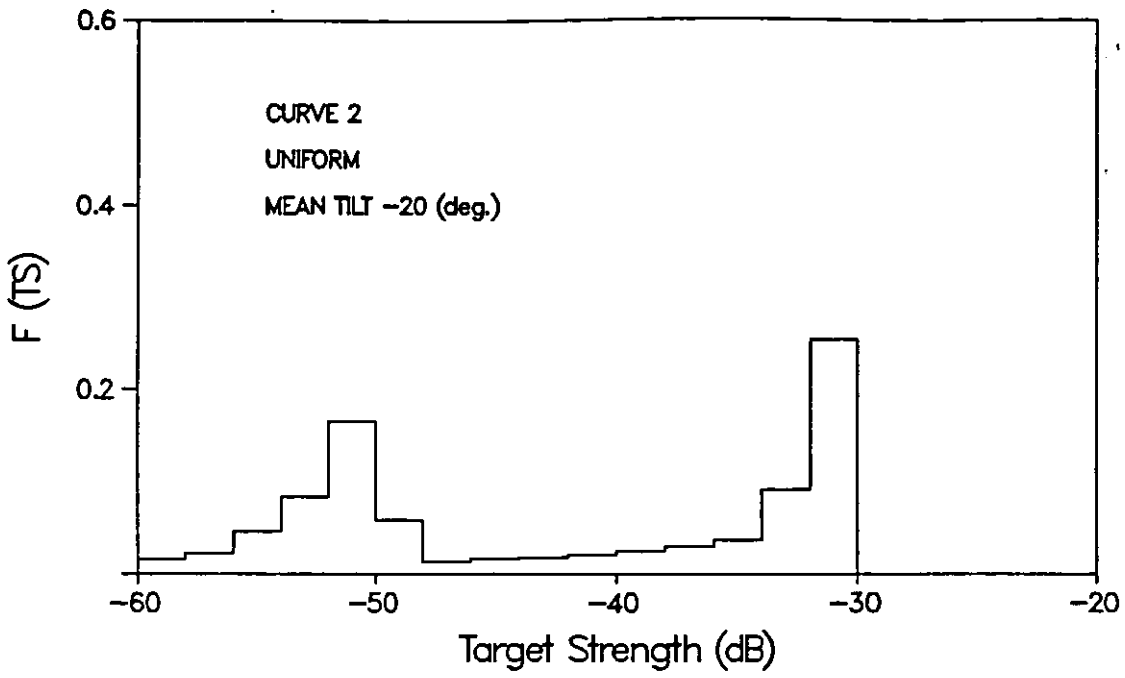

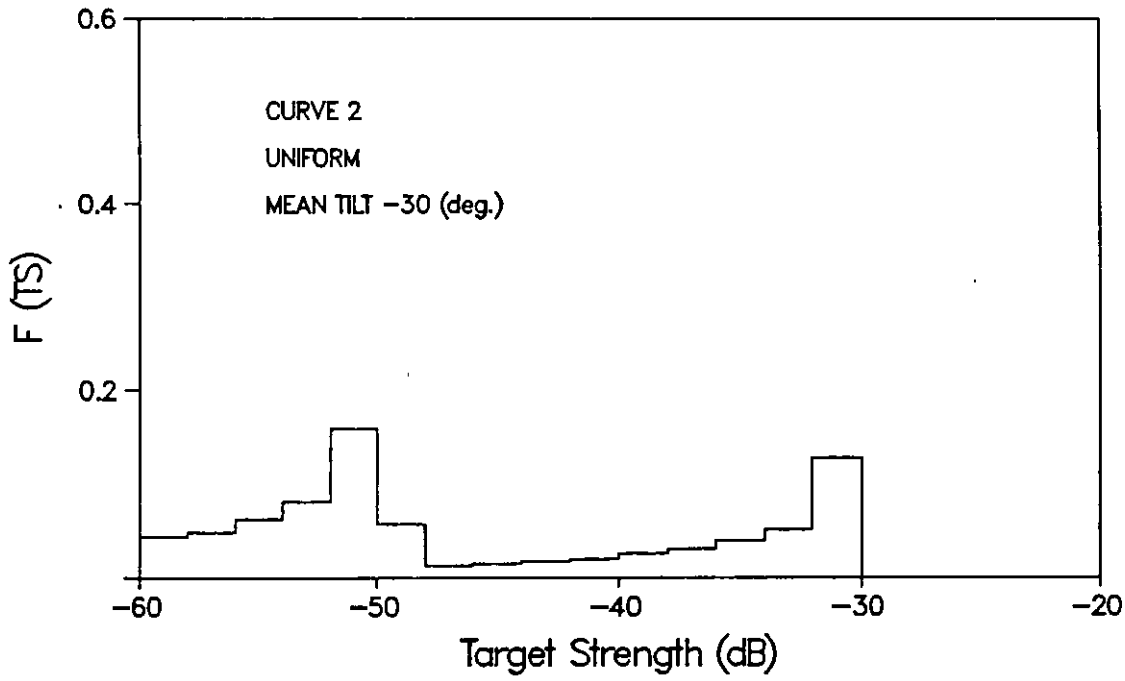

Fig.4.14 Probability distributions for the target strength of the fish obtained from the model with various assumptions.

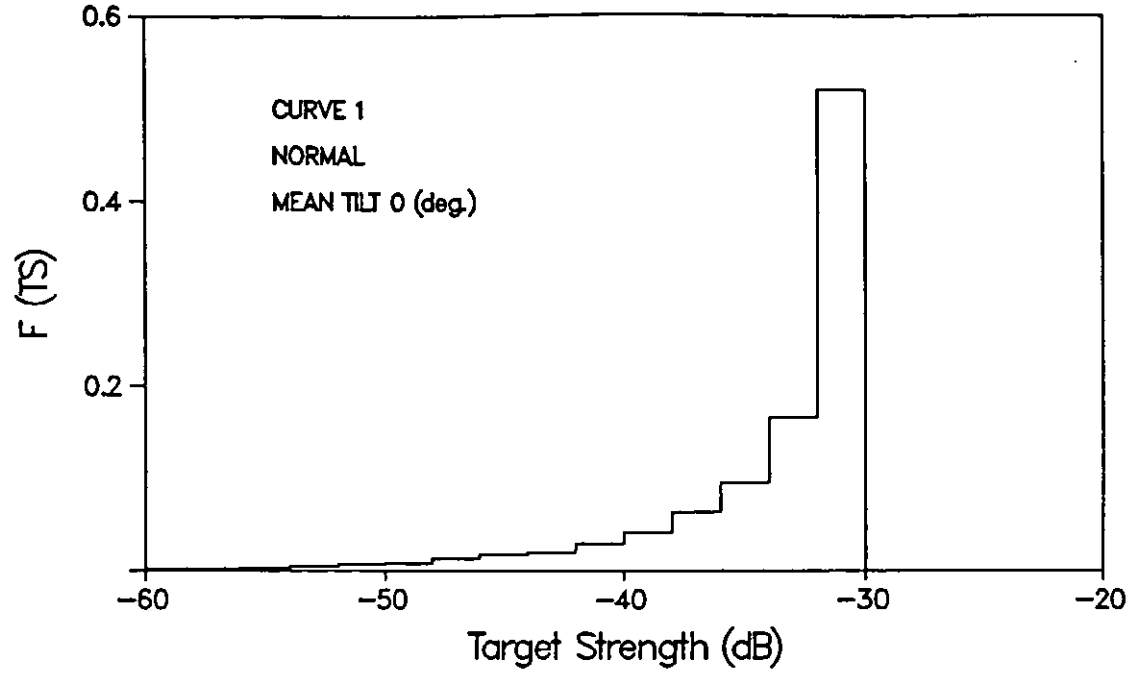

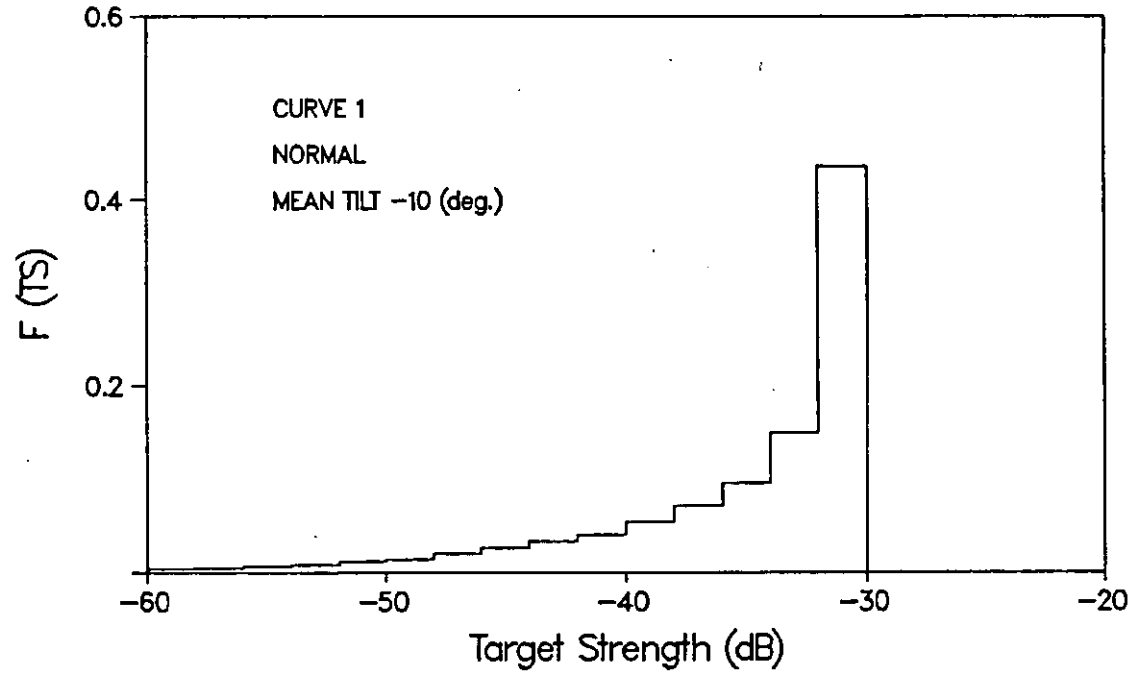

Fig.4.15 Probability distributions for the target strength of the fish obtained from the model with various assumptions.

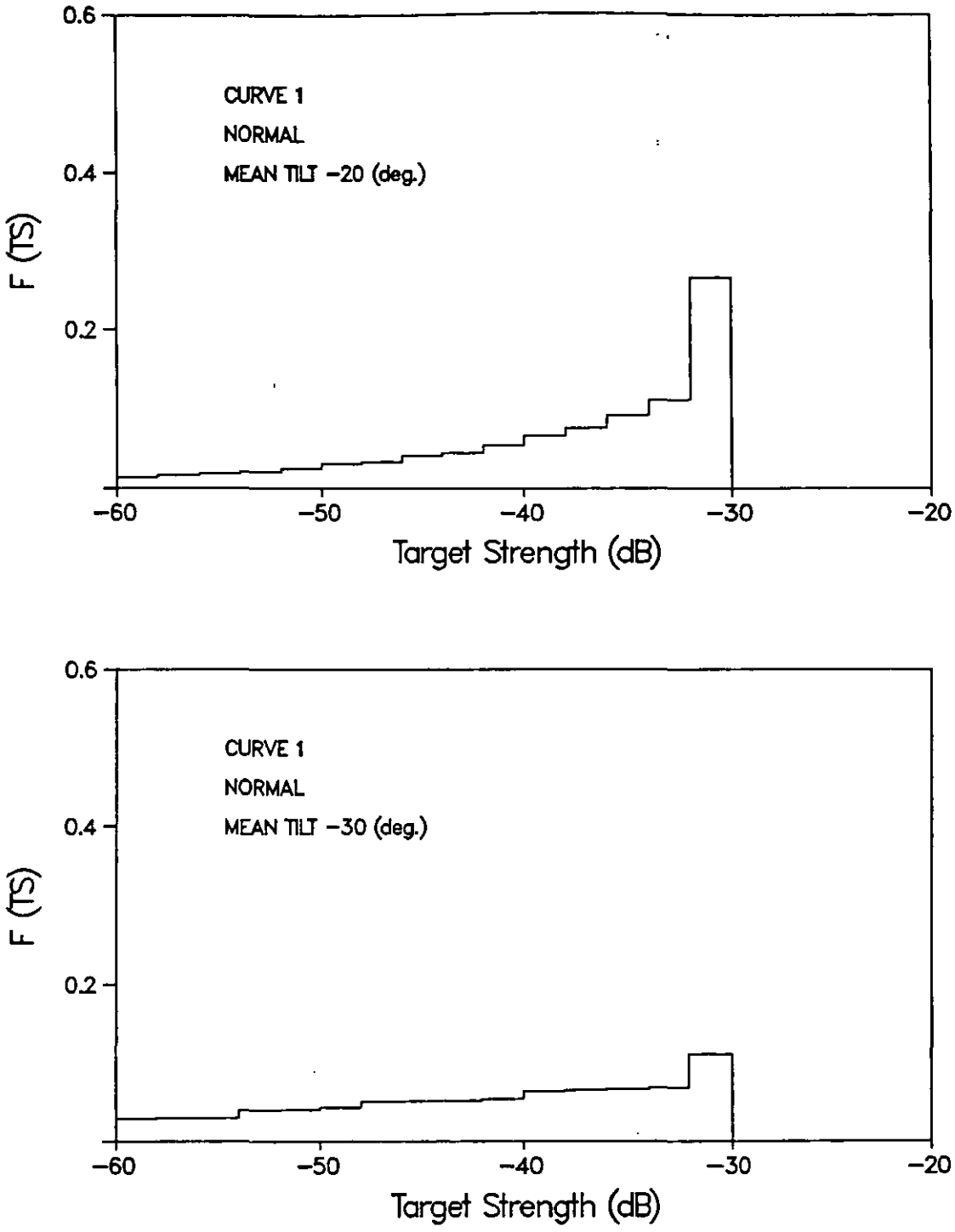

Fig.4.16 Probability distributions for the target strength of the fish obtained from the model with various assumptions.

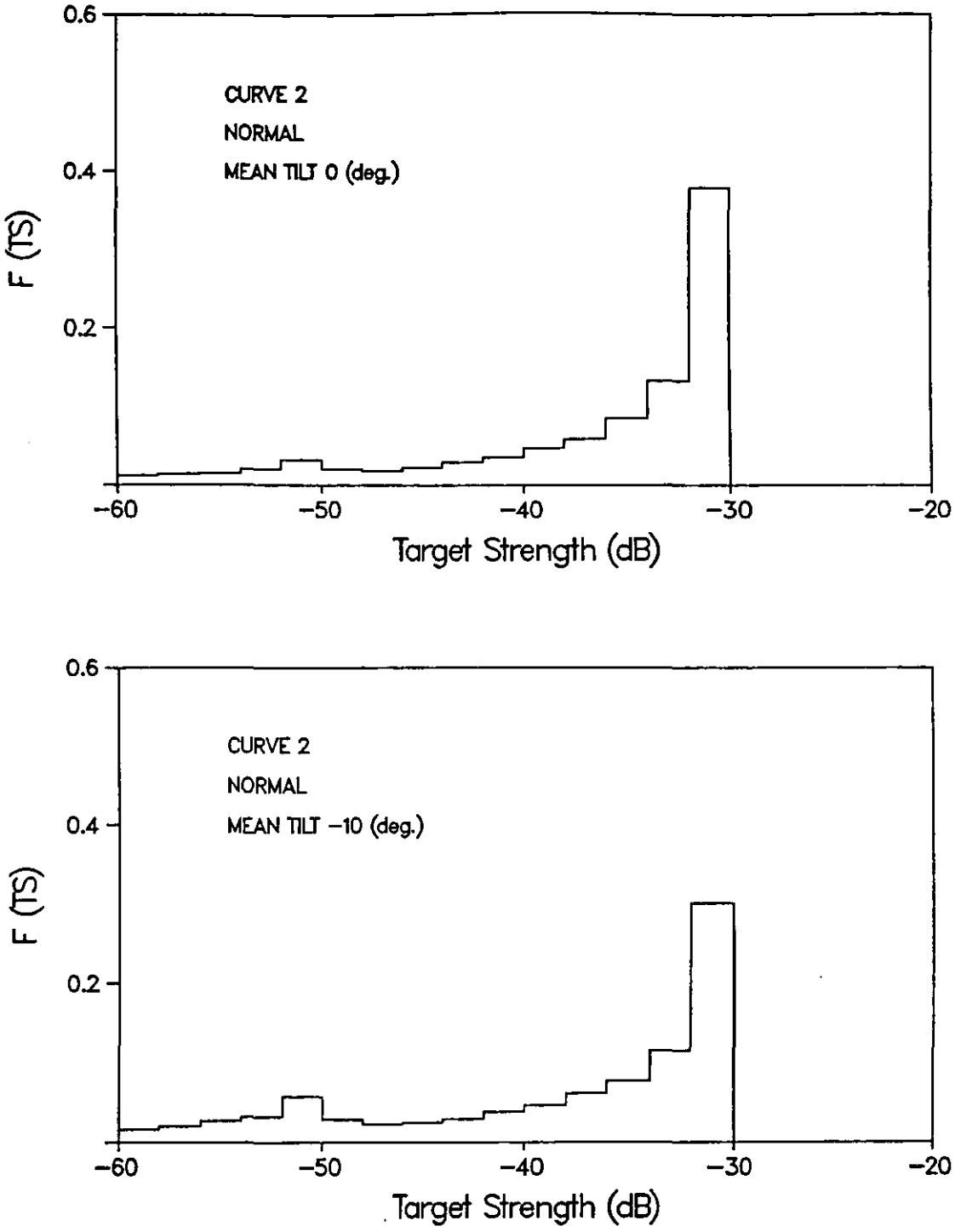

Fig.4.17 Probability distributions for the target strength of the fish obtained from the model with various assumptions.

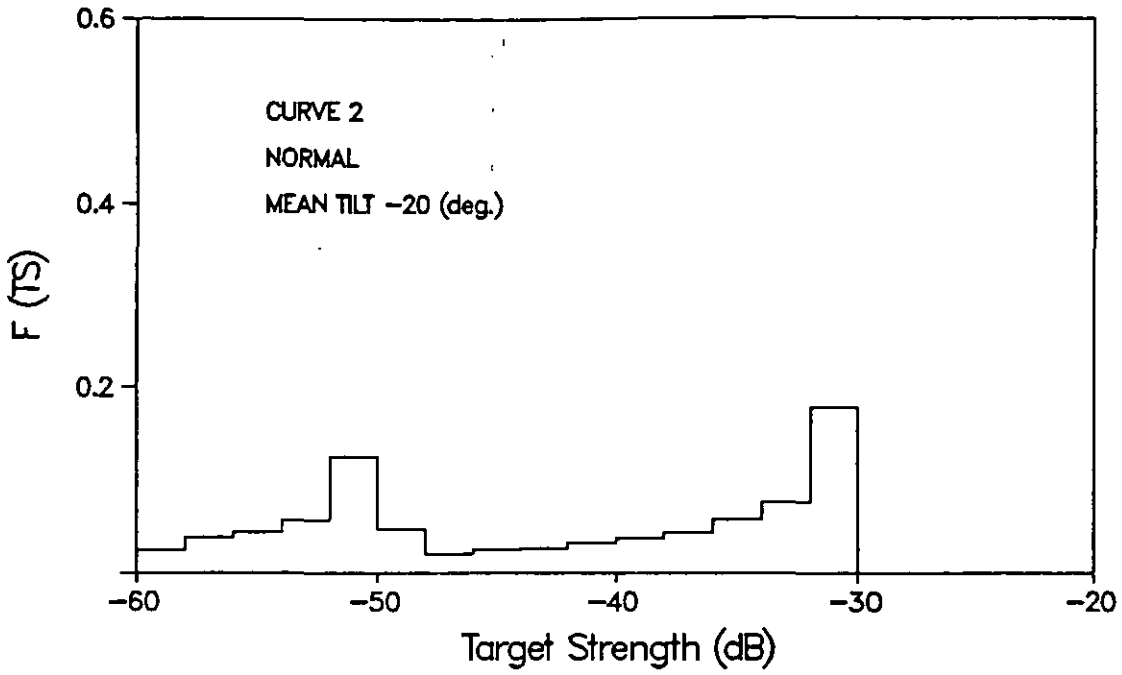

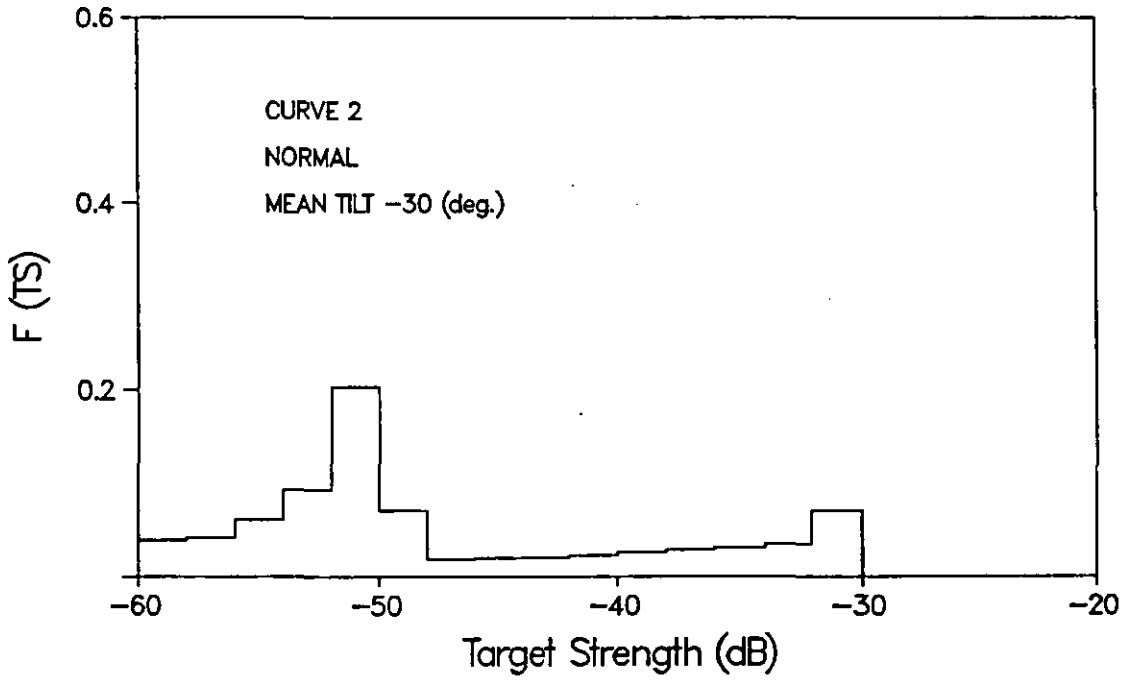

Fig.4.18 Probability distributions for the target strength of the fish obtained from the model with various assumptions.

4.5 DISTRIBUTION OF MEAN TILT ANGLE AT DIFFERENT DEPTHS

4.5.1 Introduction

Experiments have shown [10] that some fish species have avoidance reactions when exposed suddenly to low frequency noise stimuli. The hull and propeller of a vessel emits this sort of noise which can be detected by fish at distances of several hundred meters. The fish would avoid the noise source when the vessel approaches and passes over. The avoidance behaviour displayed by the fish may lead to considerable changes in both spatial and swimming orientation and this will affect the recorded target strength [5, 10]. It is obvious that the avoidance behaviour resulting in the fish being scared out of the region beneath the surveying vessel will affect any estimation of fish abundance.

4.5.2 Behaviour Model

In reference 11, it is shown that the mean tilt orientation of fish at different depths is related to noise pressure gradient at different depths and it was estimated as.

$$\beta_D = \beta_p + (\frac{\pi}{2} - \beta_p).(\frac{D_p - D}{D_p})^3 \qquad \text{..... (4 - 11)}$$

where β_p is set equal to the vertical angle of a line through points of maximum increase in pressure gradient at different depths. D_p the depth at which the stimulus originating from the vessel propeller becomes the dominating one compared to the hull stimulus (both as regards directional and gradient effect). D is the depth.

The noise pressure gradient was expressed as

$$\frac{dP_f}{dR} = dP = \frac{P_o}{R^2} .\sin\alpha.(V.\cos\alpha - V_F.\cos(\alpha - \theta)) \quad \text{..... (4 - 12)}$$

where P_o is the assumed pressure amplitude at the noise source, R the distance from the noise source center, V the vessel speed, V_F the swimming speed of fish, α vertical angle below the horizontal plane ahead of the vessel at which the fish is positioned, θ the tilt angle of the fish.

4.5.3 Consideration of Factors

The avoidance behaviour of fish is believed to be dependent on the magnitude of the noise source as well as on the speed of a vessel and on the distance of fish positioned from the noise source etc.. This can be seen from the equation (4 - 11) and (4 - 12). To estimate the mean tilt orientation of fish at different depths, the factors which affect the variation of such should be studied. The consideration of these factors is given below.

Two main noise sources were taken into account in the study of the avoidance behaviour of fish; the hull and the propeller of a vessel. The former produces a hydrodynamic pressure wave which may have, to some extent, some effect on the avoidance behaviour of a fish. The latter generates low frequency noise which is believed to be the dominating stimulus causing aviodance reaction in fish on the approach of the vessel. If the fish is positioned shallowly enough, the hydrodynamic pressure wave induced by the movement of the hull would become a strong stimulus and the region of influence may be considerably larger than the size of the vessel. In this case, the avoidance reaction in fish occurs and may results in the changes in both spatial and swimming orientation of the fish.

This will affect the magnitude of the integrated energy from the output of a sonar system and hence will bias the estimates of fish abundance.

It is observed by experiments that the shallower the fish is positioned, the greater is the integrated energy reduced. Since the pressure wave stimulus generated by the hull is proportional to the square of the speed and the size of the vessel, and the avoidance reaction is strongly depth dependent due to the stimulus gradient being inversely proportional to the cube of the depth, this suggests that the estimates of fish abundance could not be carried out in water of relatively shallow depth by using a larger vessel at quite a high speed.

In relatively deep water, the low frequency noise generated by the propeller of the vessel will become dominating. This would also cause the changes in both the distribution of the fish and its swimming orientation beneath the vessel. Although it seems unlikely that technical solutions can be found to accurately predict the distribution of fish and its target strength beneath the vessel, there is still a great need for more information about the fish behaviour to be incorporated into the estimation method of fish abundance.

4.6 DISTRIBUTION DENSITY OF FISH SCHOOL AND SIZE OF FISH

To make an estimate of fish abundance in a surveying area, it is necessary to take into account the spatial distribution of fish which has a significant effect on the accuracy of the estimation.

In reference 12, measurements were reported that fish school structure is not random and the neighbours in the school are most commonly in positions

alongside each other. Besides, fish do not approach closer than a certain distance from one another. In terms of bearing to neighbours, some species were studied by means of statistics. It is found that saithe and cod are most likely to have their nearest neighbours at around 90 deg. and herring most frequently have their nearest neighbours at 45 deg. or 135 deg.. These are the positions one would expected if herring schools were cubic lattices.

Spacing of fish, or neighbour distance of fish, is believed to be an important factor causing the occurrence of destructive and constructive interferences. To consider how often and to what extent these interferences may occur, it is necessary to know or to assume the nearest neighbour distance of fish.

The mean distance to nearest neighbours could be expressed in body lengths. Some data about this for some typical species were given in Fig.7 of reference 12. More details can be also found in that reference.

Information regarding species and size of fish can be obtained by simultaneous sampling so as to predict the target strength of the fish registered since the target strength is directly related to the size of fish.

5. COMPUTER MODELLING OF AN ECHO SOUNDER SYSTEM FOR FISH ABUNDANCE MEASUREMENT

5.1 INTRODUCTION

In Chapter 2, two common methods of processing acoustic measurements of fish - echo counting and echo integration were introduced in detail. The computer model developed for the echo-sounder system was extended in reference [21] to allow a model for fish abundance measurement, but this leaves a lot to be desired. Especially the generation of target strength should be reconsidered. The effect of the tilt angle of a fish on the target strength, and the distribution of the target strength were discussed in the preceding chapter. It was found that the probability density distribution of the target strength was not symmetrical and does not obey a Gaussian distribution as the earlier computer modelling work assumed. Therefore, this required a modification in the method of generating the target strength in the simulation. The results obtained from the modified computer model are discussed in Chapter 6.

5.2 BASIC MODEL

By considering the signal energy from fish, and with the knowledge of sonar parameters, the estimates of fish abundance could be made. The method employed in fish abundance estimation for the echo-sounder modelled in Chapter 3 was based on the energy measurement of the echoes from many fish or from a shoal. All detectable echo-returns are received by the receiving transducer and then added as the sums of squares, or incoherently, over the entire period for which the pulse is transmitted. Assuming that the mean square value of the signal

energy from a single fish is expected to be known, on dividing the total energy from the many fish by the average signal energy of the single fish, an estimation of the number of the fish insonified in the beam can be computed.

There has been some experimental evidence that the target strength of fish depends strongly on their orientation. But when an echo-sounder system is applied, in other words, when the fish is viewed in the dorsal aspect, it has been shown that the significant orientation is the tilt angle [20,33]. It has also been shown in references [4,19] that the variation of the tilt angle is random. Therefore, the calculation of the average signal energy of a single fish is hard to give in exact terms. Assuming that the probability density distribution of the tilt angle and the mean length of the fish of one species are known, the average signal energy as expected from the single fish could be estimated within a given range of the fish tilt angle (pitch and roll are ignored).

It should be noted that in this model the sonar system parameters are assumed to be known and the signal energy can be measured accurately under the ideal conditions in that no allowance was made for any propagation losses other than spreading and absorption. The propagation losses are those from the source to the fish and from the fish to the receiver, which can be compensated by the TVG amplifier in the system.

5.3 TARGET GENERATION

There are two principal sources of variability. First, the amplitudes of the detectable echo-returns depend on the positions of the fish in the sonar beam. For simplicity, the space of interest is imagined to be divided by a set of spherical

shells centered on the location of the sonar system and spaced by a range increment of ΔR. The targets are assumed to be distributed on a random basis within the any range shell ΔR. Their positions, in range as well as angularly, in the space could be generated from some probability density functions.

Second, the target strength of fish varies considerably because the fish is a complicated scattering object. As discussed in Chapter 4 the target strength will not, in general, be constant from pulse to pulse and from member to member. In the earlier modelling work refered to, it was assumed that the target strength of the fish varied according to an arbitrary probability distribution and for simplicity the Gaussian distribution was chosen. But it was found in the present work that the distribution of the target strength was not symmetrical. This led to the use of a different model for generating the random target strength.

5.3.1 Target Positions in Range

In the earlier modelling work, a Poisson model was used in generating target positions in range. But it was found in reference [22] that this model would cause anomalous results for closely spaced targets because the occurrence of constructive or destructive interference would be very dependent on the average value of the distribution used. But the case did not appear in the other model - probability density function of the uniform model [22]. It was indicated that the occurrence of the constructive or destructive interference in the uniform model was quite independent of the average value of the distribution, and their deterioration effects on the fish abundance estimates tend to balance each other when averaged over a number of trials. Therefore, the uniform model was adopted in this work to generate the target positions in range.

The random numbers representing the range values of targets were generated from the uniform distribution generator between R_{min} and R_{max}, where R_{min} is the starting position in range for the measurement and R_{max} the largest range available. These random numbers are therefore uniformly distributed within the limited range, assuming that N random samples were drawn and ordered ascending from the starting range R_{min} to the maximum range R_{max}. It should be noted that the generated random numbers must be larger than the starting range R_{min}, and one pulse length less than the maximum range R_{max} to ensure that the integral region is not beyond the maximum range R_{max}. The average spacing is determined by the following equation, namely,

$$\text{average spacing} = \frac{R_{max} - \text{Pulse length}}{\text{No.of points} + 1}$$

5.3.2 Target Positions in the θ and ϕ Domain

The target positions in the space concerned are, in general, determined by three parameters which are: the range Ri from the transducer/receiver to the target, the angular positions θ_i and ϕ_i relative to the beam axis Z as shown in Fig.3.1. It is reasonable to assume that the targets were uniformly distributed over the θ and ϕ domain. The θ_i and ϕ_i could be selected at random from a random number generator with probability density function given by a uniform distribution. The random numbers selected should be uniformly distributed in the given limit $\pm \theta_T$ and $\pm \phi_T$ respectively. $\pm\theta_T$ and $\pm \phi_T$ are the thresholds in the angular domains and can be calculated as appropriate according to the requirement of the beamwidth at the -3dB point and the dynamic range of operation of the beam pattern. The setting of the thresholds are to ensure that the received signals are from the targets rather than from noise. It should be noted

that the determination of the thresholds might affect, to some extent, the fish abundance measurement. Especially, if the beam pattern concerned was of relatively narrow beamwidth, it is not necessary to extend the thresholds much beyond the beamwidth. This has already been proved in reference [21].

Alternatively, since the position of any point in the space concerned can be defined by the three-dimension coordinates (X,Y,Z), the target position (R_i, θ_i, ϕ_i) in any shell of the space can be obtained by the same way. The random positions of the targets in the space are selected from three random number generators whose probability density functions are given by uniform distributions. This performance can be made in BBC computer. The parameters R_i, θ_i and ϕ_i can be directly calculated by using the following equations:

$$R_i = \sqrt{X_i^2 + Y_i^2 + Z_i^2}$$

$$\phi_i = tg^{-1}(Y_i/Z_i) \qquad \text{and} \qquad \theta_i = tg^{-1}(X_i/Z_i)$$

Since the area insonified by the effective acoustic beam is limited and assumed to be in a conical form with an apex angle of θ_i and ϕ_i in both the θ_T and ϕ_T domaims, the targets outside the effective beam could not be insonified. If the effective beam can move in a direction, for example, in the Y direction, and if the X_i of ith target located at X_i, Y_i, Z_i coordinates meets the following equality:

$$X_i < Z_i \, tg \, (\phi_T/2)$$

then the target will be insonified. This seems to be the case in the movement of a vessel across a shoal. In other words, the vessel is moving across the shoal as if the generated shoal is made to move across the beam. It is in fact the relative movement between the vessel and the fish shoal because both the vessel and the shoal are moving relative to each other. For convenience, the generated fish positions are assumed to be stationary while the vessel with the sonar equipment moves across the fish shoal. This method of generating target positions was used to simulate some dynamic situations.

The simple dynamic model has already been established in reference [22] for fish abundance measurement, while the present work is concentrated on the effect of the orientation of fish on the estimation of fish abundance. Therefore, some assumptions about the use of the dynamic model and some initial findings can be found in reference [22].

5.3.3 Generation of Target Strength

Target strength is not in general constant from pulse to pulse because of the variability of the many factors which contribute to its magnitude. One of the major factors will be due to the movement of the fish itself. Many published papers have shown that the target strength of a fish depends strongly on the orientation of the fish as well as on its size and on the frequency of the acoustical signal [3,33]. Therefore, to generate the target strength which is mainly dependent on the tilt angle, it is necessary to know or to assume the probability distribution that represents the way in which the tilt angle will vary in practice. In references 4 and 19 measurements are reported on different species and it is shown that this distribution is close to normal. Thus, normal distribution has been

chosen and used to describe a suitable tilt angle distribution with a mean tilt angle of θ_m and standard deviation of S_q. For simplicity, a uniform distribution for the variation of the tilt angle has also been used in the model.

As discussed in chapter 4, the tilt angle of fish might vary with depth due to the avoidant behaviour of the fish in relation to a surveying vessel and it seems to be the fact that the mean tilt angle may decrease with depth. This suggests that the mean tilt angle at different depths may be determined by the model in reference [11]. The tilt angle distribution at a given depth would be then normal.

The effect of the length of the fish on the target strength is another important factor which should be taken into account in fish abundance measurement. Many measurements are reported on different species and it is shown that the length distribution of the fish is random. But in most cases, the length distribution of the fish is asumed to be normal [16].

In chapter 4, the two functions shown in Fig.4.7 for the variation of target strength with tilt angle and size have been assumed and used to generate the target strength. It is clear by comparison with Fig.4.8 to Fig.4.10 taken from reference [3] that the curves derived from these functions are not unlike the measured curves.

From the information above, Ai can be calculated and it is obvious that the target strength is always a random value. It should be noted that the choice of the functions shown in Fig.4.7 is because they are easy to use in computer modelling and are quite close to the measured curves. Of course, more complicated models established by other authors could be incorporated if necessary.

It must be emphasized that the signal magnitudes received by the transducer for reception are, in theory, dependent on propagation losses and the target strength of fish (assuming that the noise is small enough and can be ignored). In practice, the propagation losses could be compensated by connecting a Time-Varied Gain amplifier (TVG) to the receiver. In this case, Ai only represents the target strength of the fish.

5.4 AVERAGE SIGNAL ENERGY FOR A SINGLE TARGET

It can be seen from equation (3-3) that the magnitude of the signal received from a single target depends strongly on the target strength of the fish, the beam directivity both on transmission and reception, and the transmitted pulse envelope. It must be indicated that the magnitude also depends on a number of factors such as propagation losses and sensitivity of the receiver etc.. Ideally, these factors could be compensated for and calibrated using certain circuits or equipment. If the received signal is perfectly envelope detected, the average signal energy for the single target is given by

$$\overline{V^2} = \overline{A^2 \beta^2(\theta, \phi) X^2(R)} \qquad \text{..... (5-1)}$$

where the bar signifies average value.

It is believed [34] that the positions of the fish in the sonar beam and the target strength of the fish are independent. Therefore, it is reasonable to assume that each term on the right hand side of the equation is independent of each other. Hence

$$\overline{V^2} = \overline{A^2}.\ \overline{\beta^2(\theta, \phi)}.\overline{X^2(R)} \qquad \text{..... (5-2)}$$

The problem in hand is now simplified and all that is now required is to obtain the individual averages of the terms on the right hand side of equation (5-2).

It has been discussed that the target strength of a fish will not in general be constant from pulse to pulse due to the movement of the fish itself. The movement is usually defined by the tilt angle of the fish. Therefore, to evaluate the average target strength of a fish it is necessary to know or to assume the probability distribution of the tilt angle. The average value could be evaluated using the same method as described in chapter 4. It is rewritten as follows:

$$\overline{A^2} = \int T^2(\theta)p(\theta)d\theta \qquad \text{..... (5-3)}$$

where $p(\theta)$ is the PDF of the tilt angle θ.

As discussed in chapter 4, the mean square value of the target strength depends on a number of factors which include the range of the tilt angle, the mean tilt angle, the standard deviation of the tilt angle, the frequency of the acoustic signal, and the size of the fish. The last two terms directly affect the shape and magnitude of the function for the variation of the target strength, $T(\theta)$.

If the factors mentioned above were known, the average target strength could be evaluated straight away. Four different sets of parameters (θ_r, S_q, θ_m, f) have been used in calculating the average target strength. In each set of parameters, only one was varied during the calculation while the others were kept constant.

The other terms, $\overline{\beta^2}$, and $\overline{X^2(R)}$, could be evaluated as in references [21] and [22]. The results taken from these references are shown as below:

$$\overline{\beta^2(\theta,\phi)} = \frac{\pi}{8c^2\,\theta_T\,\phi_T}\ \mathrm{erf}(2c\,\theta_T)\,\mathrm{erf}(2c\,\phi_T) \qquad \ldots\ldots (5\text{-}4)$$

$$\overline{X^2(R)} = \frac{3}{8} \qquad \ldots\ldots (5\text{-}5)$$

It should be noted in this expression that the beamwidth in both angular domains were taken to be equivalent. If the dynamic range of operation is considered, the expression above becomes

$$\overline{\beta^2(\theta,\phi)} = \frac{1}{2c\alpha_T^2}\ (1 - \exp(-2c\alpha_T^2)) \qquad \ldots\ldots (5\text{-}6)$$

where α_T is the radius on the cross section of the beam pattern, or angular threshold.

Using the information above, the average energy as expected from a single target by considering only the pulse envelope can be obtained. It must be emphasized that since the average target strength varies with the mean tilt angle, the range of the tilt angle, the standard deviation of the tilt angle distribution and the size of fish, the average energy of the single target will be affected by these factors.

5.5 COMPUTER SIMULATION OF ABUNDANCE ESTIMATES

The simulation is divided into two sections. One is static, the other dynamic. 'Static' means that the positions of targets in range were generated from a random number generator with the probability distribution of a uniform model on the acoustic axis. If a group of targets were generated in the X, Y and Z co-ordinates with the same random number generator, the situation is regarded as 'dynamic'. Since some assumptions about applying the dynamic model were given in reference [22], it is not necessary to repeat these again.

Initially, a group of targets were generated with the uniform model either on the acoustic axis or on the three dimensions in the X, Y and Z co-ordinates. Target positions in the θ and ϕ domain were also obtained. The target positions in range were ordered by their co-ordinates. The mean tilt angle with depth were obtained and hence the tilt angles could be generated from the probability density distribution of the tilt angle with the mean at a given depth and a standard deviation. The effect of the directivity of the transmission and reception beam pattern on the magnitude of impulses to be received could be calculated according to the positions of the targets in the sonar beam.

From this information, the ordered targets could be treated as impulses with random strength and were fed to the linear system with an impulse response of h(R) as in Fig.3.2. The processed output samples were linearly added before envelope detection. The output samples were then detected by a "perfect" filter as in reference [22] and the magnitudes were squared to obtain the signal energy. After that, the squared samples were added to produce an accummulated total energy. On dividing the total energy by the average signal energy for a single

target, an estimate of the number of targets insonified was obtained. A block diagram illustrating the above procedures is shown in Fig.5.1.

The simulation was designed to carry out the above calculations and to examine the effect of some important factors, such as the orientation of fish on the estimates. The estimated number of targets obtained from the simulation was compared with the known value which had been generated. The above procedures were repeated a number of times with a random number of targets generated each time. The complete set of results was plotted by the computer in the form of a graph with number of targets estimated against number of targets generated. The results from the estimation were carefully checked by means of regression analysis. The graphs representing these results and the discussions about them are given in the following chapter.

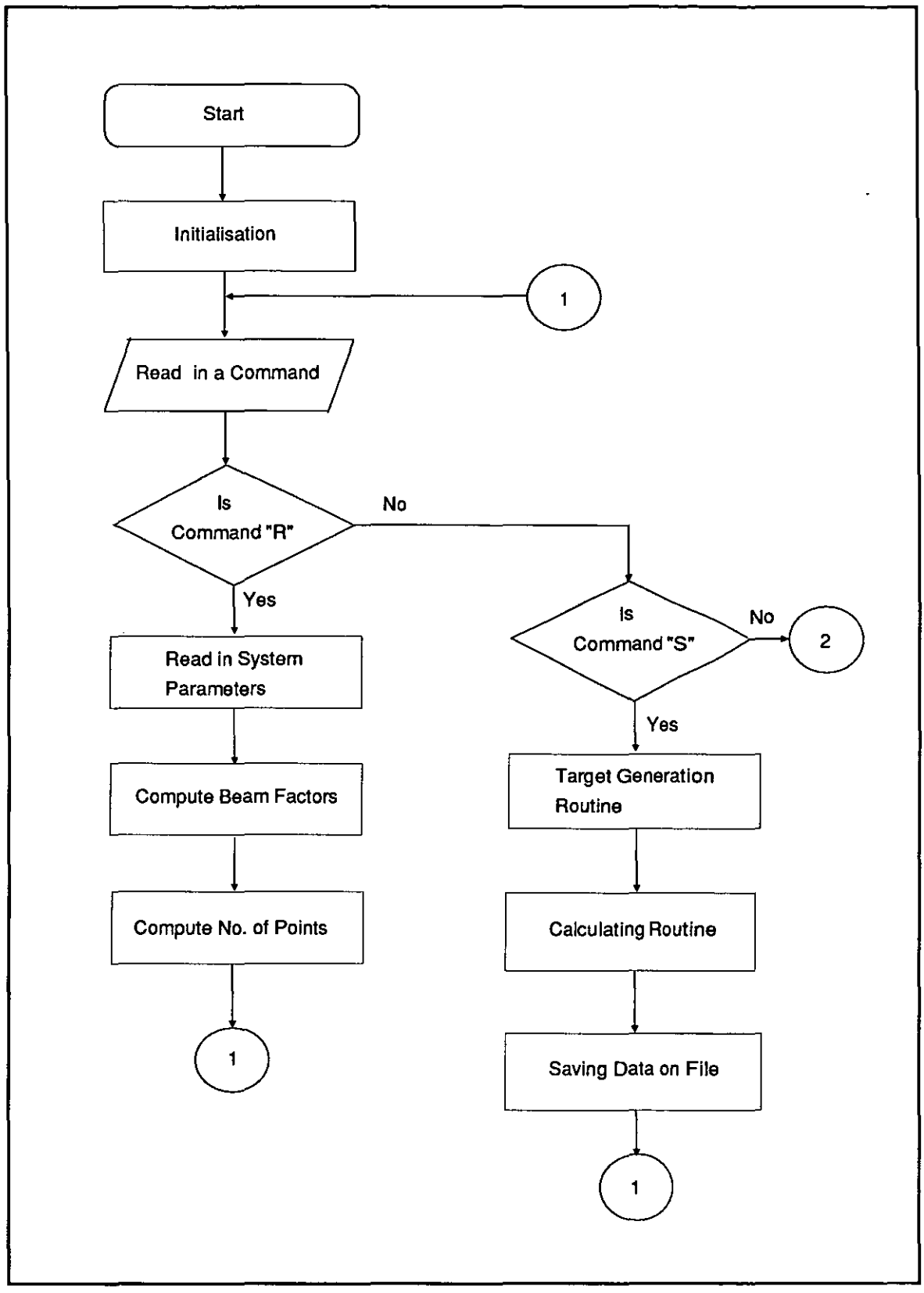

Fig.5.1 Flowchart for Computer Simulation in Fish Abundance measurement

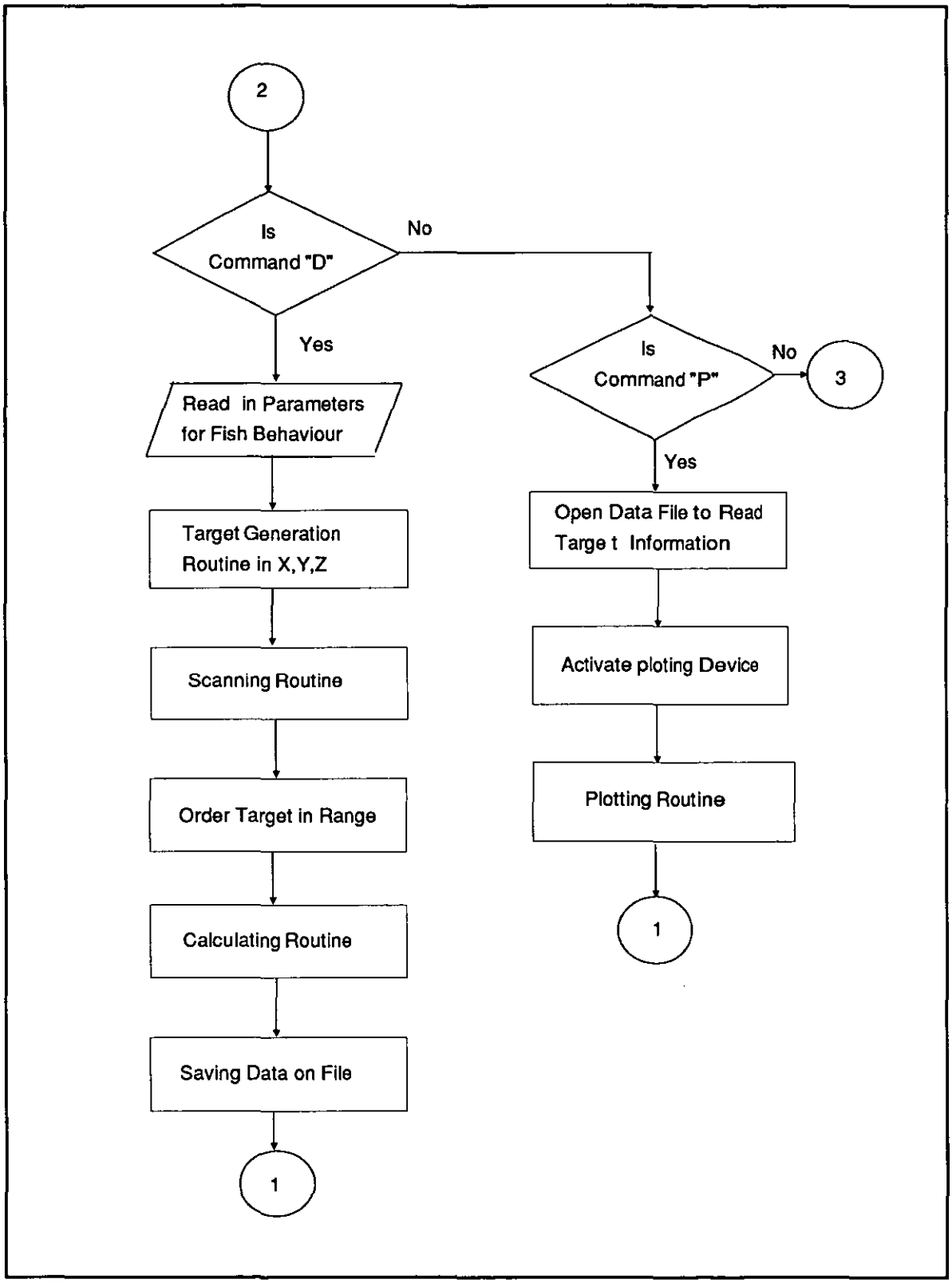
2
Is
Command "D"
No
Yes
Is
Command "P"
No
3
Yes
Read in Parameters
for Fish Behaviour
Target Generation
Routine in X,Y,Z
Scanning Routine
Order Target in Range
Calculating Routine
Saving Data on File
1
Open Data File to Read
Targe t Information
Activate ploting Device
Plotting Routine
1

Continune

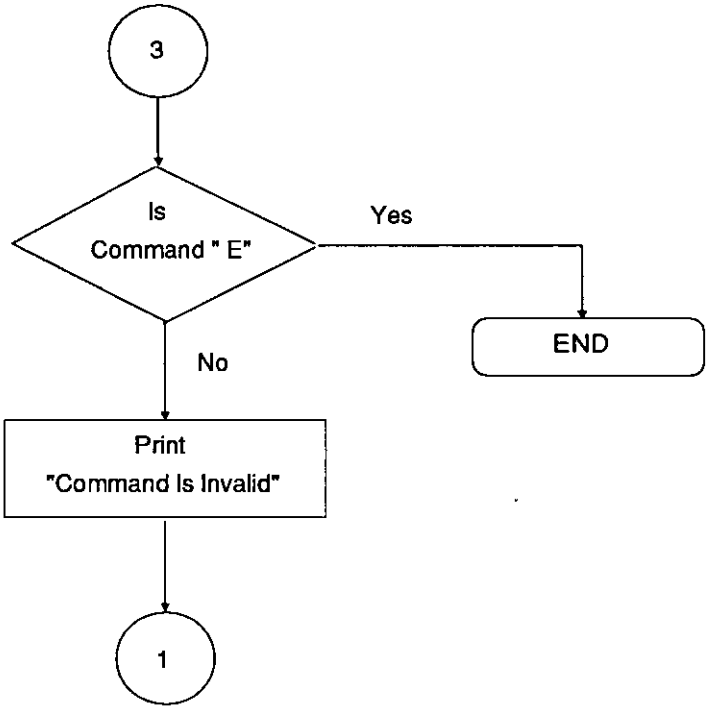

Continue

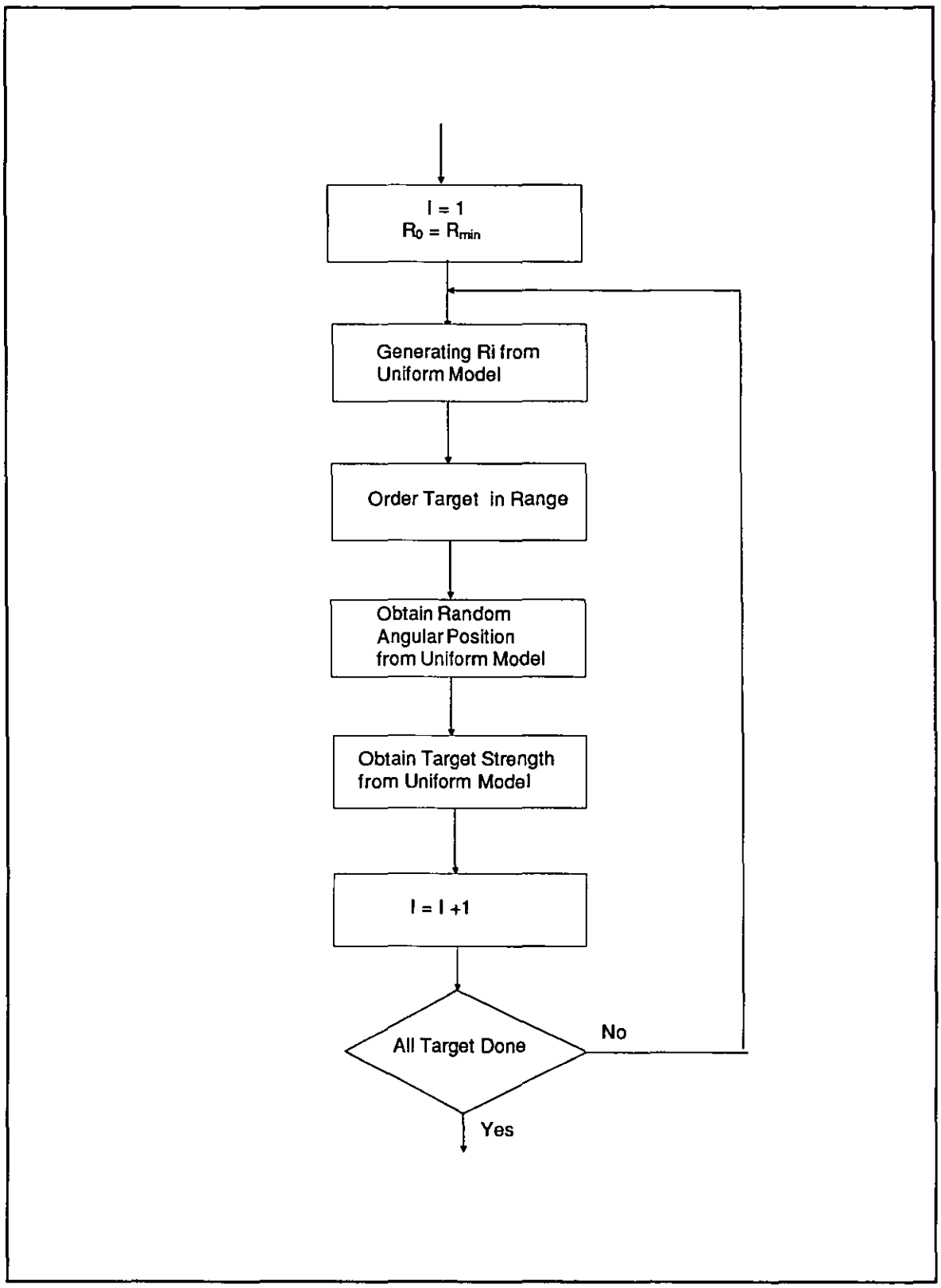

Target Generation Routine

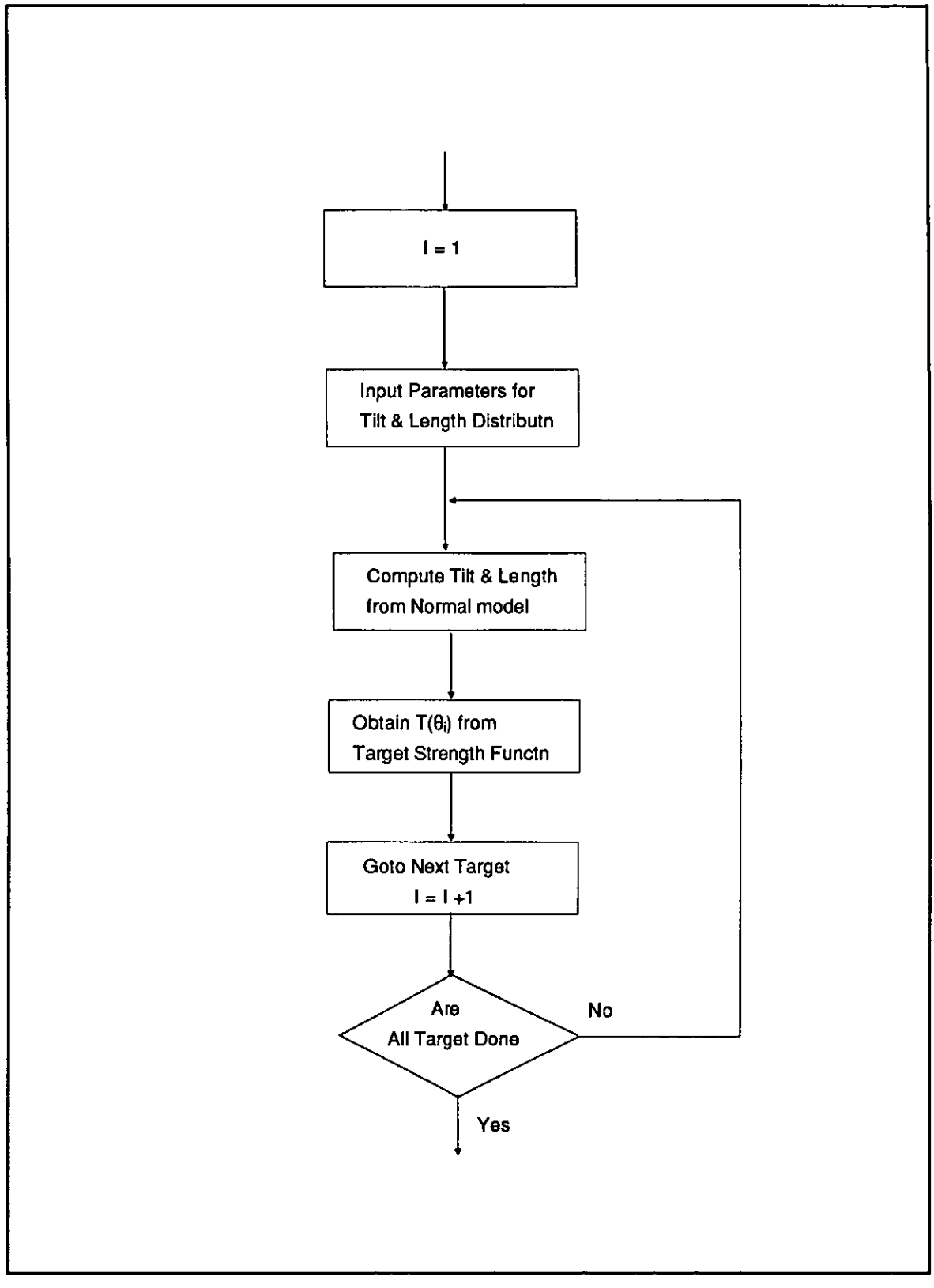

Scatterer's Target Strength Routine

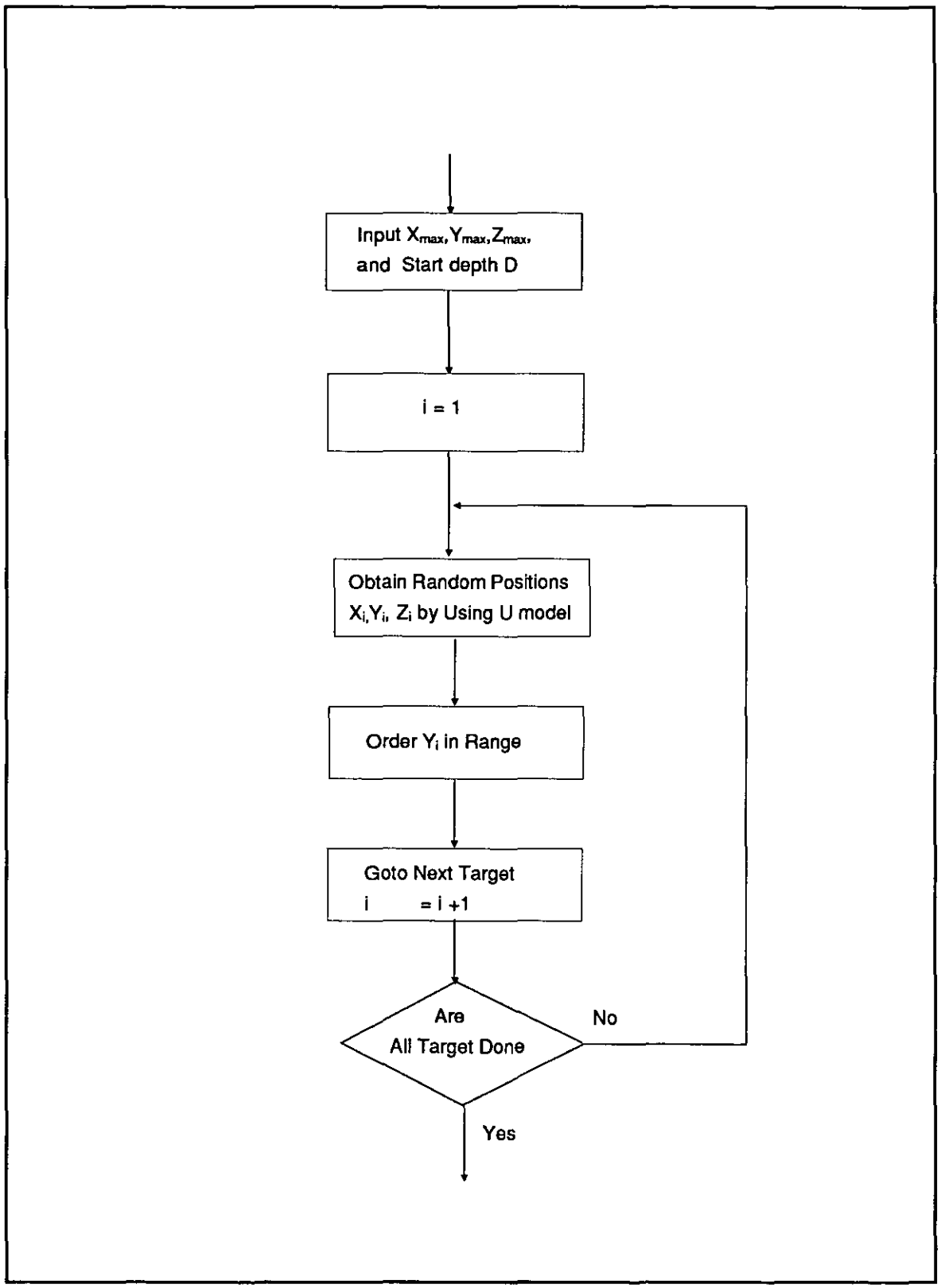

Target Positions Routine in X, Y, Z Co-ordinates

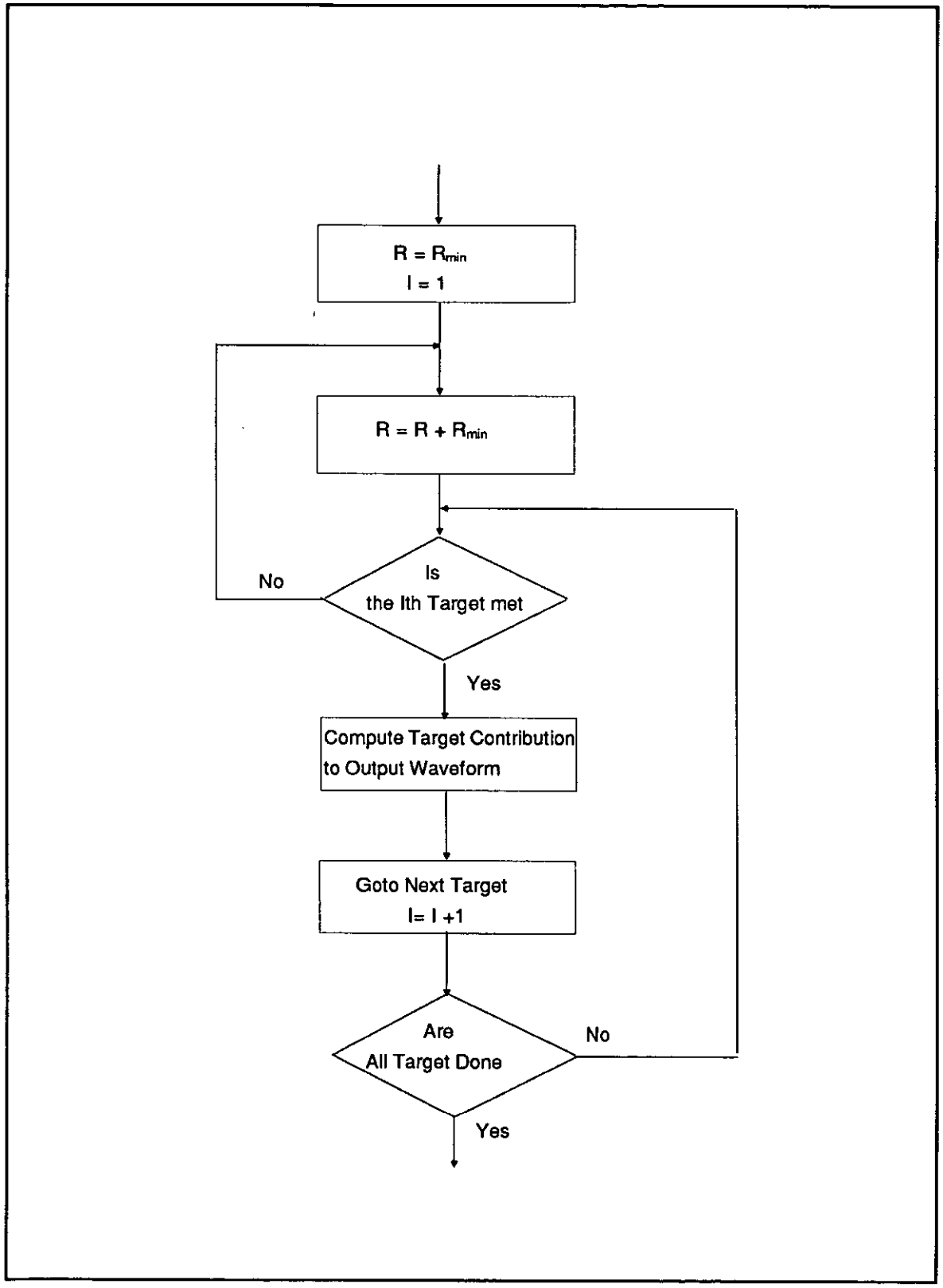

Computing Routine

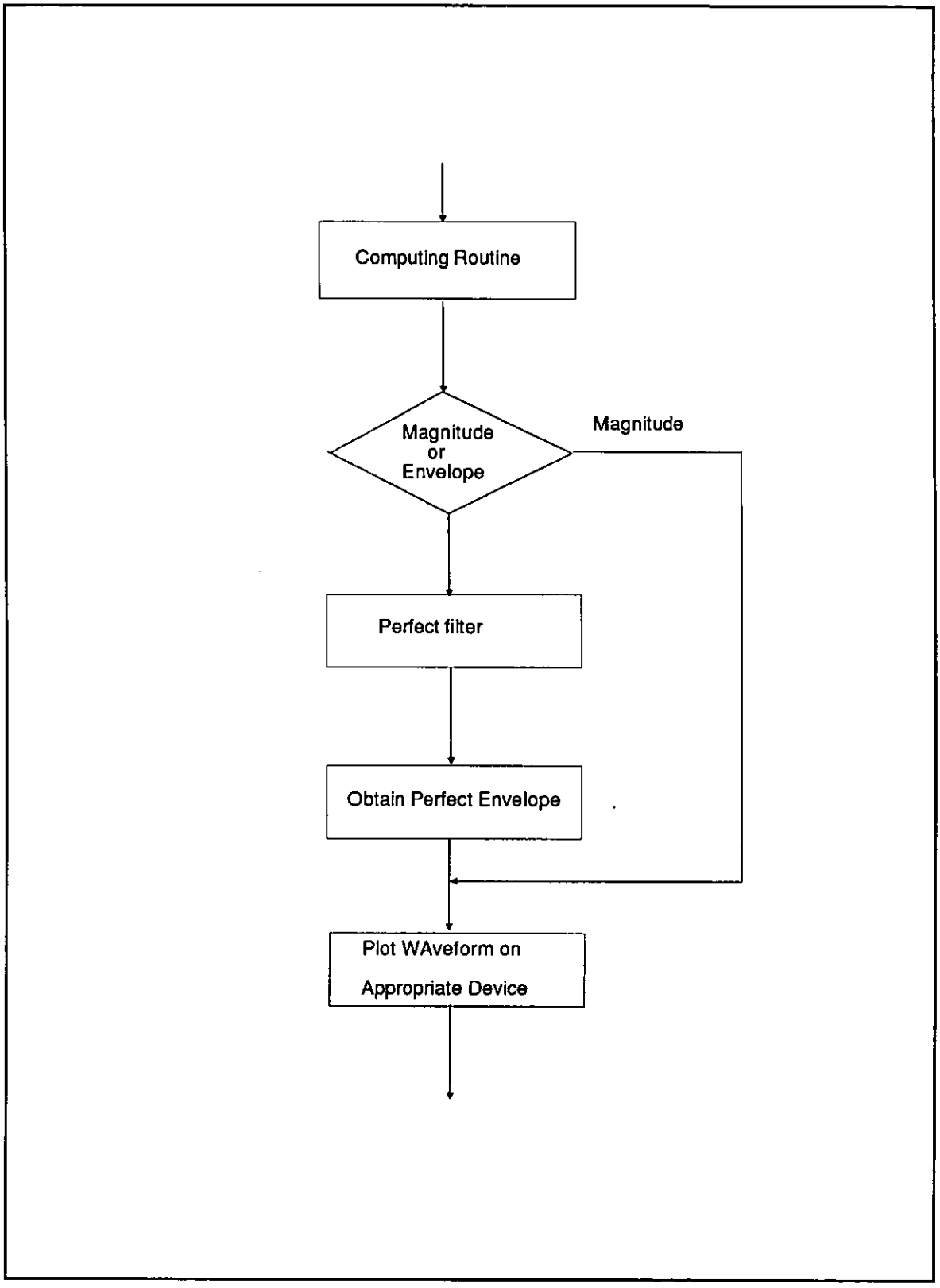

Plotting Routine

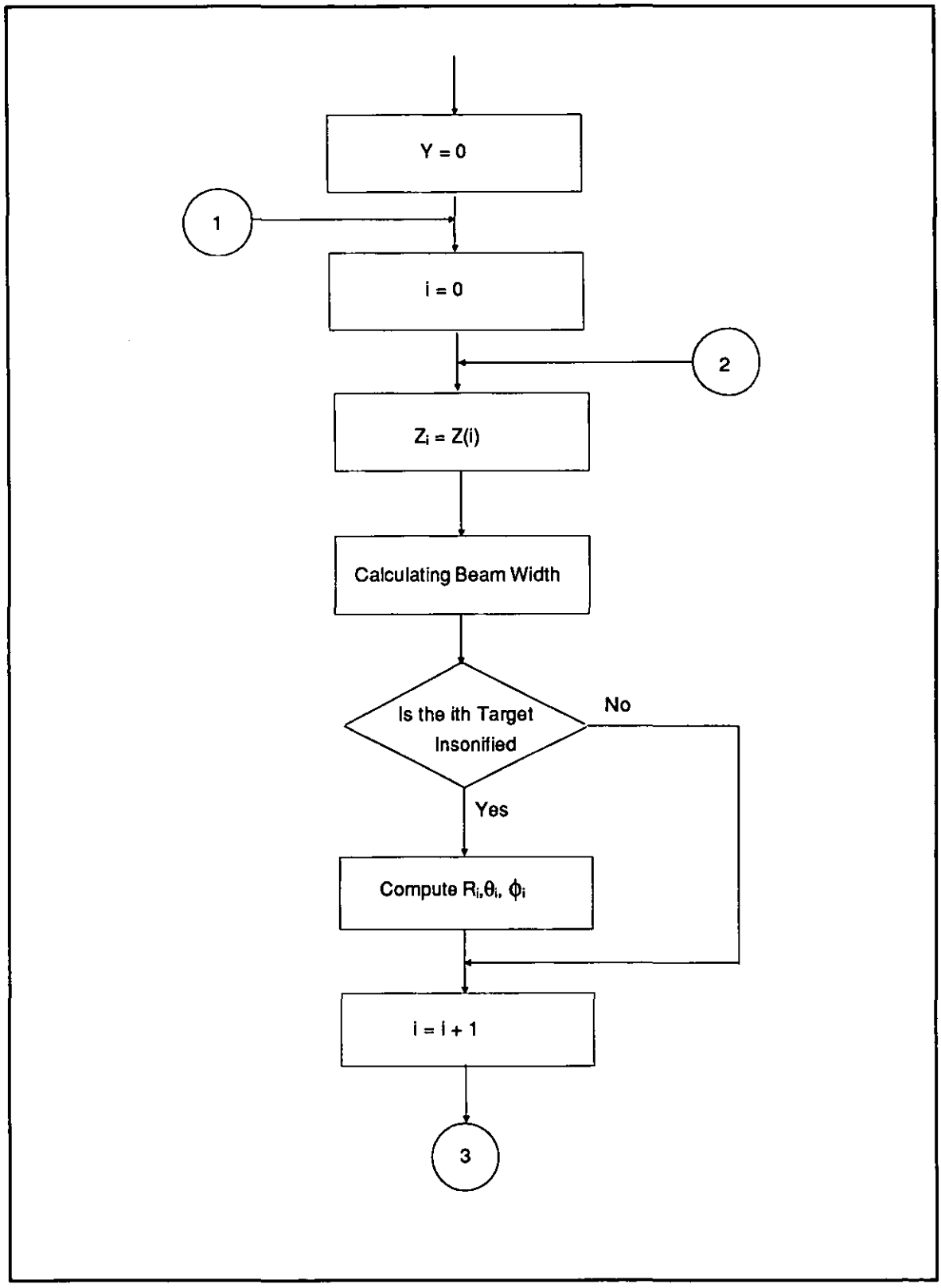

Scanning Routine

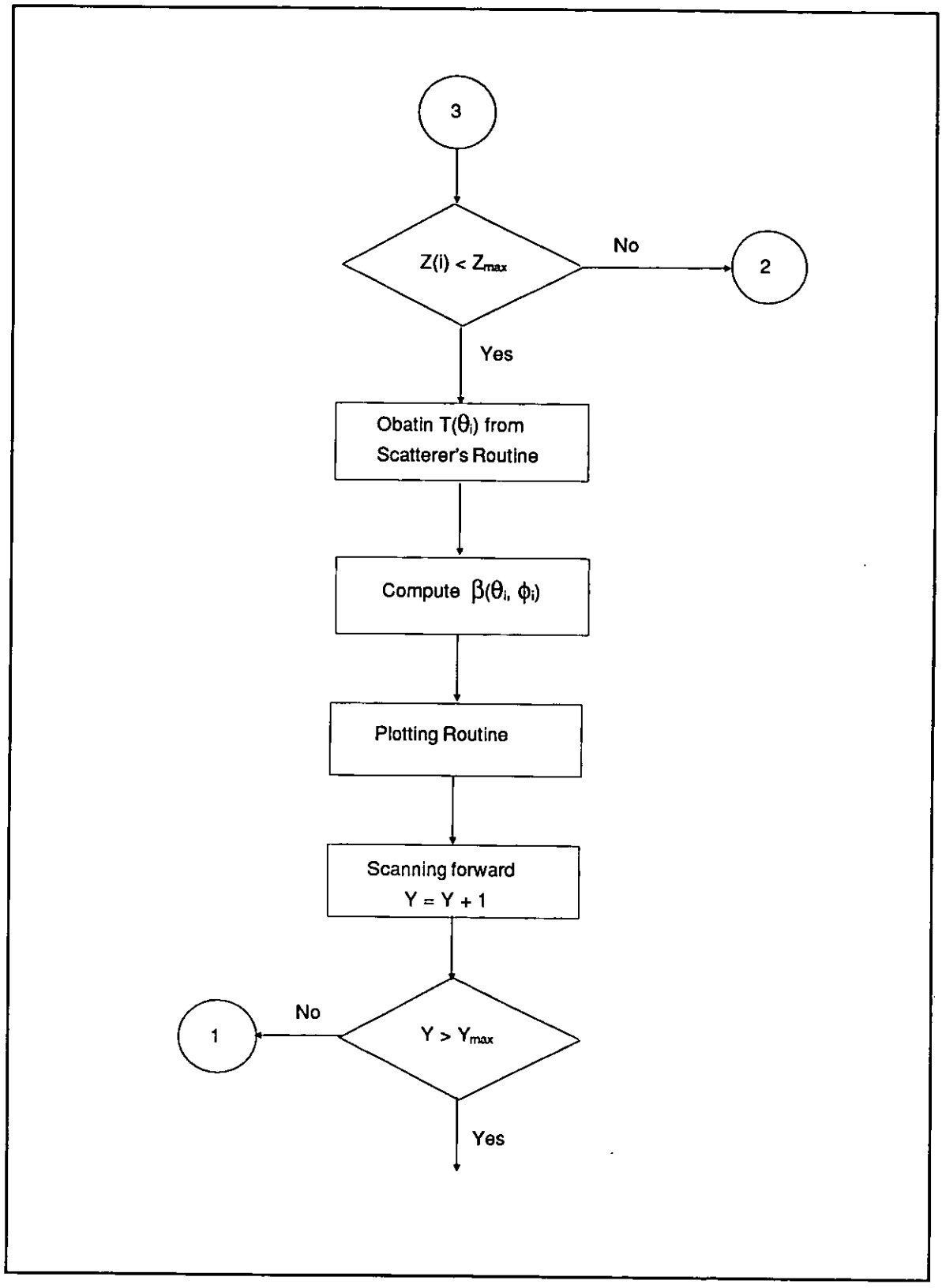
3
Z(i) < Zmax
No
2
Yes
Obatin T(θi) from
Scatterer's Routine
Compute β(θi, φi)
Plotting Routine
Scanning forward
Y = Y + 1
No
1
Y > Ymax
Yes

Continue

6. DISCUSSION OF RESULTS OBTAINED FROM COMPUTER SIMULATION IN FISH ABUNDANCE MEASUREMENT

Based on the sonar modelling discussed in chapter 5, computer simulation of an echo-sounder system on fish abundance measurement was carried out, in which some factors of fish behaviour, such as the variation of fish tilt angle, were taken into account. The results obtained from the computer simulation were presented in the form of regression graphs.

6.1 THE EFFECT OF THE AVERAGE TARGET SPACING AND THE PULSE LENGTH ON THE ESTIMATION

As the previous work in reference [21], different average target spacings in range were arbitrarily chosen and used in the simulation. For each value of the average target spacing, several sets of results were obtained, where each set of results was conducted with a particular pulse length which was normalised in range unit. The choice of the pulse length was also arbitrary, but was, to some extent, subject to the average target spacing. It could be observed from Fig.6.1 to Fig.6.4 that if targets were distributed in range with any average target spacing larger than the adopted pulse length, the number of estimated targets was close to that of generated targets. For a particular value of pulse length, this kind of estimation became worse with the decrease of average target spacing. The results of the initial simulation on fish abundance measurement were in accordance with those in reference [21].

6.2 THE EFFECT OF THE PDF OF TILT ANGLE ON THE ESTIMATION

The probability density function of tilt angle was assumed to be either normal or uniform in the computer simulation of chapter 5. Some parameters on the PDF of tilt angle which were discussed in chapter 4 were applied in the simulation. For convenience, pulse length in normalised range unit was chosen to be 10 and average spacing of targets 15. This choice ensures statistically neither constructive nor destructive interference takes place and hence the energy measurement taken would be desirable [22].

For each model of the PDF of tilt angle, several sets of results were obtained where each set of results was conducted with some parameters of the PDF. Regression analysis was used through the simulation in order to observe the accuracy of the estimation and the effect of the PDF of tilt angle on the estimation. The regression coefficient and the regression constant of the best-fit straight line through the scattered points for each set of the results were computed. The variance and the correlation coefficient of the scattered points on the graph about the best-fit straight line were also calculated.

For the study of the effect of the PDF of tilt angle on the estimation, each of the parameters of the PDF was investigated. It could be observed from Figs.6.1 to 6.6 that the regression coefficients and the variance were considerably affected by these parameters. When the range of the tilt angle or the standard deviation of the tilt angle increased, the regression coefficients deviated from unity. For bigger mean tilt angle the correlation coefficients became small. The effect of uniform and normal models of the PDF of tilt angle on the simulation was similar under

certain conditions. Discussion and explanation of these results are given as follows.

6.2.1 The Effect of the Normal Model on the Estimation

When the range of the tilt angle or the standard deviation of the tilt angle increased, the regression coefficients deviated from unity. This can be seen from Figs.6.1 to 6.2. Since the target strength function is basically symmetrical about a certain tilt angle and the normal distribution is symmetrical about its mean tilt angle, the variation of the mean tilt angle results in the variation of the central position of the distribution, and hence, the average target strength derived from the equation (4-7) varied. For individual targets, the target strength generated from the target strength function varied with the mean tilt angle to the given tilt angle distribution. The bigger the standard deviation or the absolute value of the mean tilt angle, the smaller the average target strength. The target strength function curve is quite smooth around the symmetrical centre of the function, but the target strength decreased very quickly above a certain tilt angle. The target strength generated in this case is very variable. This is why the variance of the regression line increased as the mean tilt angle increased.

The magnitude of target strength depends on the standard deviation of tilt angle distribution. The bigger the standard deviation, the wider the variation range of the target strength. As a result, the number of targets estimated compared with the number of targets generated tend to have a big bias at a given average target strength.

The range of tilt angle, θ_r, determines the integral limits of calculating average target strength. For quite small standard deviation S_q, the effect of θ_r on the average target strength MSV is not significant as described in chapter 4. However, the range of tilt angle, θ_r, affects the values of individual target strength. It is apparent that the variance of the regression line increases as the range of tilt angle increased.

6.2.2 The Effect of the Uniform Model on the Estimation

It is known that the curve of normal distribution approaches uniform distribution as the standard deviation of the normal distribution increases. It can be seen from Figs.6.5 to 6.6 that the results which examined the effect of the range of tilt angle, θ_r, and the mean tilt angle θ_m on the estimate are similar to those obtained by using the normal model as tilt angle distribution. But the slope of the regression line increases quickly upon the increase of the range of tilt angle. In other words, the number of targets estimated is more than that generated. Since the average target strength obtained by using uniform distribution is lower than that obtained by using normal distribution as shown in Figs.4.8b and 4.9c when the range of tilt angle exceeds 40, the number of targets estimated is more than that generated. The over-estimate suggests that the normal distribution can be replaced by the uniform one in the case of quite big standard deviation of tilt angle distribution.

6.3 THE EFFECT OF THE TARGET STRENGTH FUNCTION ON THE ESTIMATION

It has already been shown in reference [3] that size of fish and acoustic frequency affect the target strength function and the calculation of average target strength. Fig.6.4 showed that for a bigger size of fish or higher acoustic frequency the target strength is more sensitive to the tilt angle, i.e., the target strength obtained from the target strength function depends strongly on the tilt angle. Therefore, under the condition of a given tilt angle distribution, the results for any individual trace are either very scattered, or the variance of the regression line increased as the fish size or the acoustic frequency increased.

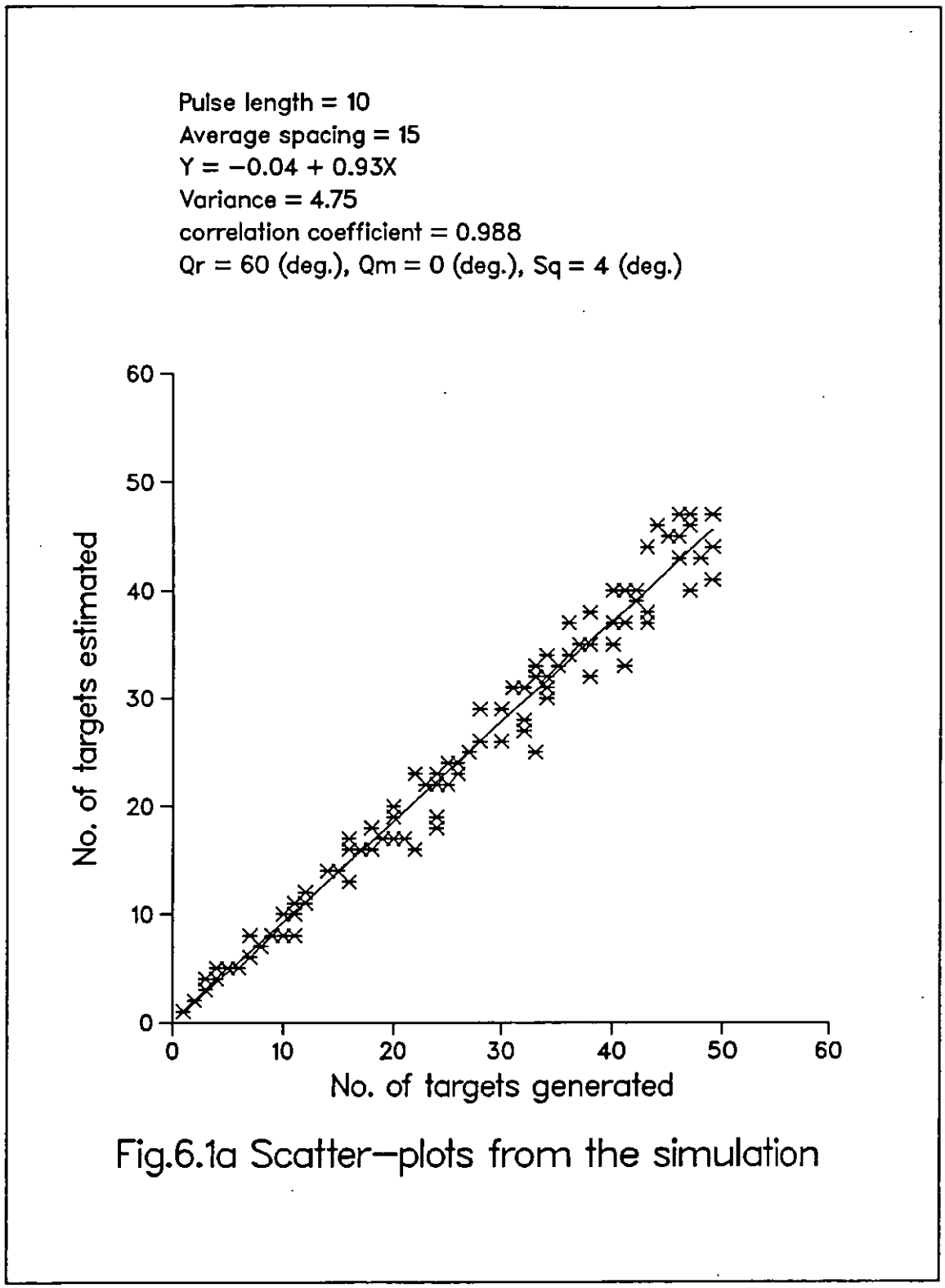

Fig.6.1a Scatter–plots from the simulation

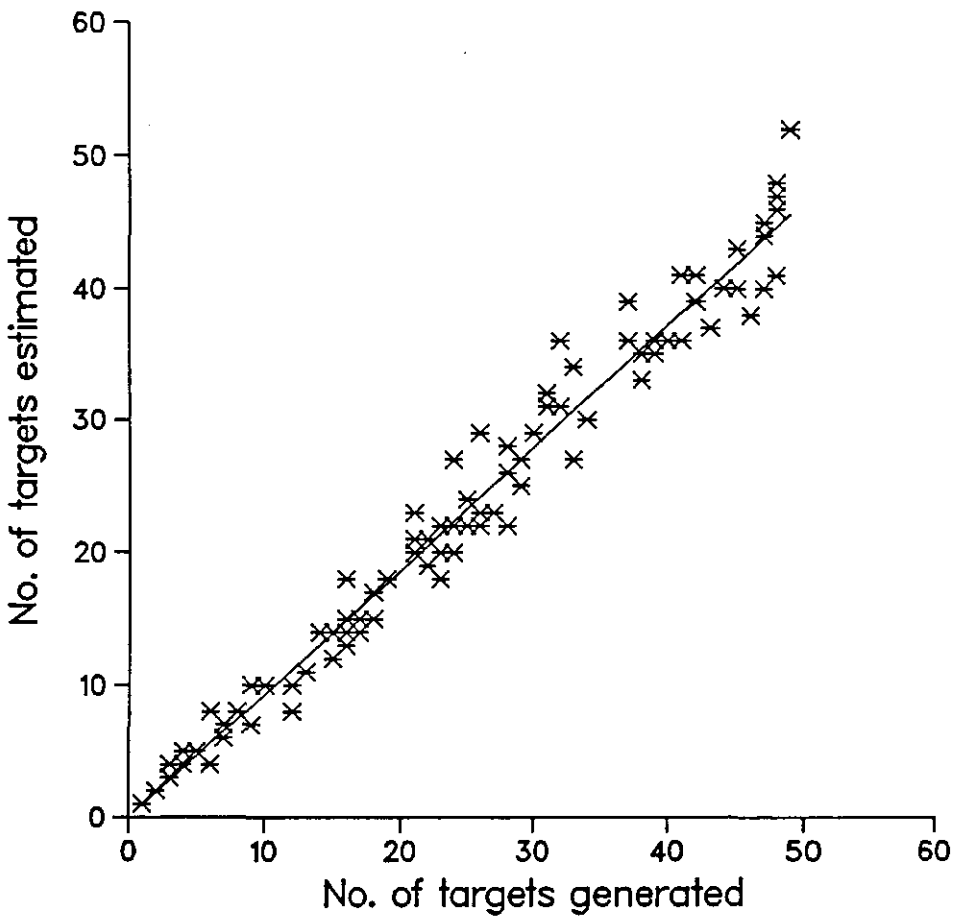

Fig.6.1b Scatter–plots from the simulation

Pulse length = 10
Average spacing = 15
Y = 0.89 + 0.88X
Variance = 12.11
correlation coefficient = 0.96
Qr = 60 (deg.), Qm = 0 (deg.), Sq = 12 (deg.)

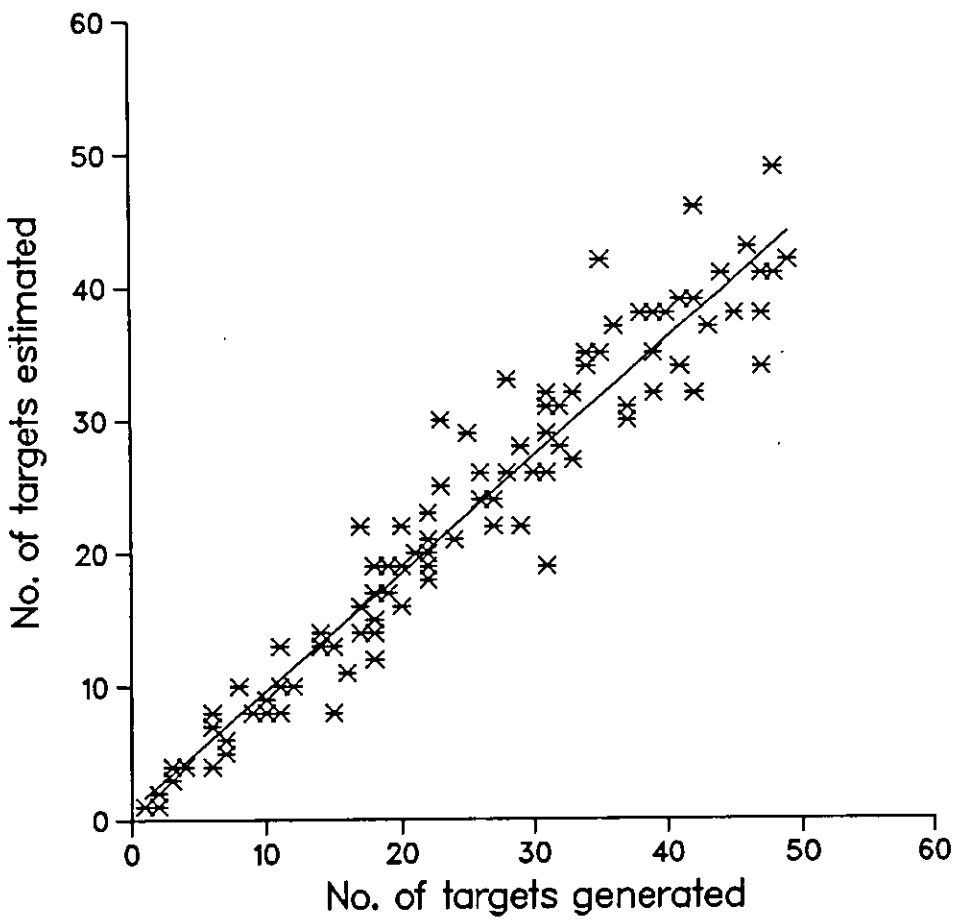

Fig.6.1c Scatter–plots from the simulation

Pulse length = 10
Average spacing = 15
Y = −0.05 + 0.94X
Variance = 12.97
correlation coefficient = 0.96
Qr = 60 (deg.), Qm = 0 (deg.), Sq = 16 (deg.)

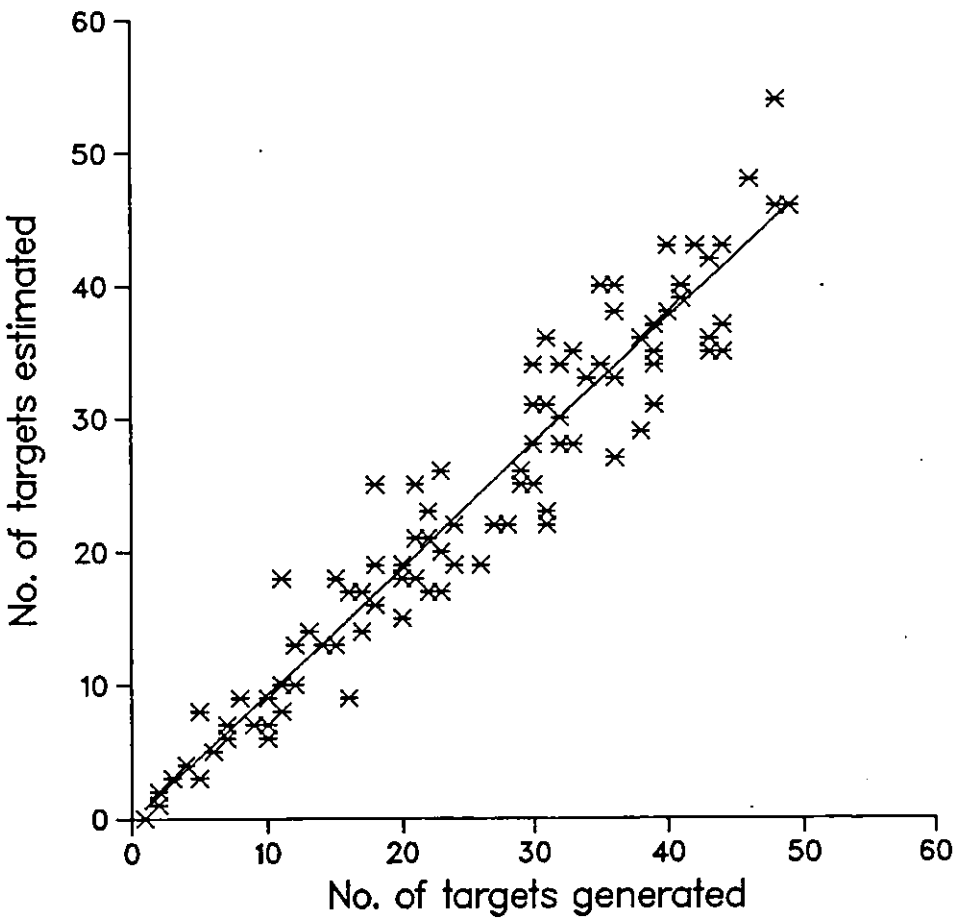

Fig.6.1d Scatter–plots from the simulation

Pulse length = 10
Average spacing = 15
Y = 0.74 + 0.9X
Variance = 15.27
correlation coefficient = 0.95
Qr = 60 (deg.), Qm = 0 (deg.), Sq = 20 (deg.)

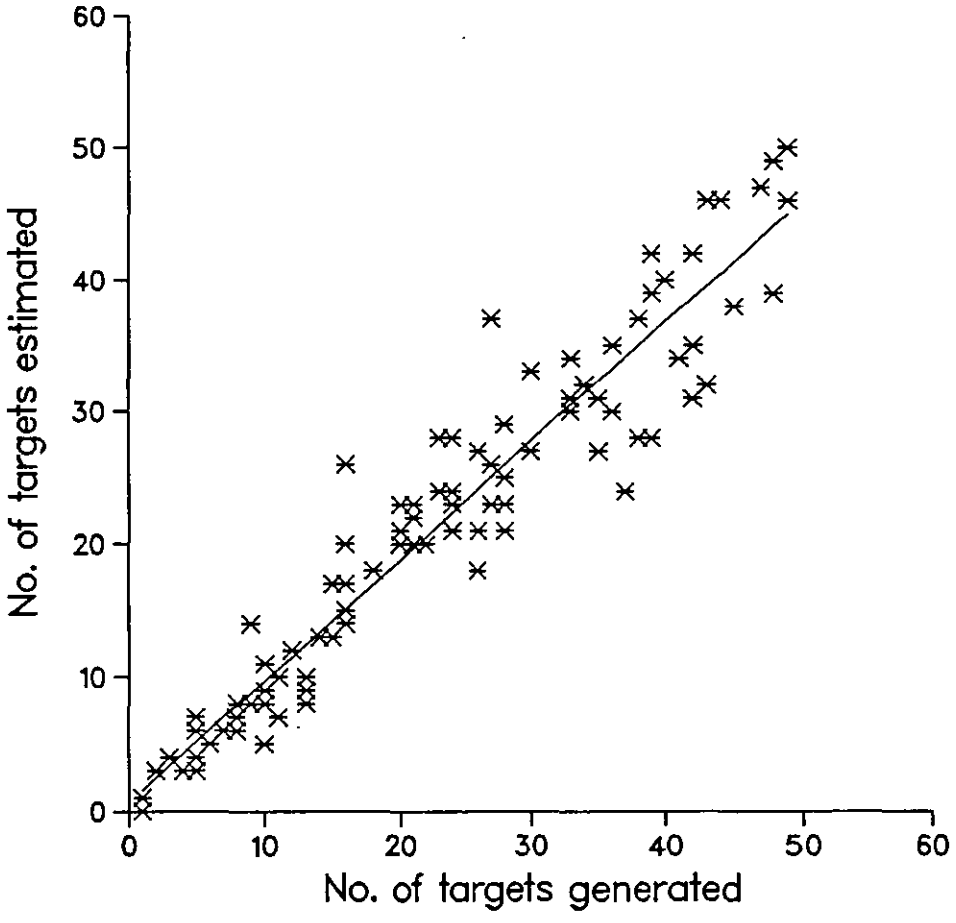

Fig.6.1e Scatter-plots from the simulation

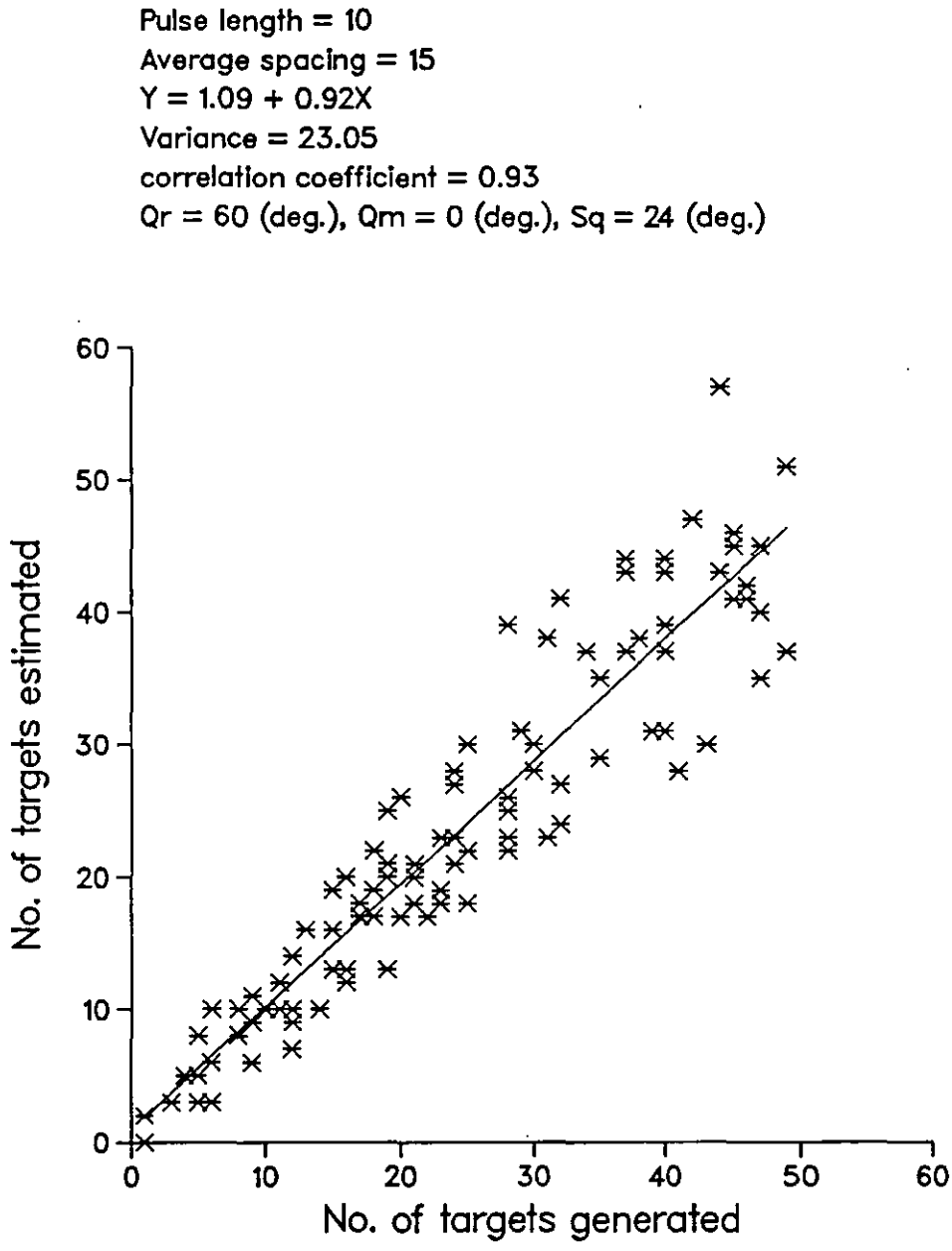

Fig.6.1f Scatter–plots from the simulation

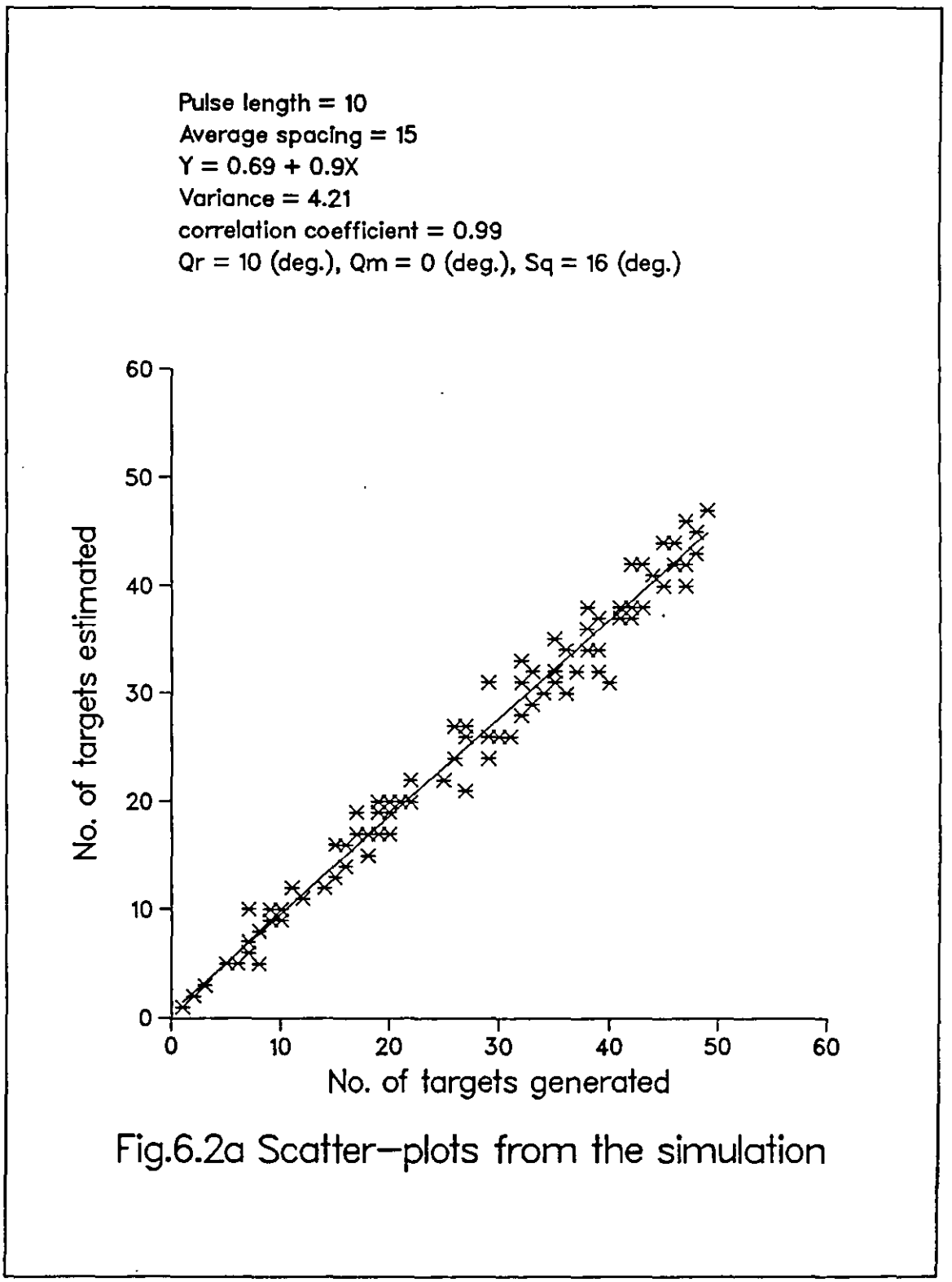

Fig.6.2a Scatter–plots from the simulation

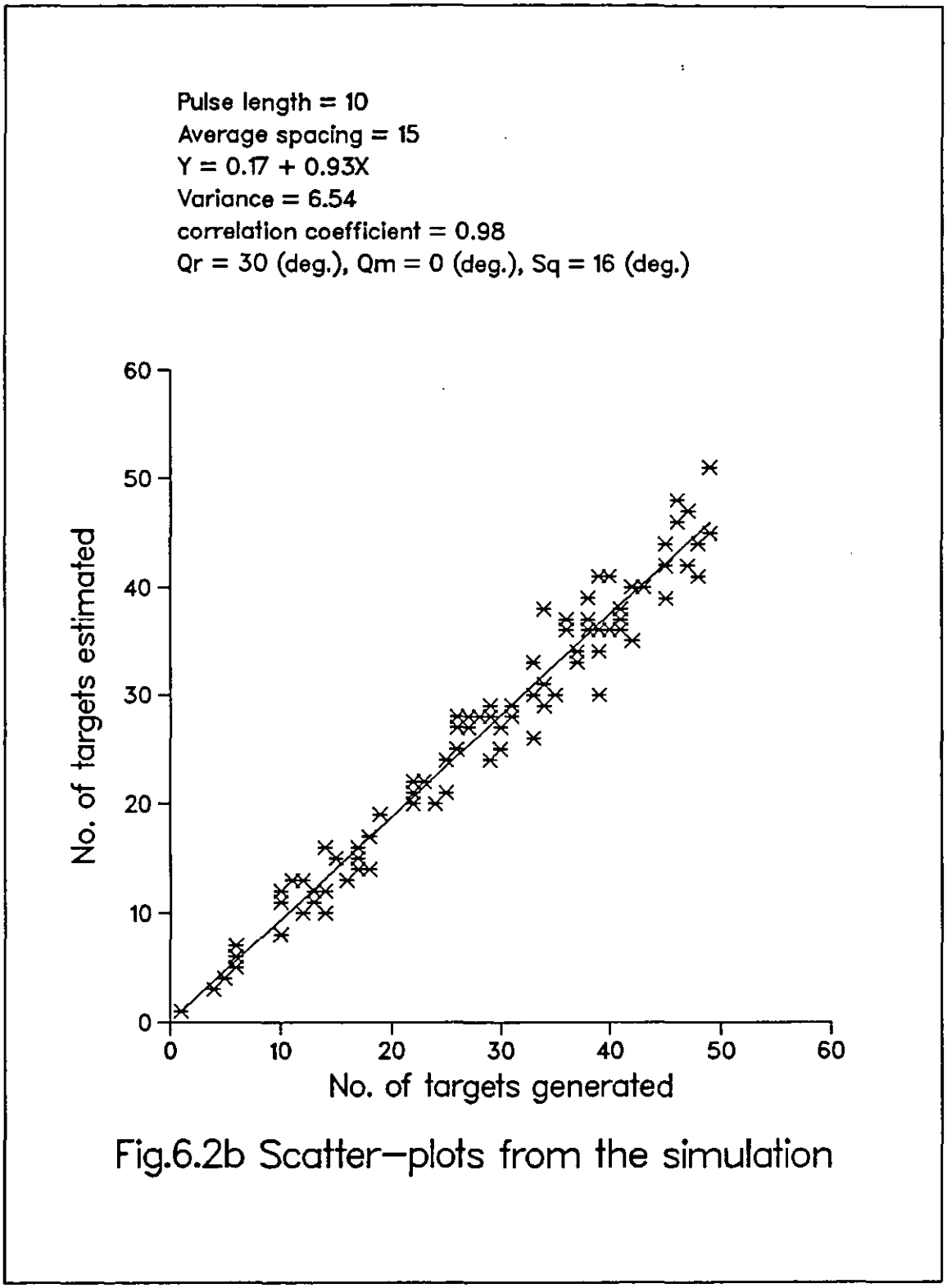

Fig.6.2b Scatter–plots from the simulation

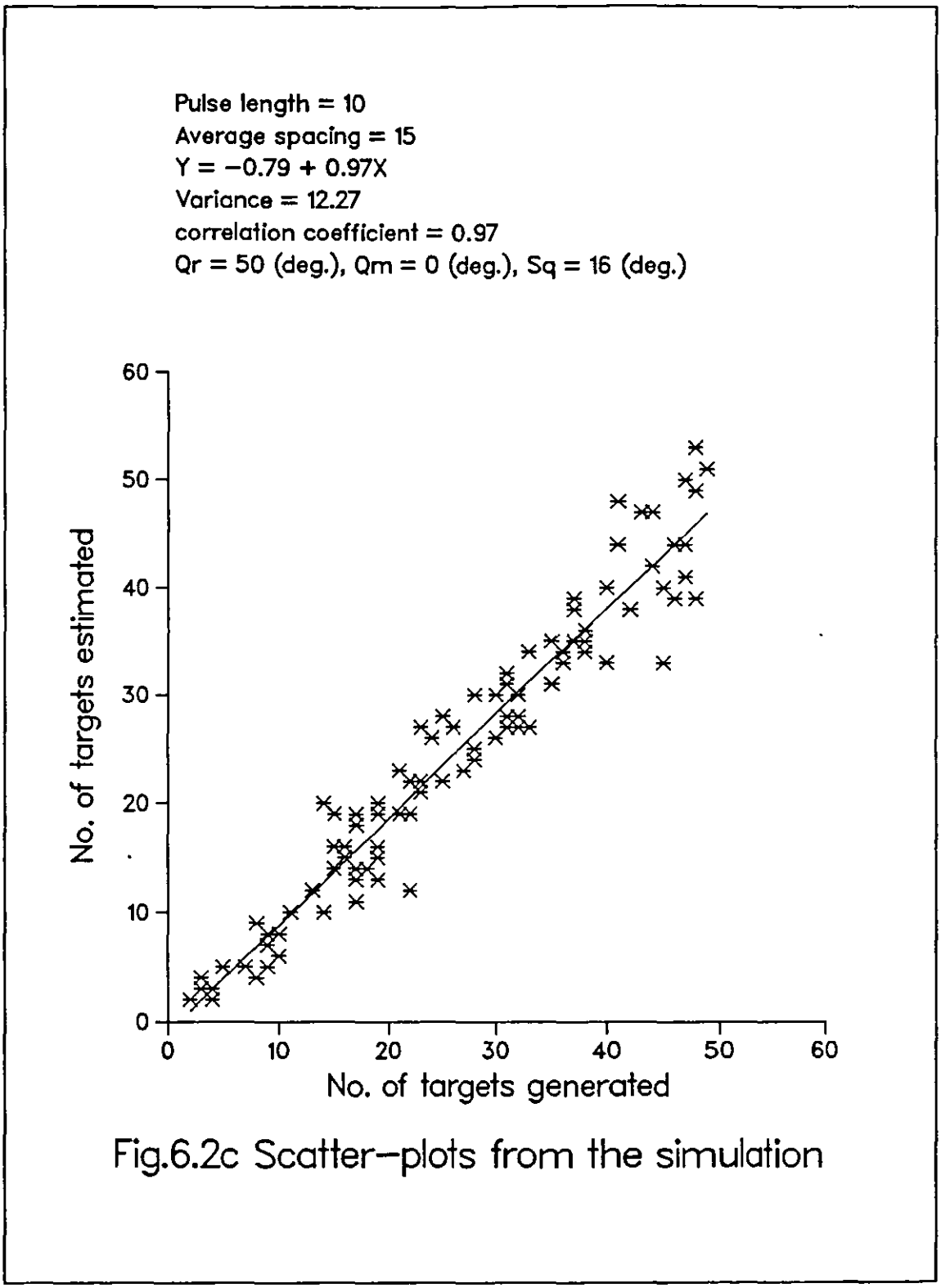

Fig.6.2c Scatter–plots from the simulation

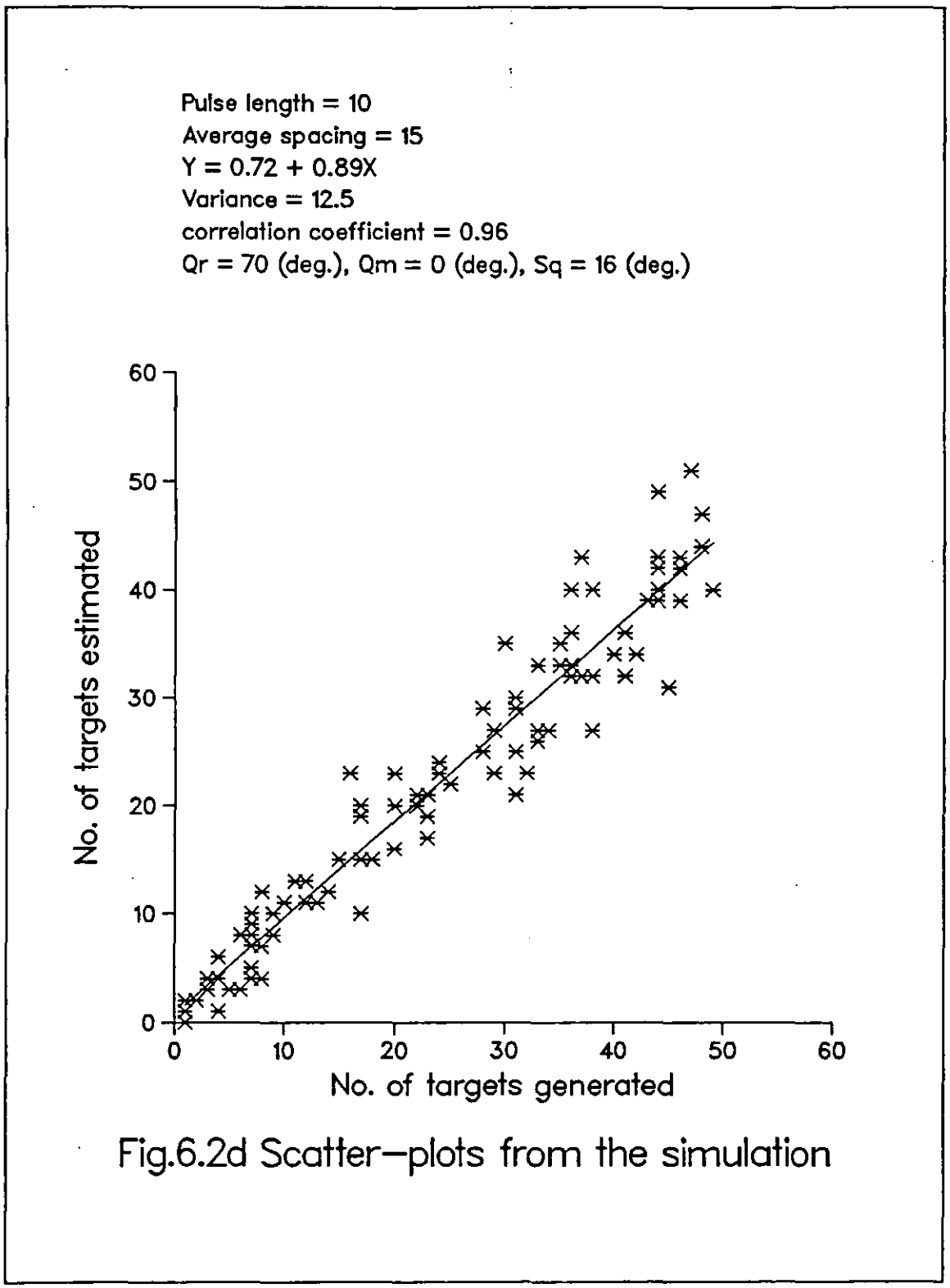

Fig.6.2d Scatter–plots from the simulation

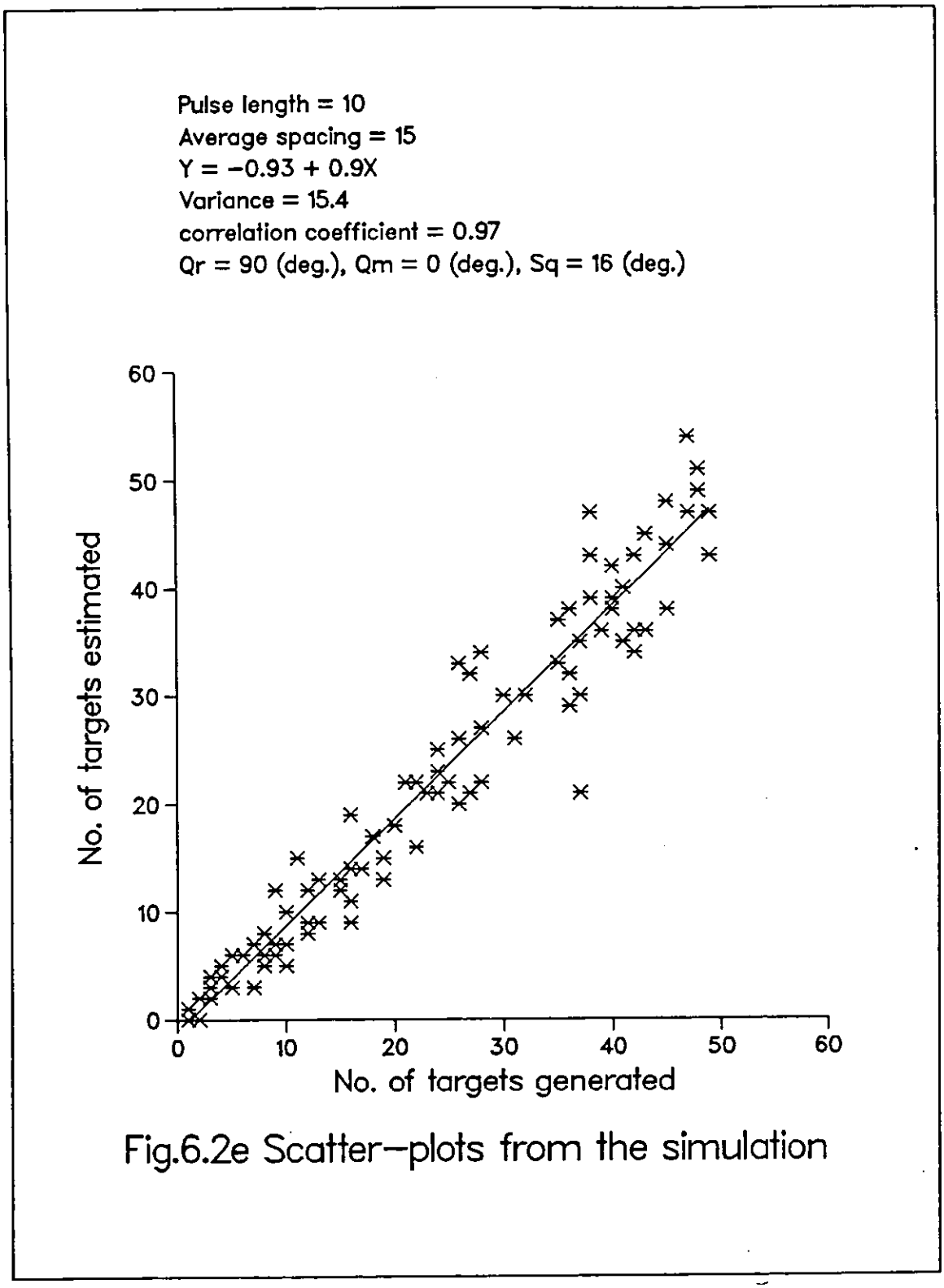

Fig.6.2e Scatter–plots from the simulation

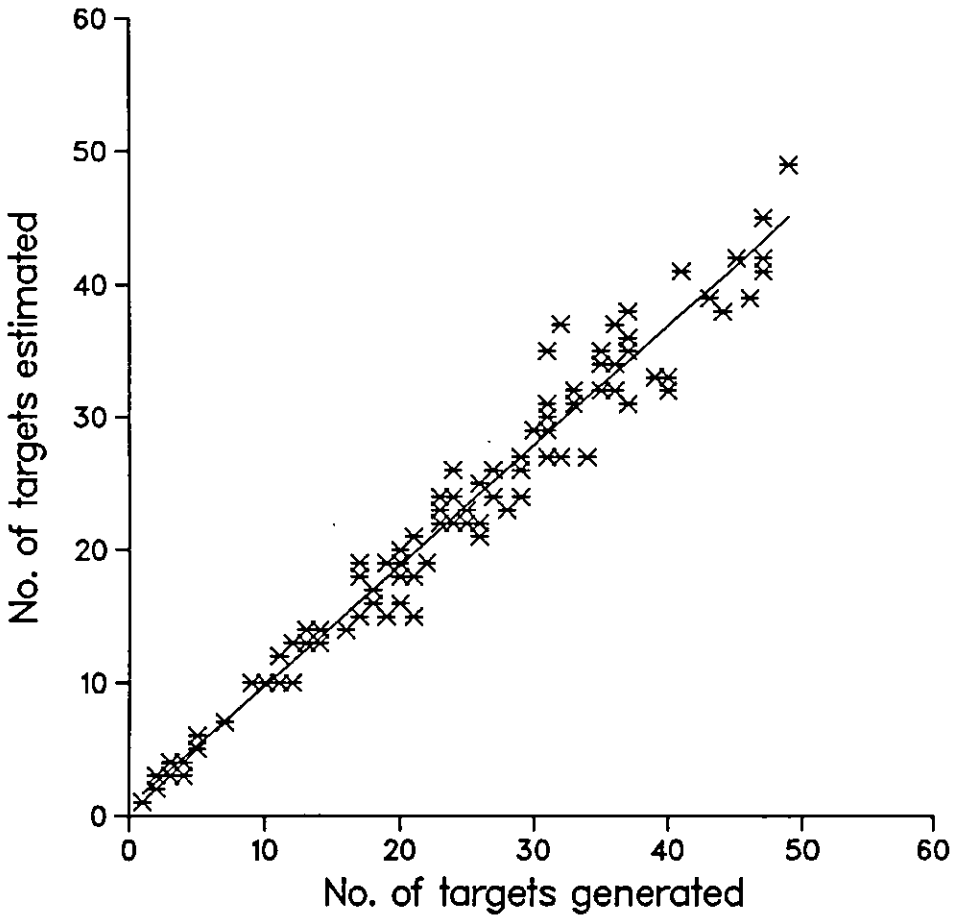

Fig.6.3a Scatter–plots from the simulation

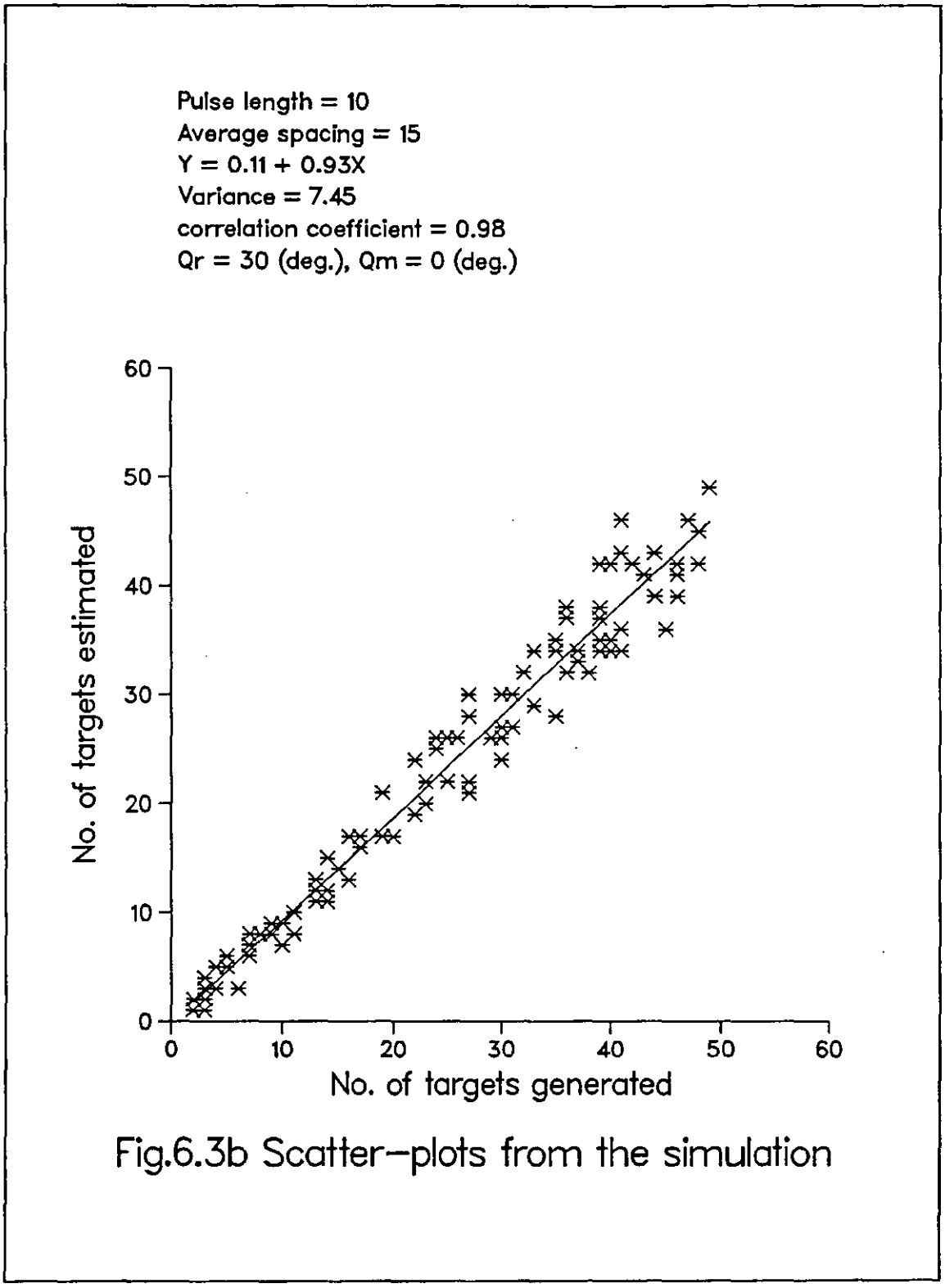

Fig.6.3b Scatter-plots from the simulation

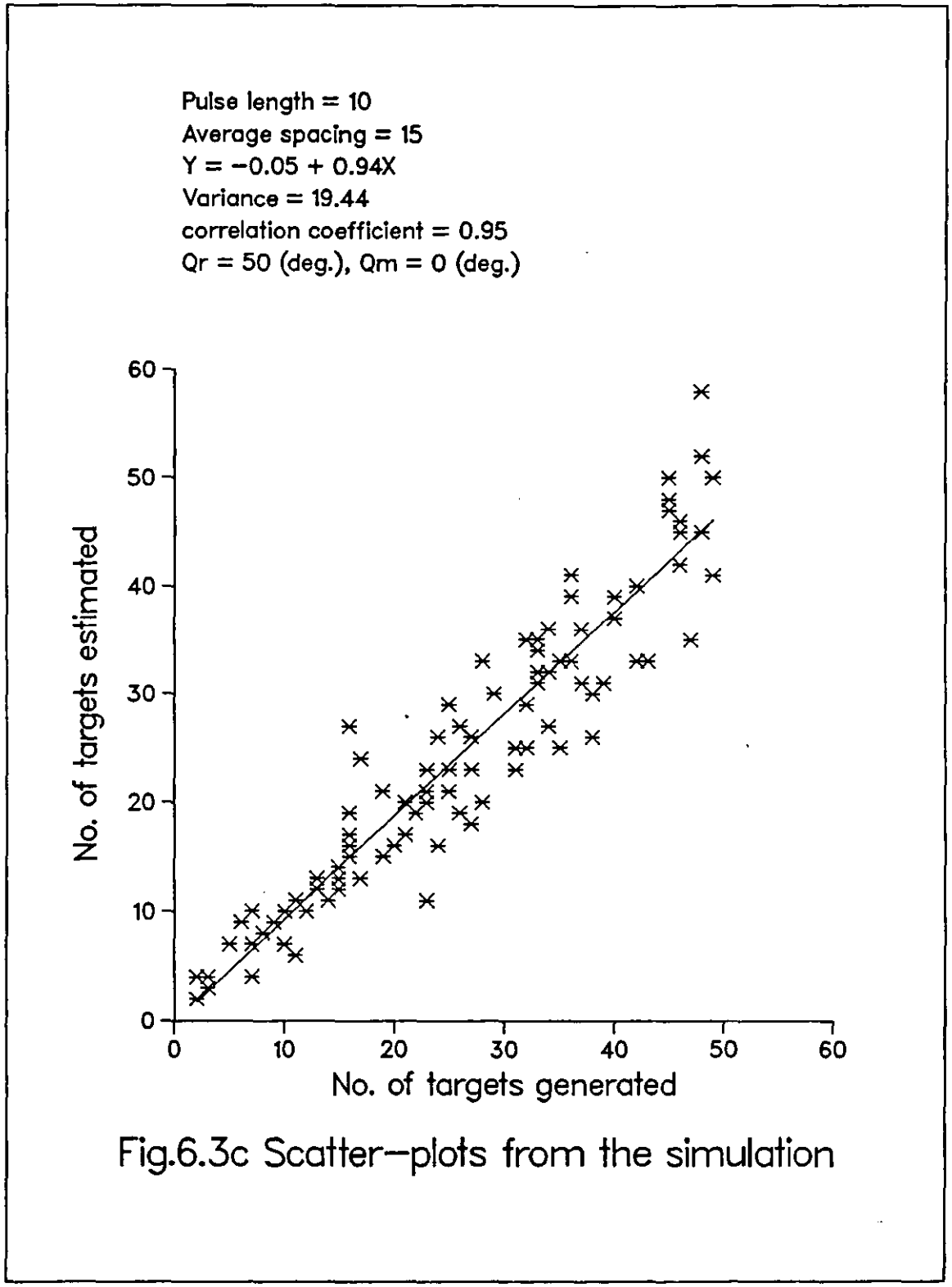

Fig.6.3c Scatter–plots from the simulation

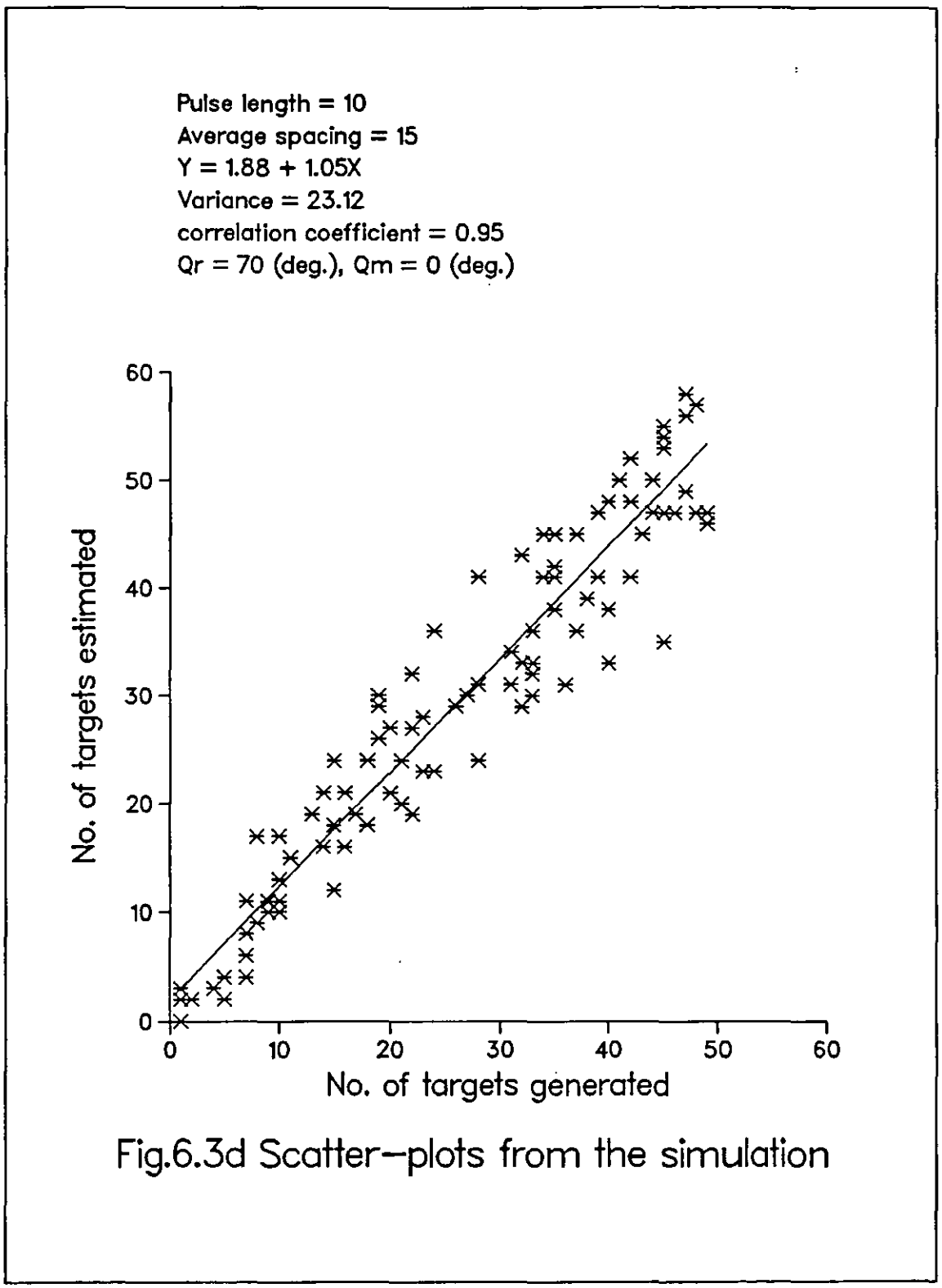

Fig.6.3d Scatter-plots from the simulation

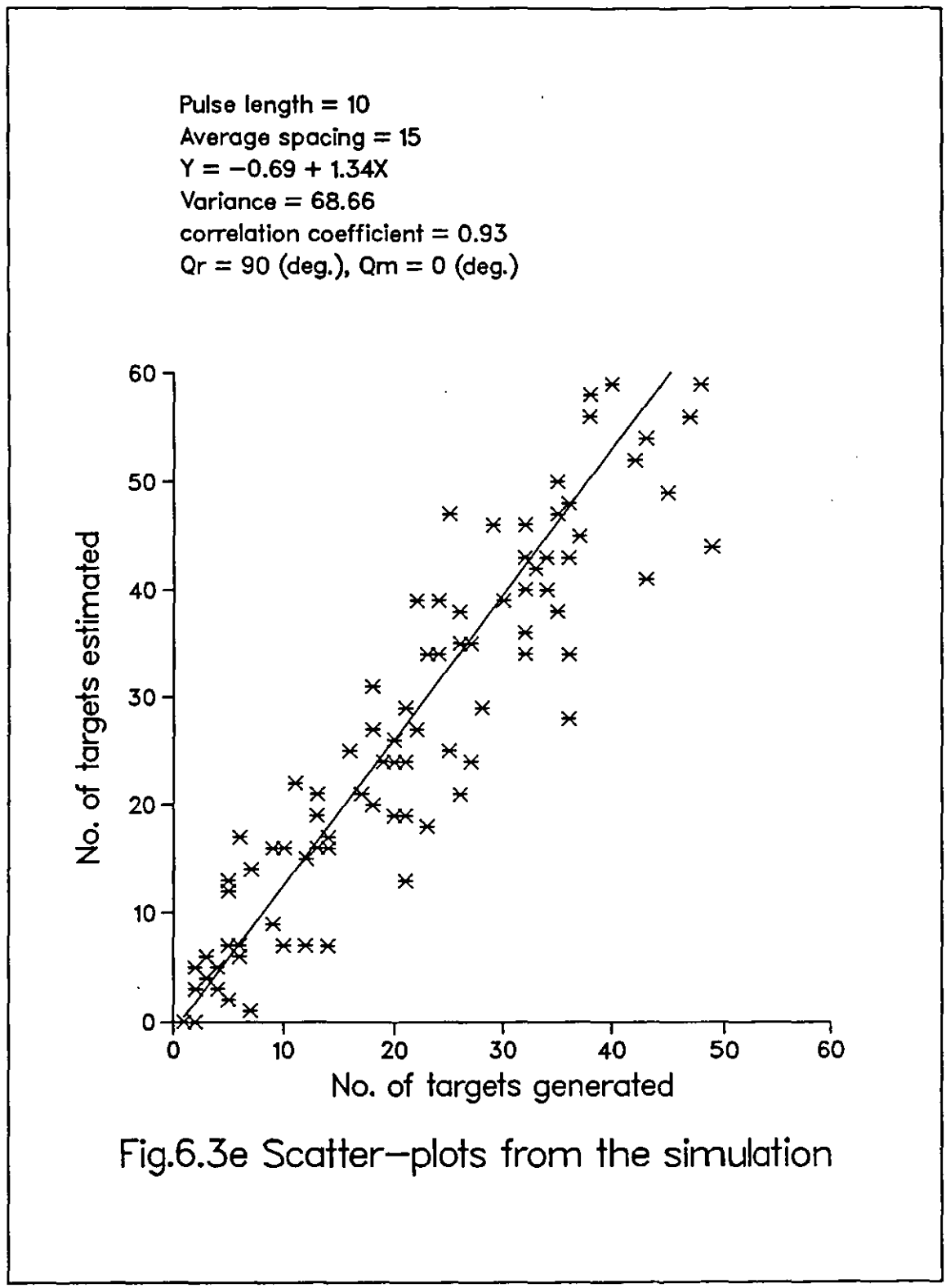

Fig.6.3e Scatter–plots from the simulation

Pulse length = 10
Average spacing = 15, constant of beam pattern = 4
Y = −0.7 + 0.96X
Variance = 8.35
correlation coefficient = 0.97
Qr = 90 (deg.), Qm = −4 (deg.), Sq = 16 (deg.)

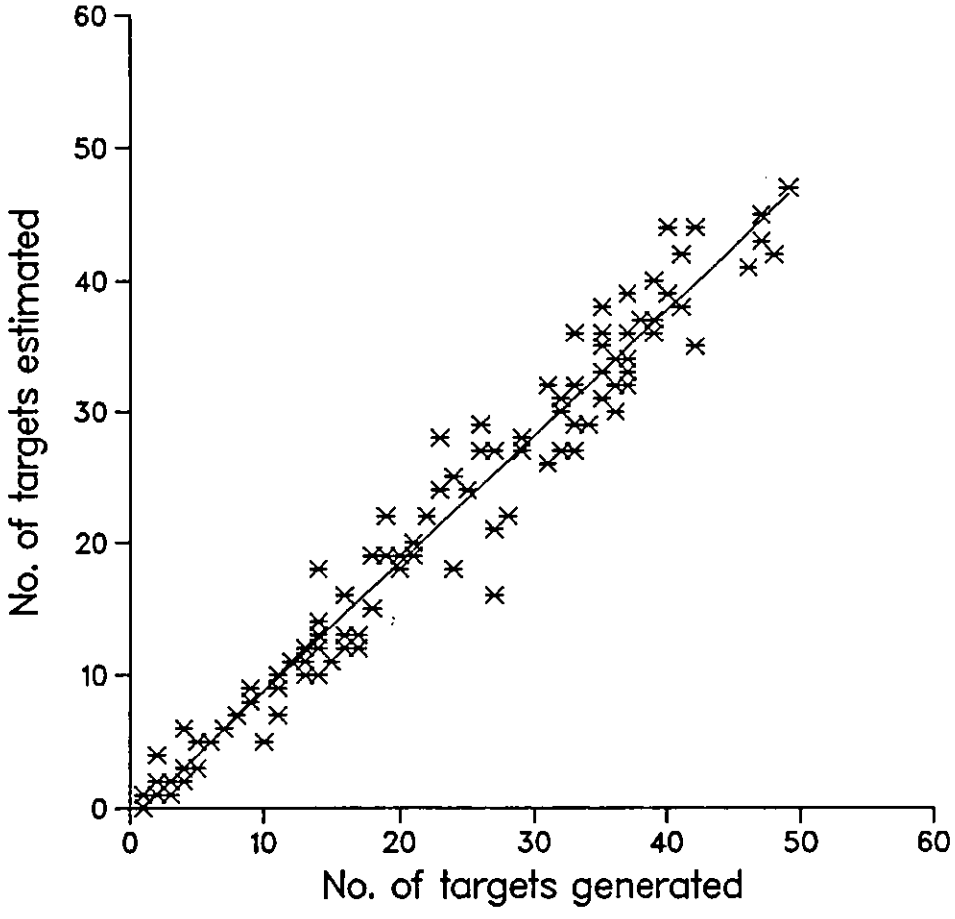

Fig.6.4a Scatter−plots from the simulation

Pulse length = 10
Average spacing = 15, constant of beam pattern = 7
Y = −0.32 + 0.95X
Variance = 13.96
correlation coefficient = 0.96
Qr = 90 (deg.), Qm = −4 (deg.), Sq = 16 (deg.)

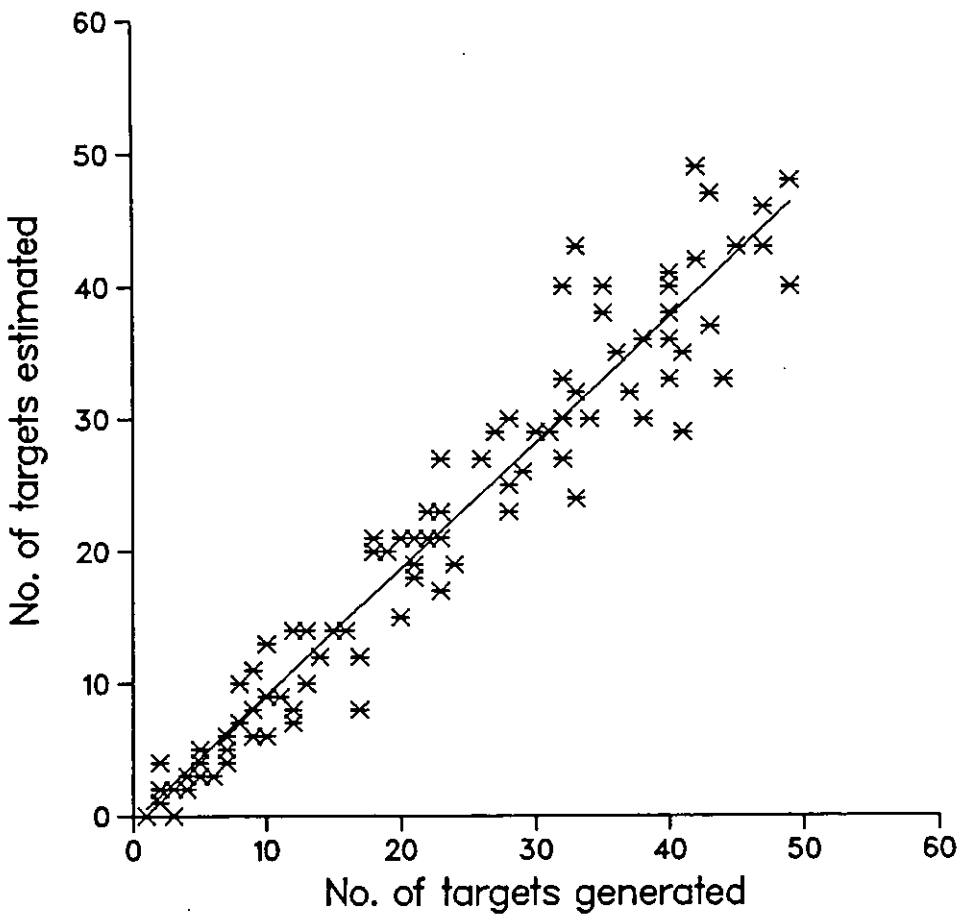

Fig.6.4b Scatter−plots from the simulation

Pulse length = 10
Average spacing = 15, constant of beam pattern = 10
Y = 0.15 + 0.95X
Variance = 34.09
correlation coefficient = 0.93
Qr = 90 (deg.), Qm = −4 (deg.), Sq = 16 (deg.)

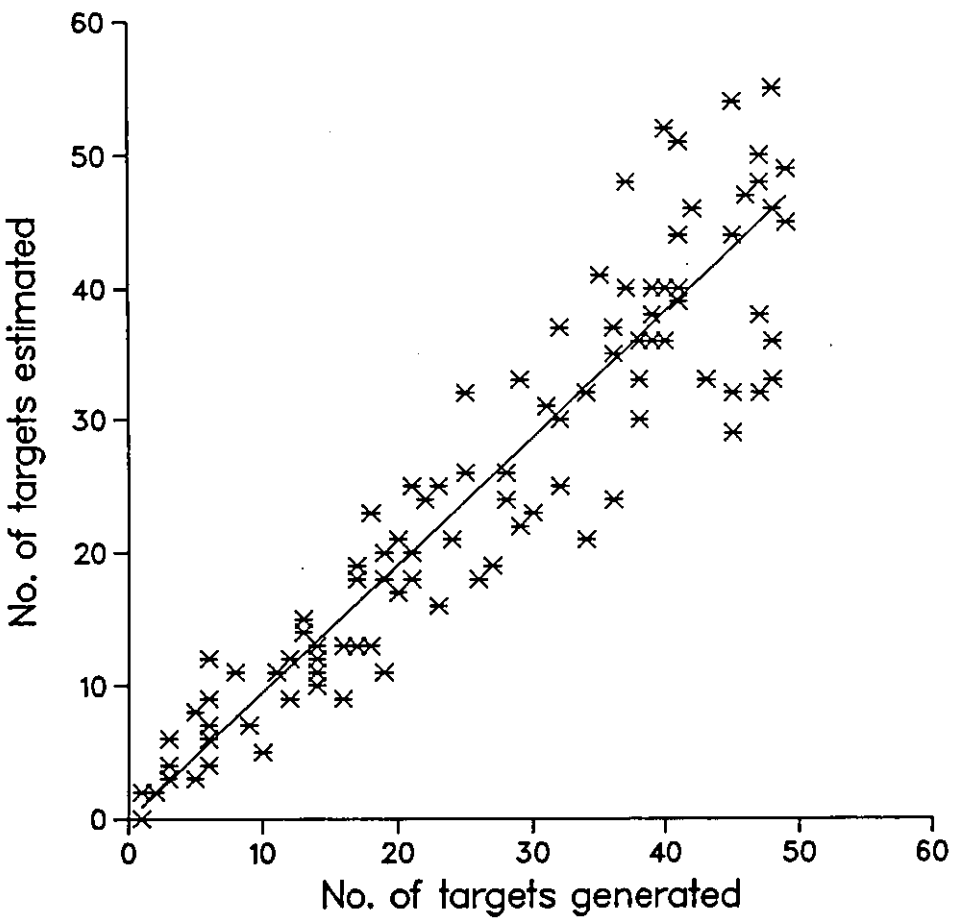

Fig.6.4c Scatter–plots from the simulation

Pulse length = 10
Average spacing = 15, constant of beam pattern = 13
Y = 0.65 + 0.9X
Variance = 42.01
correlation coefficient = 0.88
Qr = 90 (deg.), Qm = −4 (deg.), Sq = 16 (deg.)

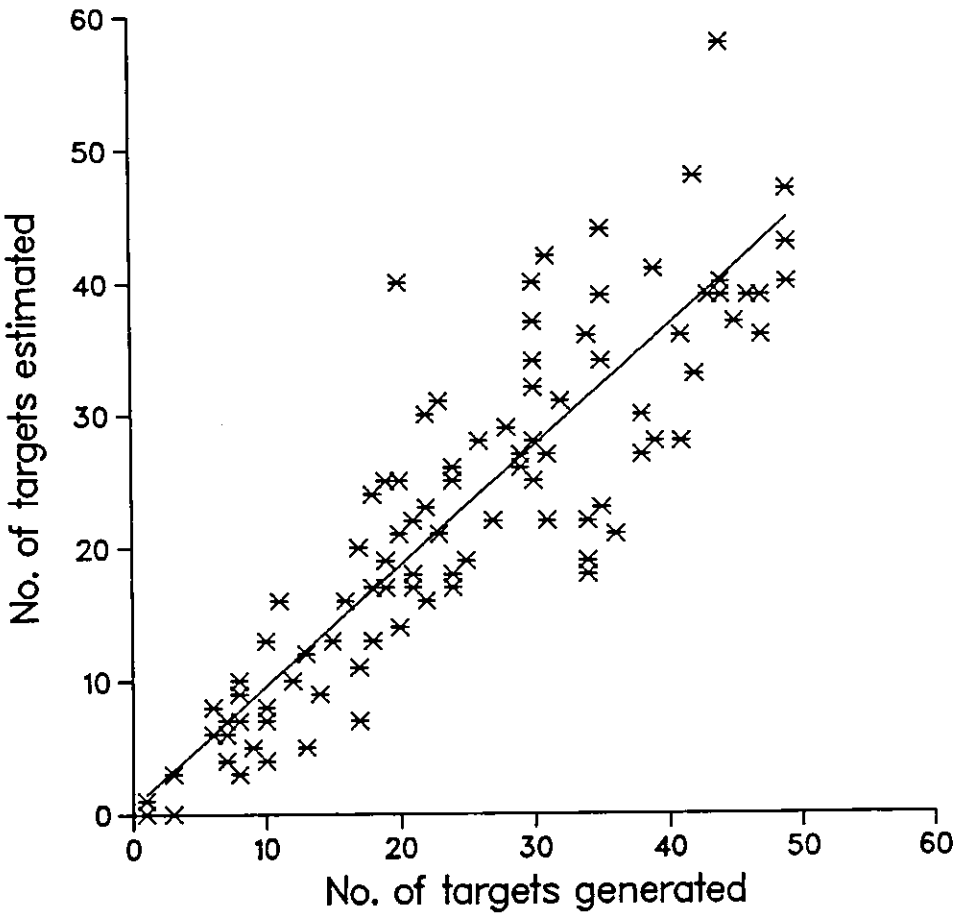

Fig.6.4d Scatter–plots from the simulation

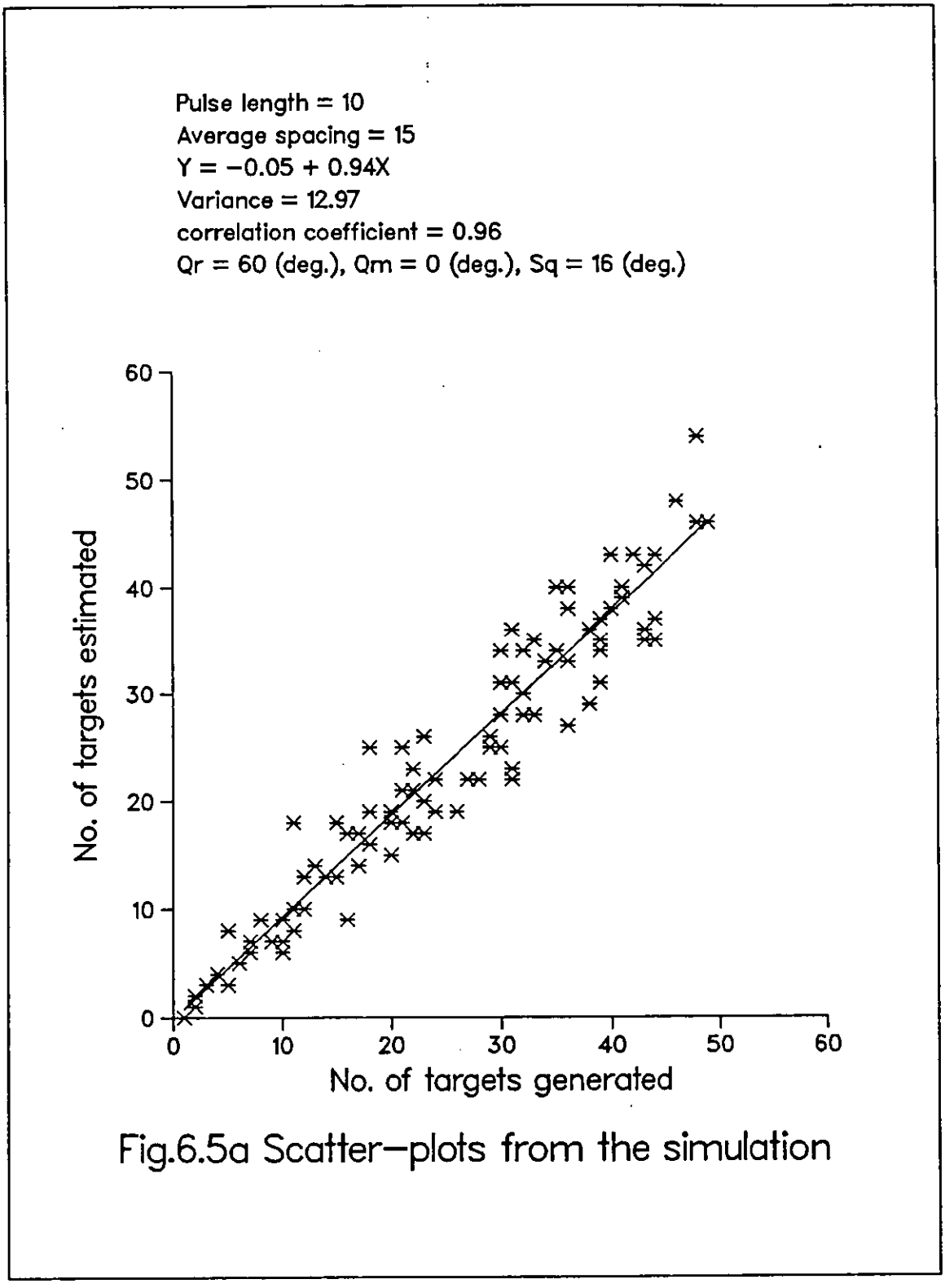

Fig.6.5a Scatter–plots from the simulation

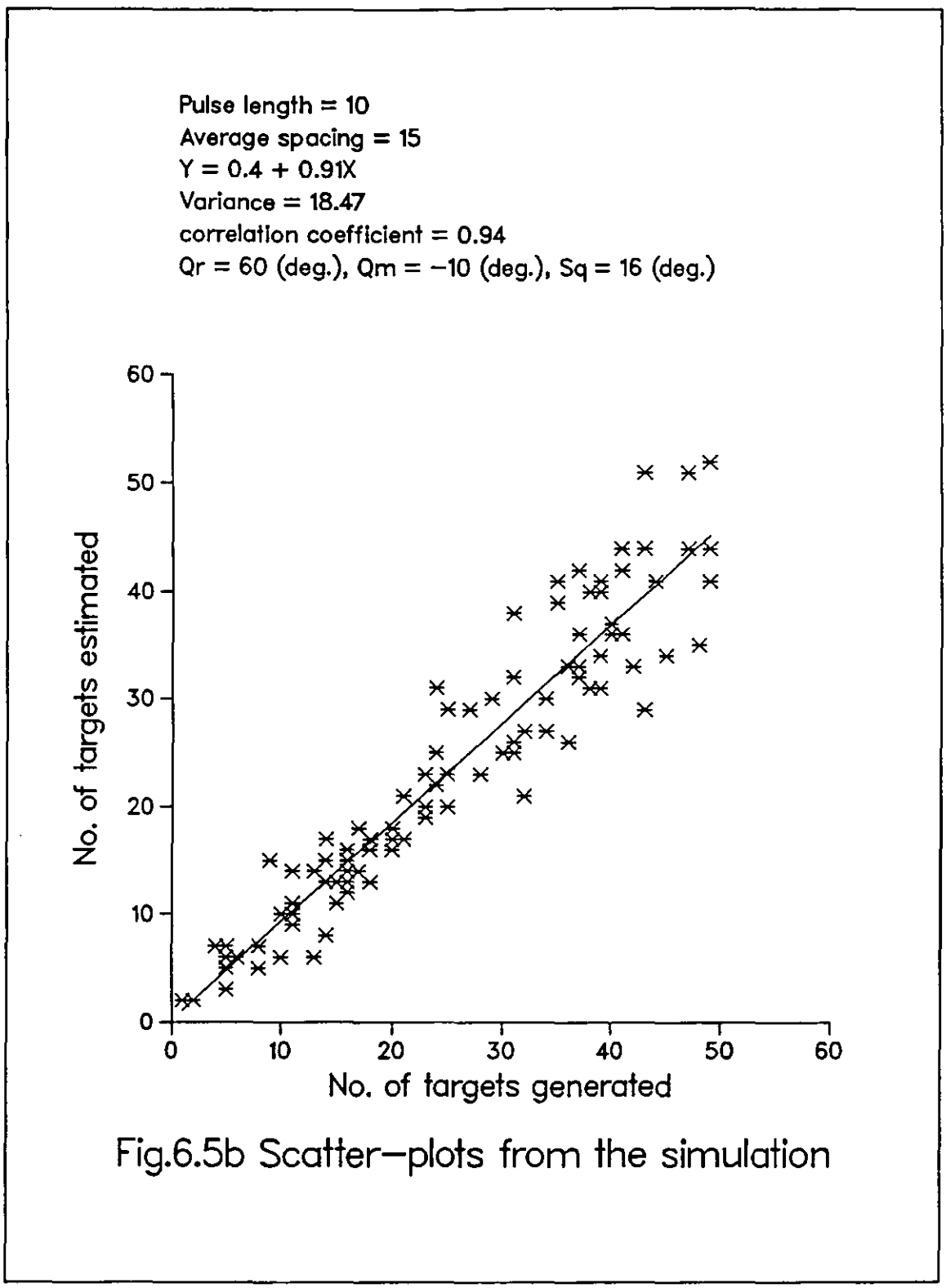

Fig.6.5b Scatter–plots from the simulation

Pulse length = 10
Average spacing = 15
Y = 0.37 + 0.94X
Variance = 41.28
correlation coefficient = 0.89
Qr = 60 (deg.), Qm = −20 (deg.), Sq = 16 (deg.)

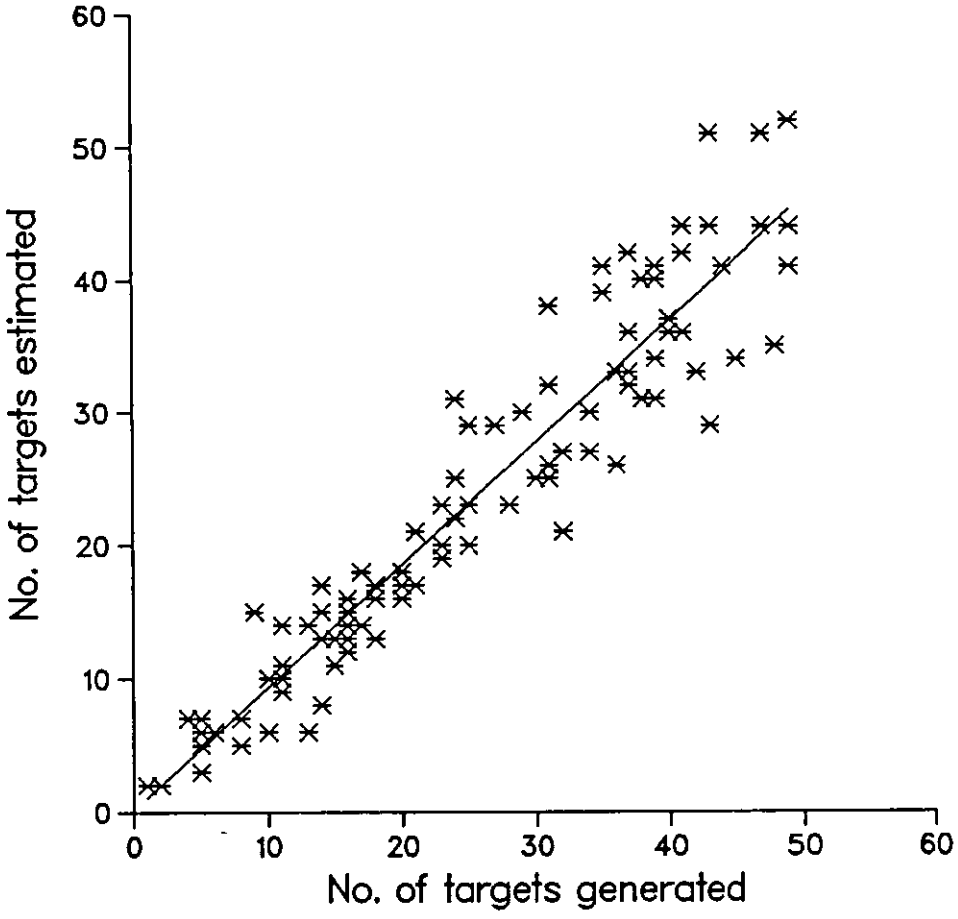

Fig.6.5c Scatter–plots from the simulation

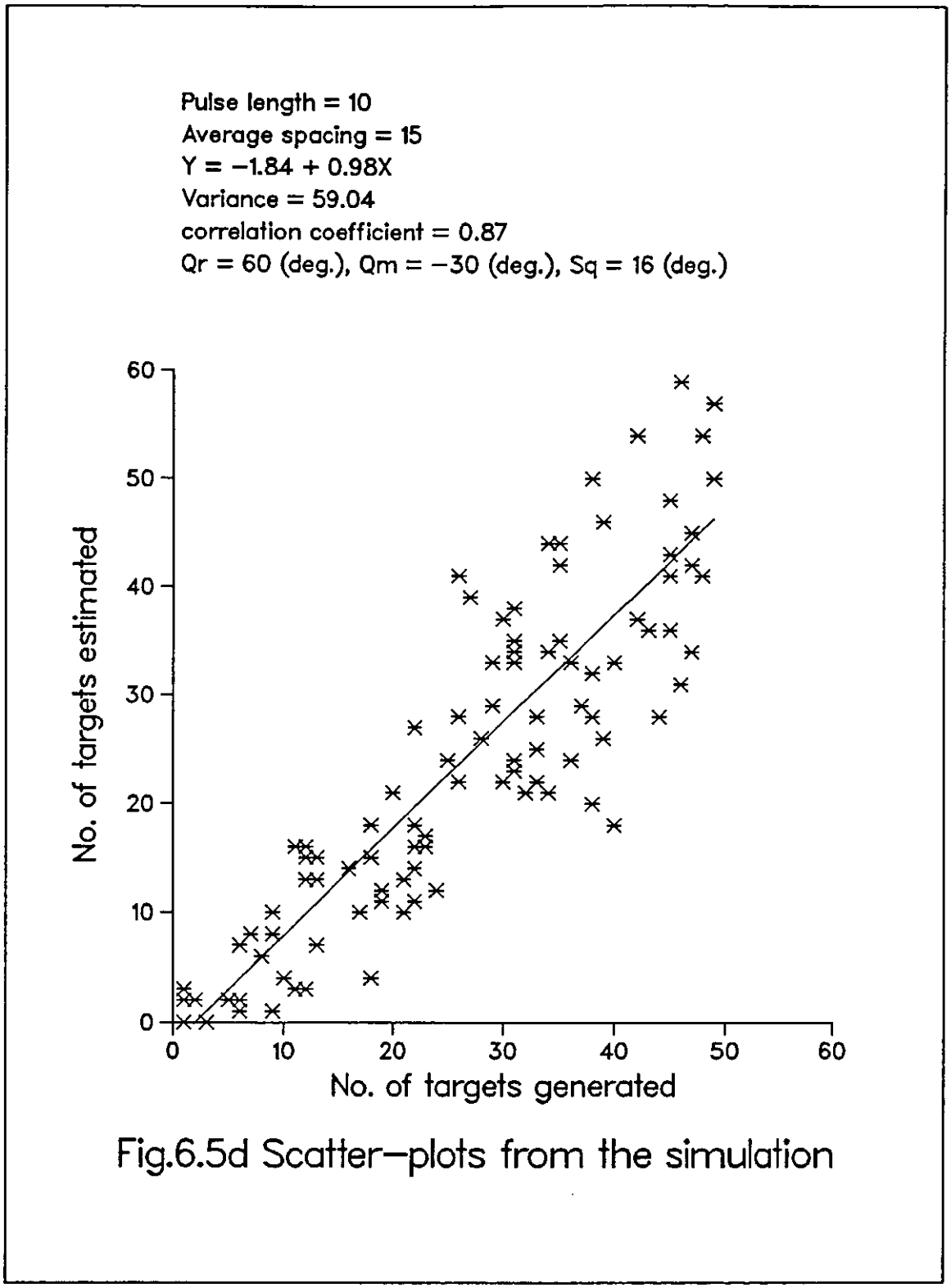

Fig.6.5d Scatter–plots from the simulation

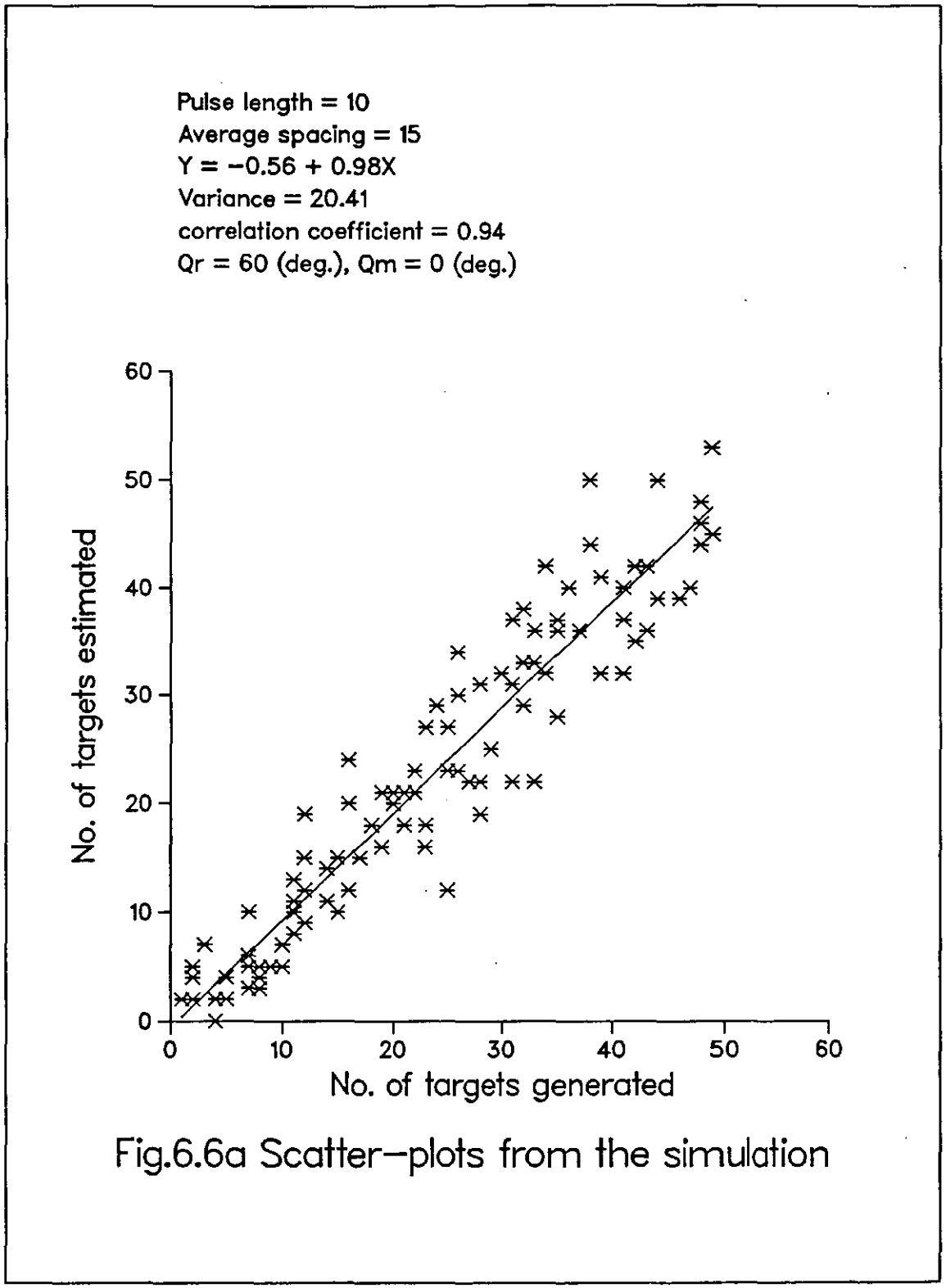

Fig.6.6a Scatter–plots from the simulation

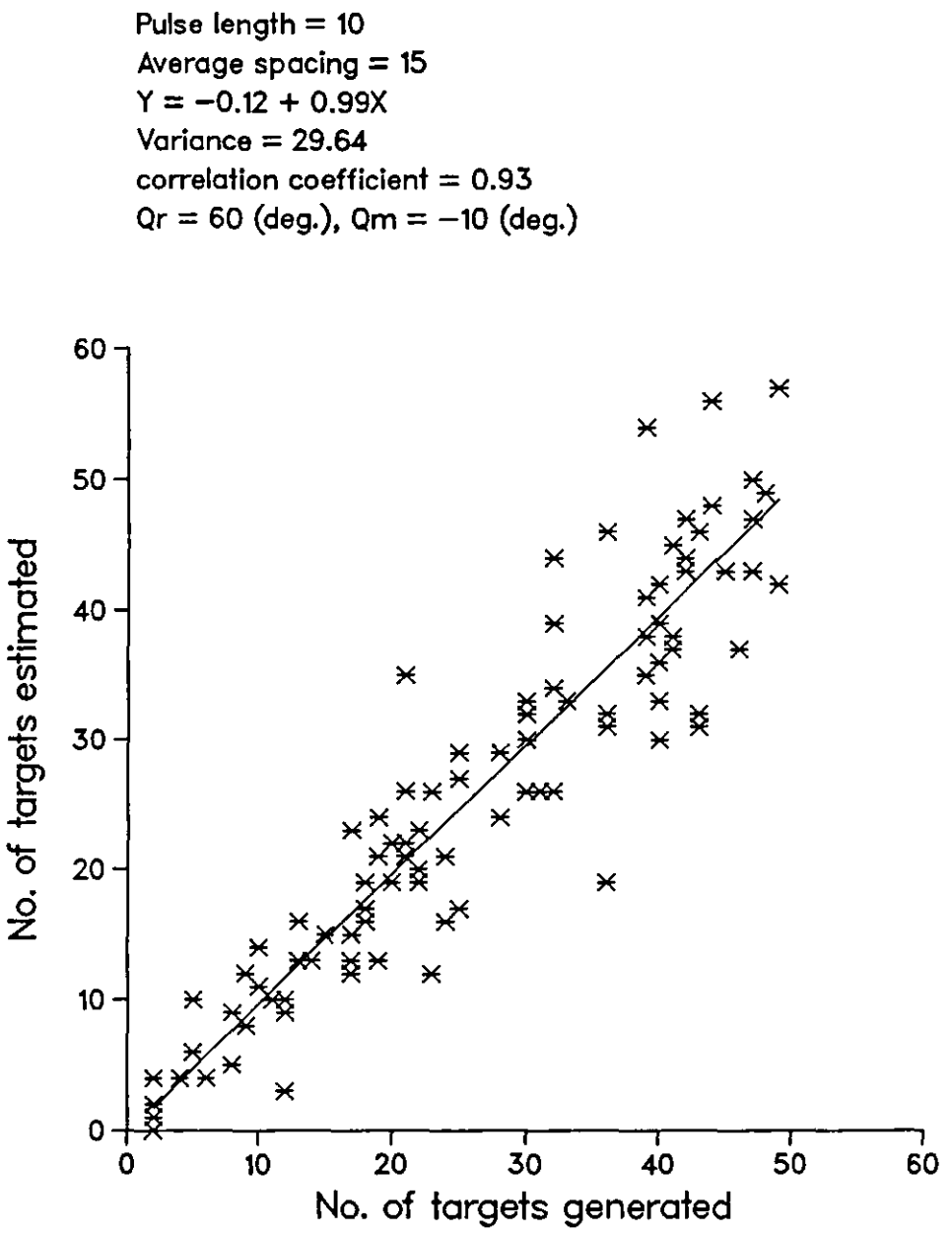

Fig.6.6b Scatter–plots from the simulation

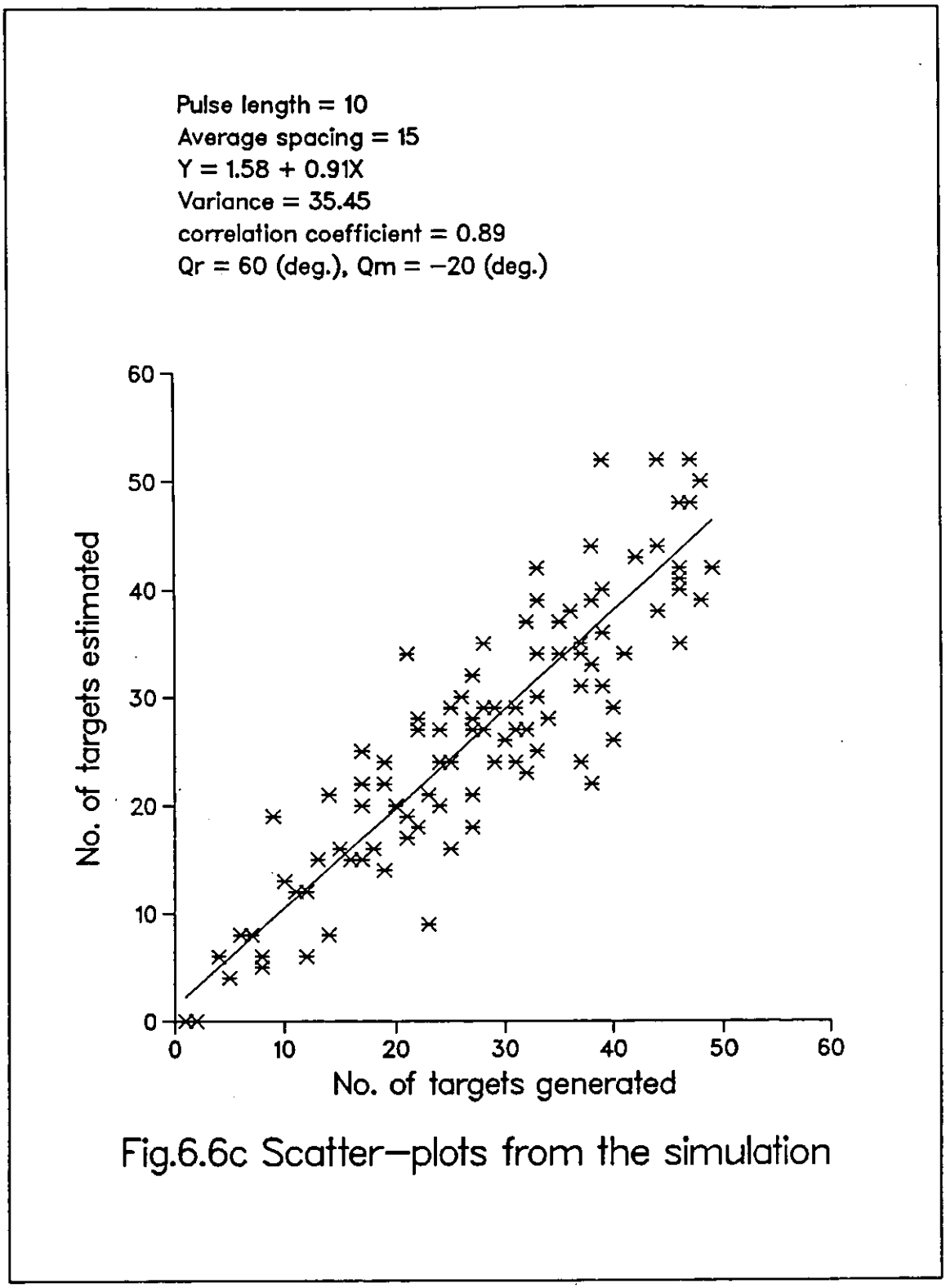

Fig.6.6c Scatter–plots from the simulation

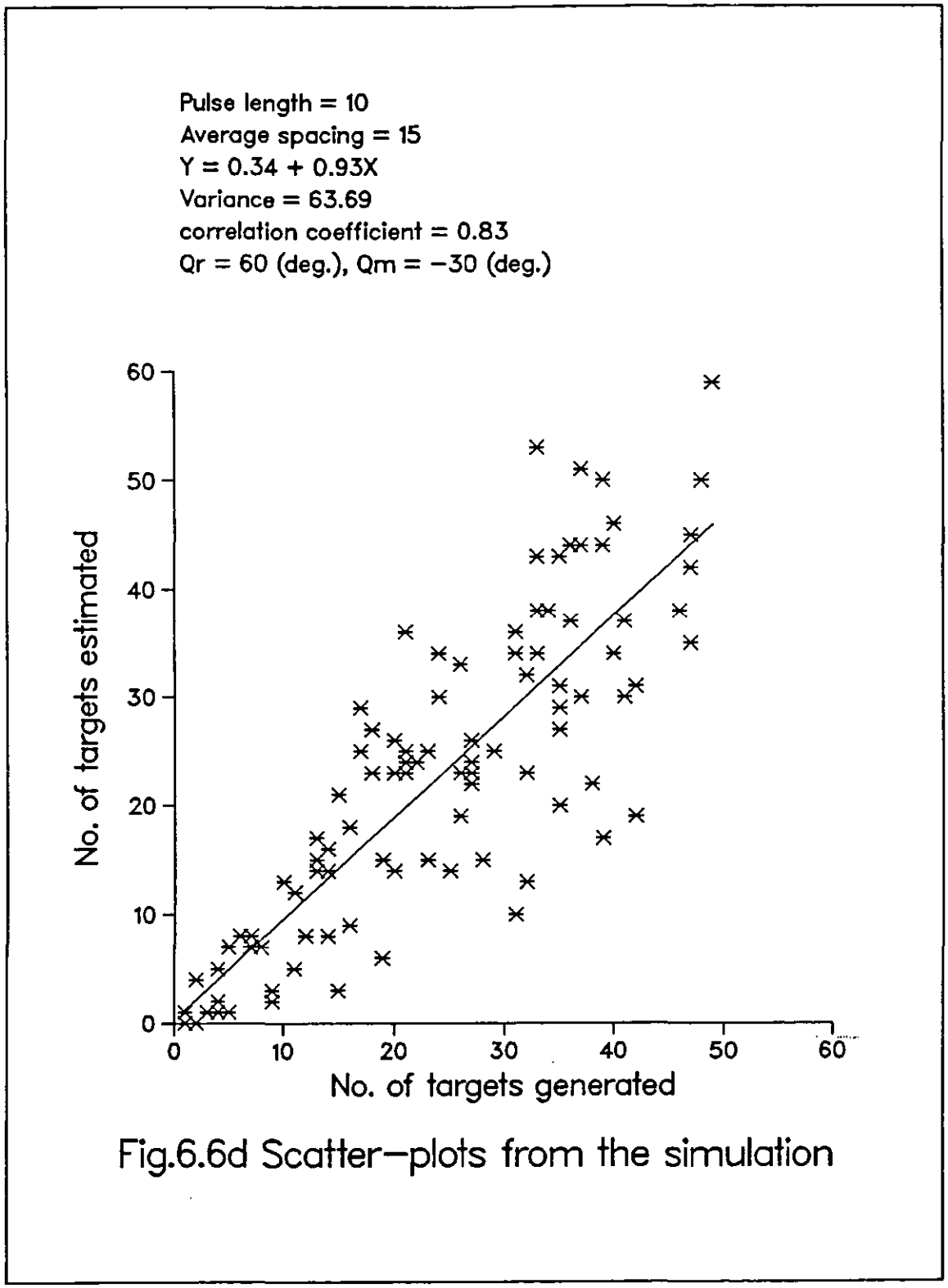

Fig.6.6d Scatter–plots from the simulation

7. PRACTICAL WORK

7.1 INTRODUCTION

This chapter describes the work done and results obtained on the measurement of the target strength for different kinds of spheres. The data used for the analysis was collected from experimental apparatus originally designed for another purpose but modified for use in determining the target strength of the different kinds of spheres. All the measurements were carried out using a frequency of 3 MHz in a large water tank.

Low frequency (e.g. 38 KHz) is the sonar frequency normally used on fish surveys. For calibrating purposes, reference targets are required to have a perceived target strength at this frequency. However, some quite high frequencies (e.g. 3 MHz) are also adopted and used for some particular purpose. For the same reason, one method of calibrating sonars operating at this frequency might be to measure the echo from a standard target. Target strengths of copper, tungsten spheres and a table tennis ball have already been obtained at low frequency and it is shown that they are quite good as standard targets for calibration [36]. But, there is a little information published about the target strengths of these spheres at 3 MHz. Therefore, it is necessary to do some experiments in order to get some knowledge about the target strengths of these spheres at 3 MHz. The results presented here are promising but these are subject to some uncertainty and require some further validation before they can be relied upon.

7.2 MEASUREMENT OF TARGETS

7.2.1 Determination of Target Strength

In active sonar the parameter target strength refers to the echo returned by an underwater target. Target strength is normally defined as [23]

$$TS = 10 \log(Ir/Ii) \qquad \ldots\ldots (7 - 1)$$

where Ir is the intensity of return at 1 metre and Ii the incident intensity. Since intensity is proportional to pressure squared, then

$$TS = 20 \log(Pr/Pi)$$

In the present experiments, the transmit transducer, the hydrophone and each sphere to be used were aligned on the acoustic axis and the diagram of the measurement geometry is shown in Fig.7.1. For the incident intensity of sound at the hydrophone as a receiver, Ii, then on applying the sonar equation and adding propagation losses, the incident intensity at the sphere as a target

$$Ii' = Ii - TL_1 - \alpha R$$

where TL_1 and αR are the spreading loss and absorption loss from the receiver to the target, where $R = R_2 - R_1$. For the target of strength TS dB, the intensity of return at the target

$$Ir' = Ii' + TS$$

Table 1. The target strengths of three spheres at around frequency of 3 MHz.

TYPE OF SPHERE	TARGET STRENGTH (dB)			PULSE LENGTH (μs)
	2.83 MHz	2.95 MHz	3.03 MHz	
Table tennis ball	-43.5	-42.7	-43.1	10
Copper sphere	-46	-48.7	-48.9	10
Tungsten sphere	-40.9	-41.6	-41.2	10

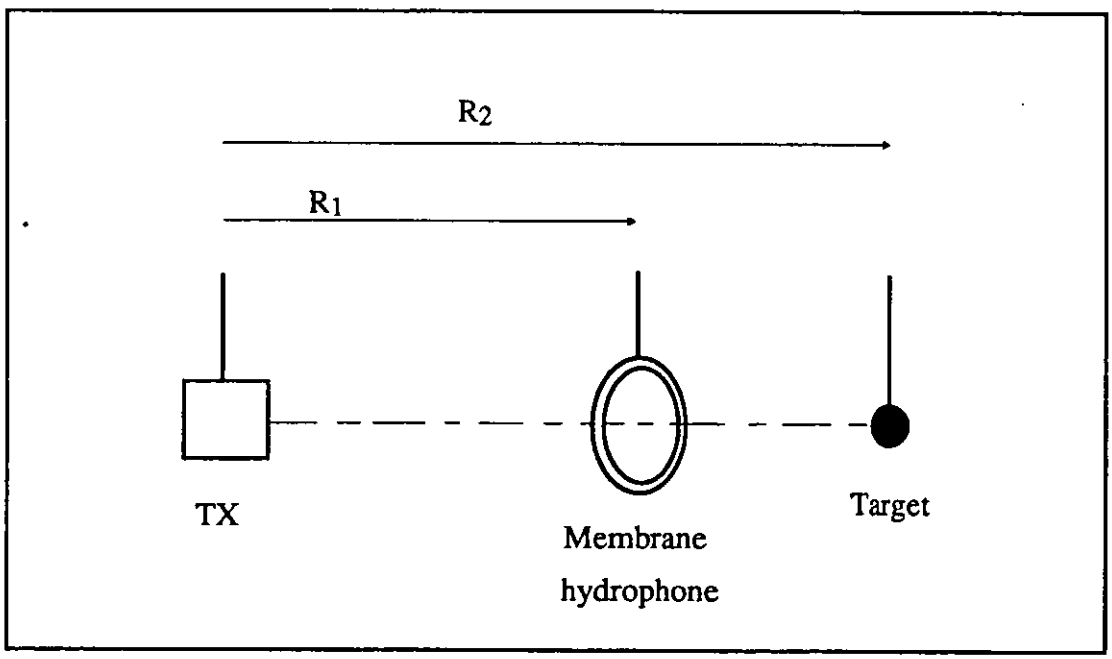

Fig.7.1 Diagram of measurement geometry.

and the intensity of the return at the receiver, Ir, by adding the propagation losses from the target to the receiver

$$Ir = Ii - TL_1 - TL_2 - 2\alpha R + TS \qquad \text{..... (7 - 2)}$$

where TL_2 is the spreading loss from the target to the receiver. The difference in voltage levels equals the difference in acoustic levels and the voltage output from the receiver is proportional to the pressure of the acoustic signal, thus by rearranging equation (7 - 2)

$$TS = 20 \log(Vr/Vi) + TL_1 + TL_2 + 2\alpha R.$$

In order to obtain target strength by using graphic solution, the equation above can be represented as

$$20 \log(Vr/Vi) = TS - TL_1 - TL_2 - 2\alpha R \qquad \text{..... (7 - 3)}$$

The basic idea of measuring the target strength of an underwater object is to compare the echo voltage Vr from the target at range R with that Vi from the transducer at range Ri. Here, there are the only three quantities that need to be measured in the experiment, except the range Ri because the hydrophone used was always kept on the acoustic axis, i.e., the reflected values to be measured were in the direction of the incident sound. There was no necessity for the transducers to be calibrated, nor for the sending level to be measured, so long as it was constant.

It should be noted that in using the measurement equipment, Vr and Vi were measured at different gain settings. R was measured from the face of the hydrophone to the nearest point on the target and the returned signals were just that returned from this point as the echo spread spherically. It may be more realistic to assume spreading of the echo from the centre of the sphere [38]. But in the present experiment, it has not been assumed so.

7.2.2 Propagation Losses

It is known that in travelling through the water, an underwater sound signal becomes delayed, distorted, and weakened. The propagation losses may be considered to be the sum of a loss due to attenuation and a loss due to spreading. The classical theory of attenuation attributed one of the propagation losses to the thermal conductivity and the viscosity of the medium. The thermal conductivity loss for water turns out to be negligible and the significant loss in water is caused by the viscosity of the medium which includes shear viscosity and bulk viscosity [37]. The attenuation rate for freshwater can be expressed as [37]

$$\alpha = 4.34/(\rho c^3)\ (4\mu/3 + \mu')\ \omega^2 \quad \text{(dB/m)} \qquad \ldots\ldots (7 - 4)$$

where ρ is the water density (kg/m^3), c the sound speed (m/s), ω the angular frequency (rad/s), μ the dynamic coefficient of shear viscosity and μ' the dynamic coefficient of bulk viscosity (N.s/m^2). Since the sound speed and the dynamic coefficients of the shear and the bulk viscosity for freshwater are constant at a given temperature T, the attenuation coefficient can be calculated by using their physical constants. If

$\rho = 1000$ kg/m^3,

$c = 1461$ m/s (for $T = 14\ ^{o}C$)

$f = 3$ MHz ($\omega = 2\pi f$)

$\mu = 1.2 * 10^{-3}$ N.s/m^2 (for $T = 14\ ^{o}C$)

$\mu' = 3.3 * 10^{-3}$ N.s/m^2 (for $T = 14\ ^{o}C$)

then the attenuation coefficient at 3 MHz can be obtained from equation (7 - 4) and is approximately 2.42 dB per metre in freshwater. It can be seen from equation (7 - 4) that the magnitude of the attenuation in a particular medium is very dependent on the operating frequency.

Spreading loss is a geometrical effect representing the regular weakening of sound signal as it spreads outward from the source. For the range from the hydrophone to the target as shown in Fig.7.2a, the spreading loss

$$TL_1 = 20 \log(R_2/R_1)$$

and the spreading loss TL_2 from the target to the hydrophone

$$TL_2 = 20 \log(R_4/R_3)$$

The relationship between the spherical spreading loss and the range is shown in Fig.7.2b.

7.2.3 Interference

The spheres as targets in the experiment have to be placed at some desired position from the transmit transducer. One of the main reasons is that the effect of near field could occur which is caused by the constructive and destructive

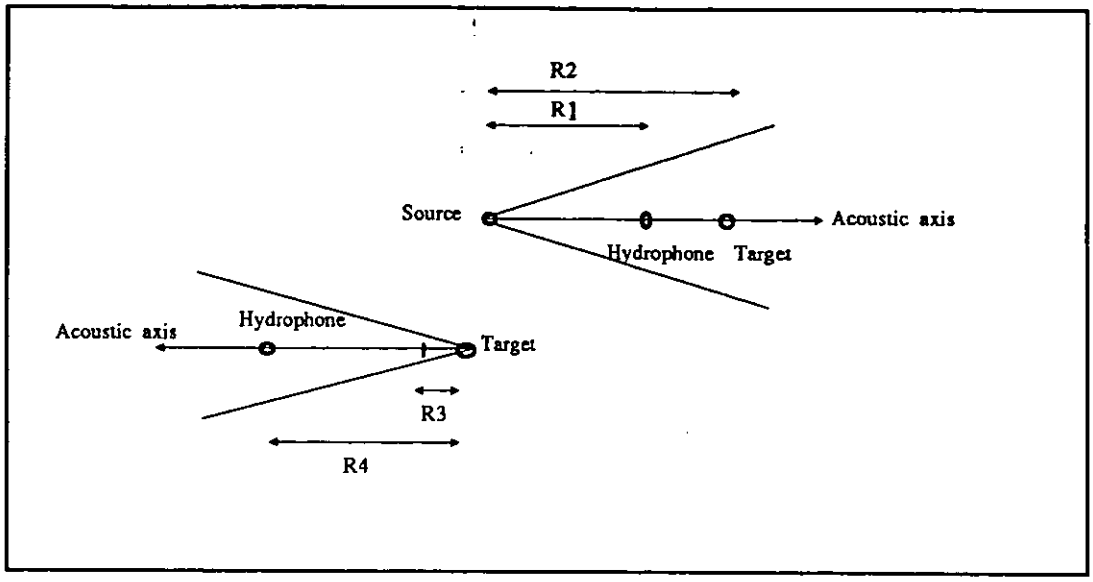

Fig.7.2a Signal spreading geometry in the water.

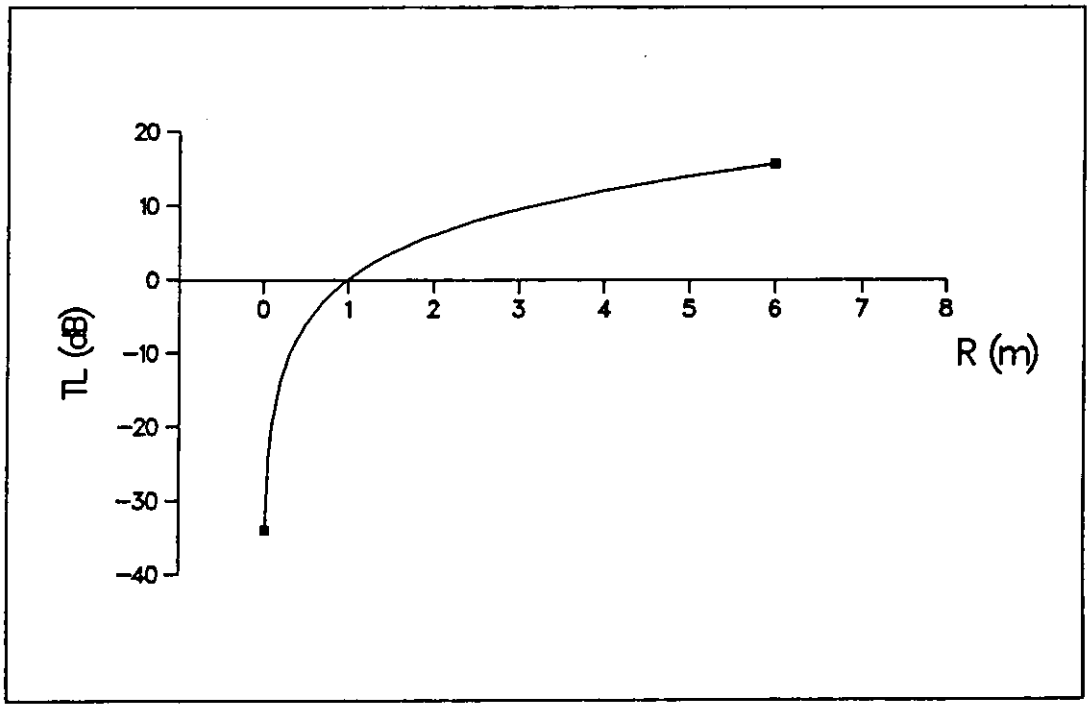

Fig.7.2b Spherical spreading loss function.

interferences of the radiation from different subareas of the transducer face [38]. The near field is normally calculated by the following equation,

$$\text{Near Field} = D*D/\lambda$$

where D is the diameter of the transducer and λ the wavelength of operating frequency. At a frequency of 3 MHz the wavelength is 0.5 mm and the diameter of the transducer used in the work is 25 mm. Therefore, the near field in this case is about 1.25 metres.

The other main reason is that the results would be invalid, in many cases, for use at longer ranges, since the echoes from the target are too weak to be detected perfectly, due to the propagation losses of the underwater sound signal and the ambient noise level in the water tank laboratory. This means that the spheres to be used should be located at some desired position in the experiments.

In addition, the surface and bottom of the water tank both reflects and scatters sound and this may create an interference pattern in the underwater sound field. This pattern is caused by constructive and destructive interference between the direct and reflected sound from both the surface and the bottom. The combined pattern makes the measurement of the return from the target inaccurate. Therefore, the targets could not be placed either near the water surface, or near the bottom.

7.2.4 Procedure of Measurement

The experiment was carried out as follows:

(1). The transducer for transmission, the hydrophone and a sphere were aligned as accurately as possible. The hydrophone was first used to make sure that the maximum voltage was measured at 1.7 metres from the transducer by means of the movement of the rack. This means that the hydrophone is on the acoustical axis of the transducer. One of the spheres was then placed in front of the hydrophone and was very carefully aligned on its "acoustic axis".

(2). The hydrophone was moved along the acoustic axis towards the transducer and the data measured by the hydrophone every 4 cm displacement. The data includes the echo voltages derived from the target, and from the source (transducer). As the distance between the hydrophone and the target increased (movement of the hydrophone towards the transducer), the echoes reflected by the target became too weak to be detected properly beyond a certain distance, while the incident voltage from the source continued to increase. Therefore, different gain settings were chosen to ensure that both voltages measured from the target and from the transducer were properly recorded. The two sets of recorded data were represented as the return from the target, Vr, and as the incident voltage, Vi.

(3). A digital frequency meter was used to measure the signal frequency accurately. The target strength of each sphere was measured at the frequencies of 2.83 MHz, 2.95 MHz and 3.03 MHz with pulse length of 10 μs by using a slight offset in frequency from the 3 MHz

(4). All the data recorded from the outputs of the receiver were then converted into respective input values corresponding to the different gains used.

Thus, by using the equation (7 - 4), a number of values at any distance were obtained for analysis.

7.3 EXPERIMENT SITE, TARGETS AND INSTRUMENTATION

The experiment was carried out in the large water tank whose dimensions are approximately 8 metres long by 6 metres wide in which the water depth is normally 2 metres. Across the 6 metres width at one side is a rigid assembly supporting a rack drive 'railway' on which the synthetic aperture measuring head runs.

A number of table tennis balls of about 37 mm diameter, a copper sphere of 30 mm diameter as well as a tungsten sphere of 40 mm diameter were used as the targets for the practical experiment. These spheres were suspended in nylon hairnets and located at 1.9 metres from the transducer for transmission and about 60 cm below the surface of the water.

The transmit transducer operating at 3 MHz was originally designed for acoustic visualization work and has a beamwidth of around 1 degree. This transducer was fixed on the synthetic aperture measuring head and could be panned and tilted by a suitable controller. The transducer could be moved along the 'railway' with the trolley across the 6 metres width. Movement of the trolley was activated by two stepper motors controlled by microcomputer or by hand.

A membrane hydrophone was used in the experiment, which is transparent for sound going through from one side to the other. The hydrophone was mounted on a wooden support which was attached to a 3 dimensional orientation

control rack. The rack was supported by a mounting frame above the water surface. The orientation controller can change tilt, pitch, roll and displacement vertically or horizontally. Moreover, the orientation controller can move forward or backward to the target at a range of from 1 cm to 70 cm. With this rack the hydrophone could be kept on the acoustic axis when moving. The configuration of the rack with the membrane hydrophone is shown in Fig.7.3.

Signal generator, power amplifier for transmission and low noise signal amplifier for reception were used in the present experiments and this part of the set up and measurement equipment is shown in Fig.7.4.

7.4 RESULTS

Using the data obtained in procedure 4, a graph was drawn with the vertical axis in linear scale (dB) and the horizontal axis in logarithmic measures representing range (cm). The vertical axis represents 20 times the logarithm to the base 10 of the ratios of the voltages from the target, Vr, to the incident voltage Vi. The horizontal axis represents the range R from 1 cm to 100 cm. The regression best-fit straight line with a calculated slope of about -20 passes through these scattered points. According to the definition of target strength, the point on the best-fit straight line corresponding to the vertical axis is the target strength when the range R is equal to 100 centimetres. This is shown in Fig.7.5.

It should be noted that this method of obtaining target strength assumes that only spreading propagation loss is accounted for. But in fact, sound attenuation caused by absorption is significant at a frequency of 3 MHz. By considering the sound attenuation in the course of the measurement, some compensated

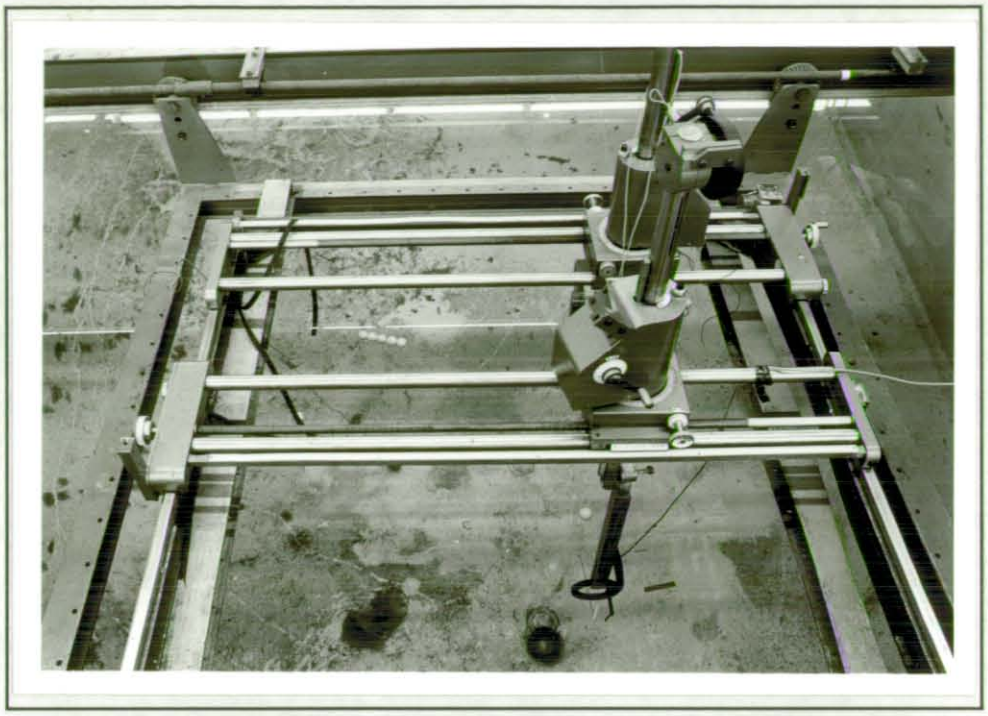

Fig.7.3 3 dimensional orientation control rack with the membrane hydrophone.

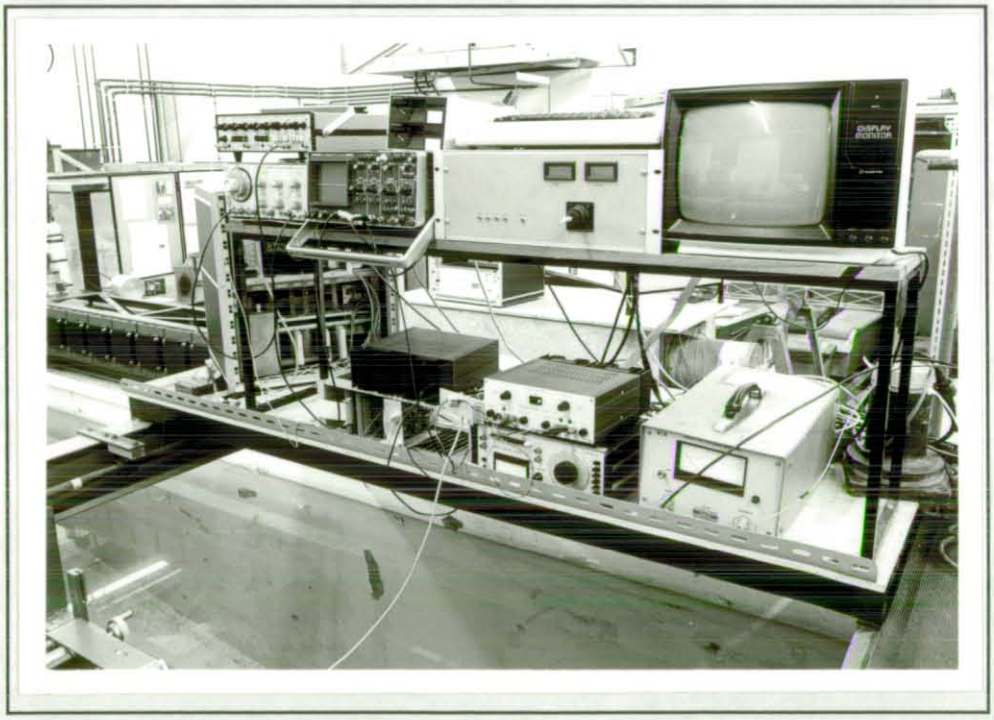

Fig.7.4 Part of the set up and measurement equipment in the practical experiment.

regression best-fit straight lines were obtained at attenuation coefficient of 2.42 dB/m. These are shown in Fig.7.6. The values corresponding to the vertical axis from these curves at the range of 1 metre were regarded as "real" target strength. It could be found from the graphs compensated by the attenuation coefficient of 2.42 dB/m that the target strength of the table tennis ball is -43 dB, the target strength of the tungsten carbide sphere about -42 dB and the target strength of the copper sphere about -48 dB. The target strengths of these spheres at different frequencies are given in Table 1. The echoes from these spheres at different pulse length were taken and are shown in Fig.7.7.

7.5 DISCUSSION

The measured target strength for the table tennis ball, tungsten carbide sphere and copper sphere at 3 MHz are basically consistent with those expected. All measured target strengths at 3 MHz are slightly lower than the theoretical values at about 40 KHz [36,39]. However, the theoretical values are not directly comparable due to the different frequency used. But it would be helpful to predict the target strength of any sphere at 3 MHz.

It can be seen from Fig.7.7 that the magnitude of the echoes from any sphere is not affected by differing pulse length, i.e., the target strength of these spheres is not pulse length dependent. However, the target strength depends on the carrier frequency and the diameter of these spheres. It should be noted that target strength is dependent on the density of spheres [36]. But this was not examined in the present experiment.

From most of the results the measured data plotted tended to a straight line with a certain slope within the range of 40 cm. Above that range the calculated values, 20log(Vr/Vi), decreased significantly, resulting from the attenuation of the signal in propagation. It could also be caused by the precision of the measurement system under conditions of very weak echoes. However, the regression line tended to have a slope of about -20 with a smaller standard deviation after compensation for attenuation. The slope characteristics of the measured values with range is basically consistent with theory. The conclusion to be drawn here is that these results are promising and suggest that a closer investigation of these target strengths should be undertaken by using a precise wide-band amplifer in the receiver.

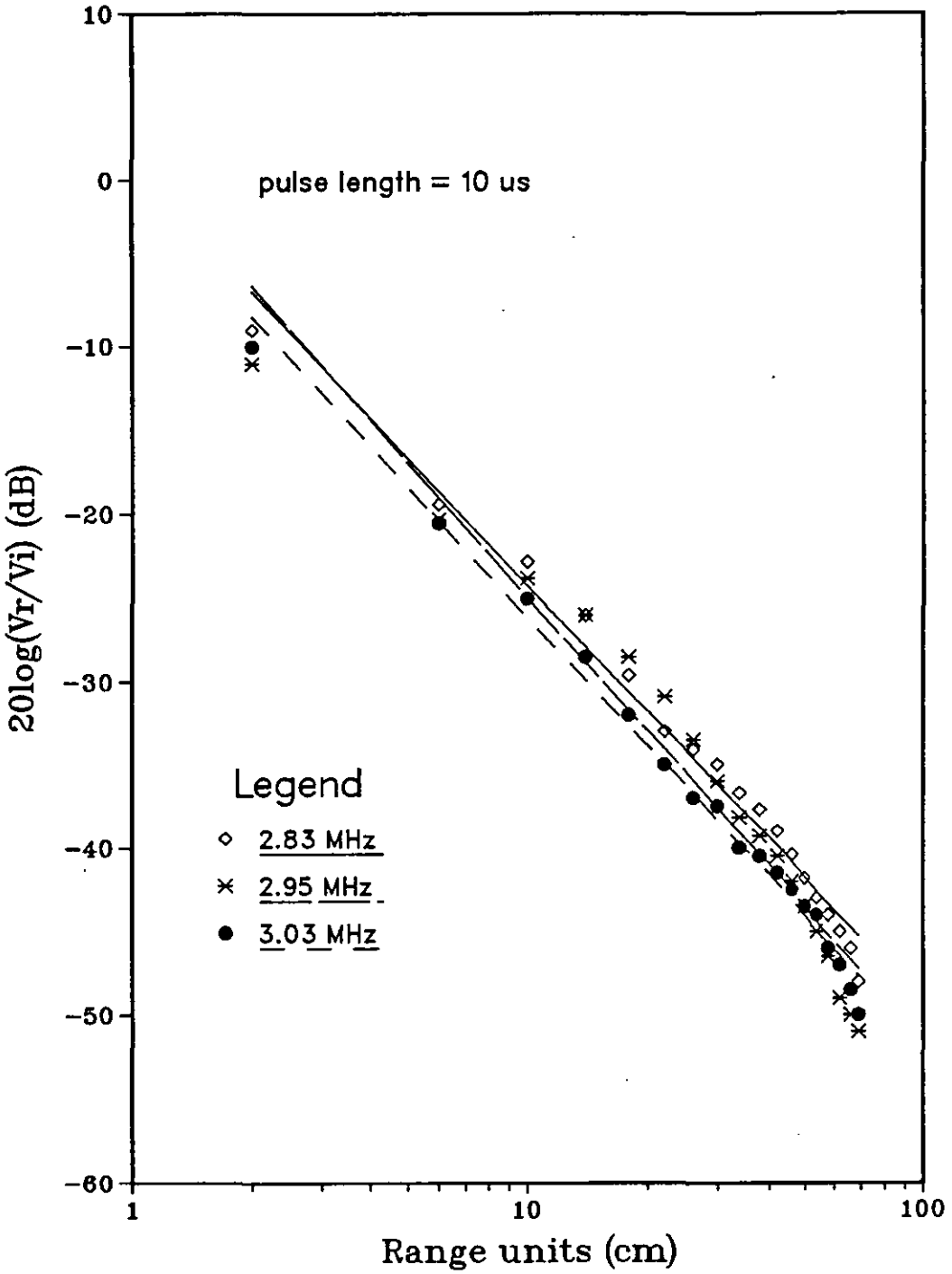

Fig.7.5a Measurement of TS for copper sphere.

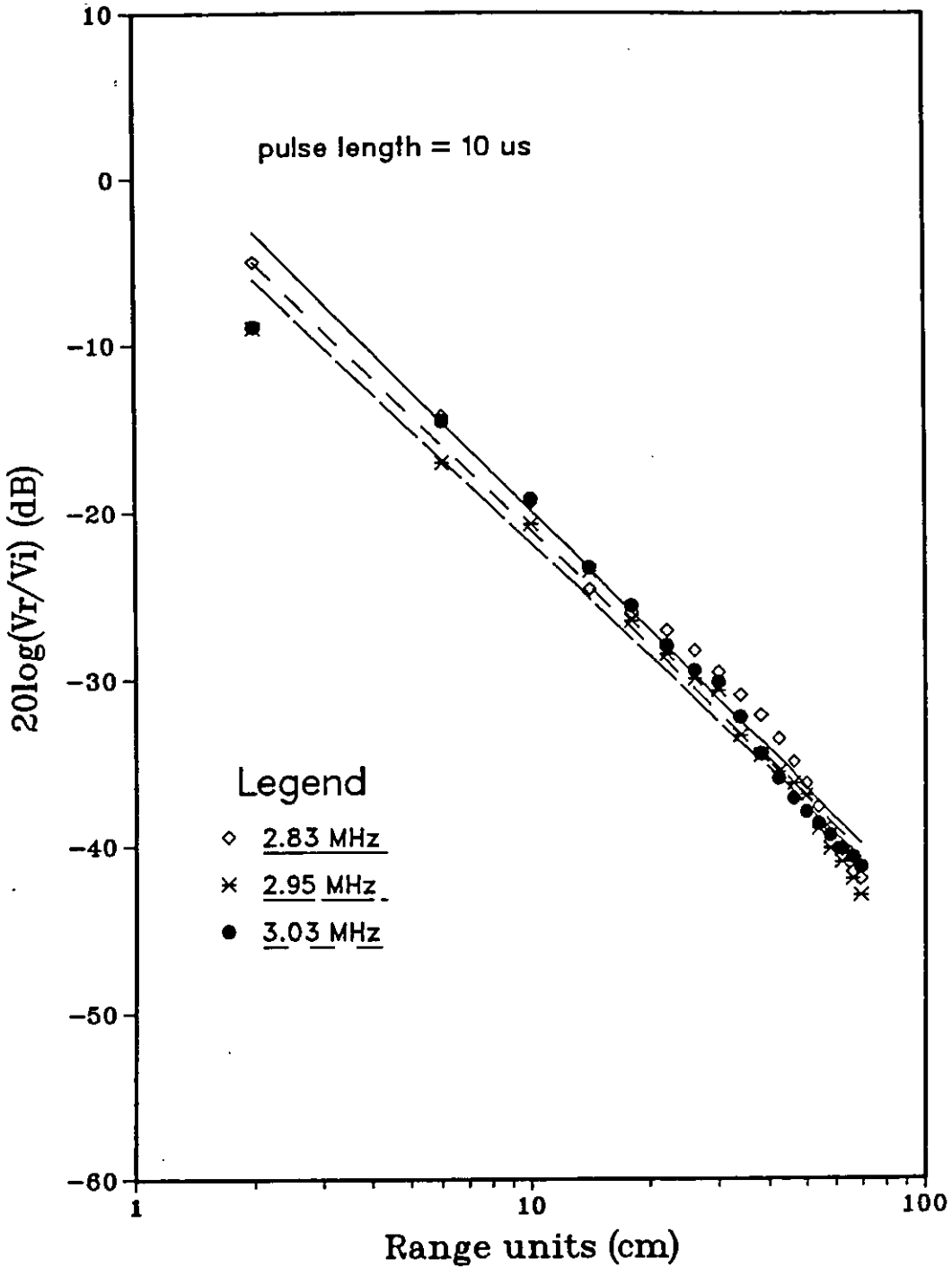

Fig.7.5b Measurement of TS for tungsten sphere.

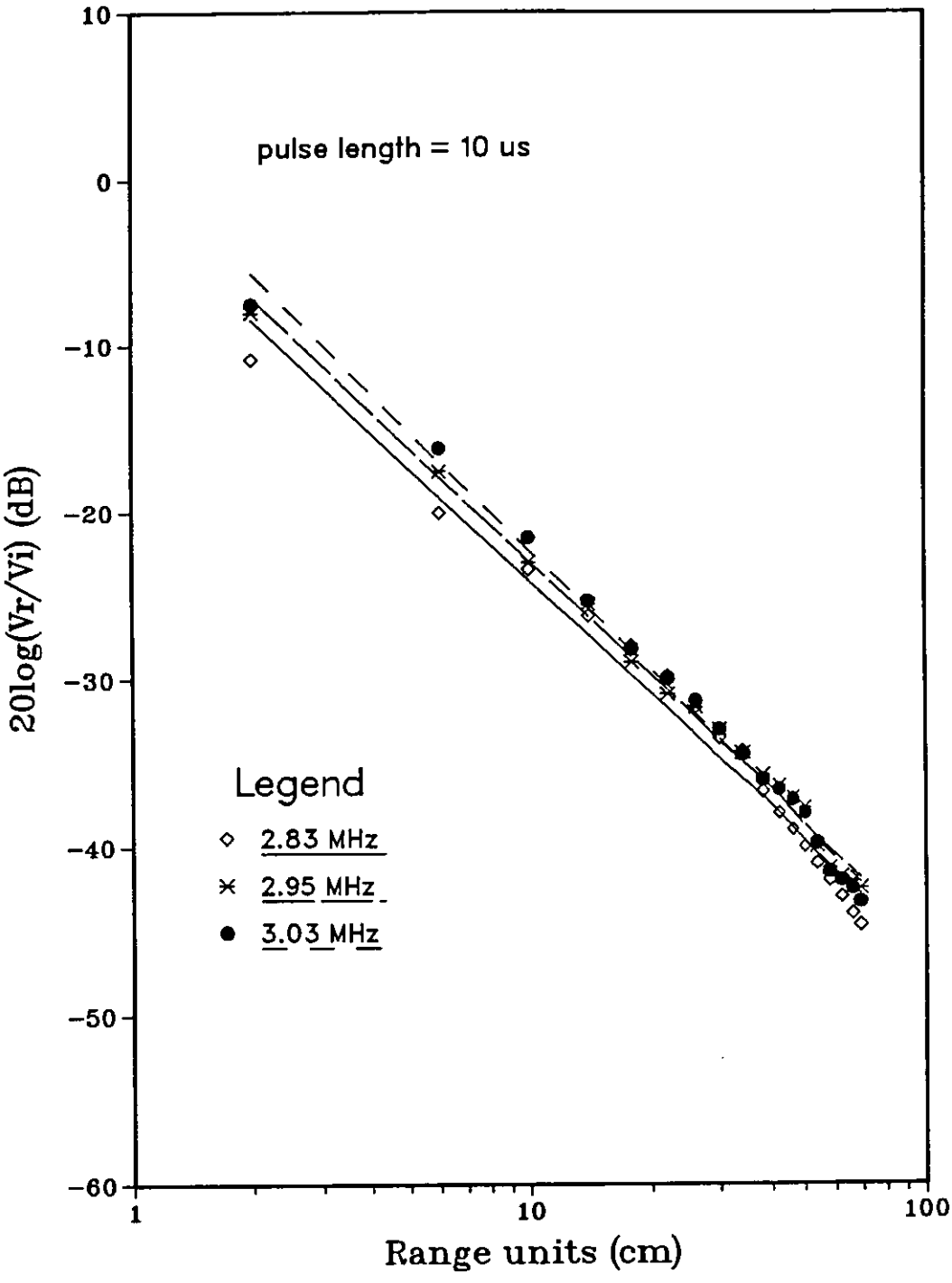

Fig.7.5c Measurement of TS for table tennis ball.

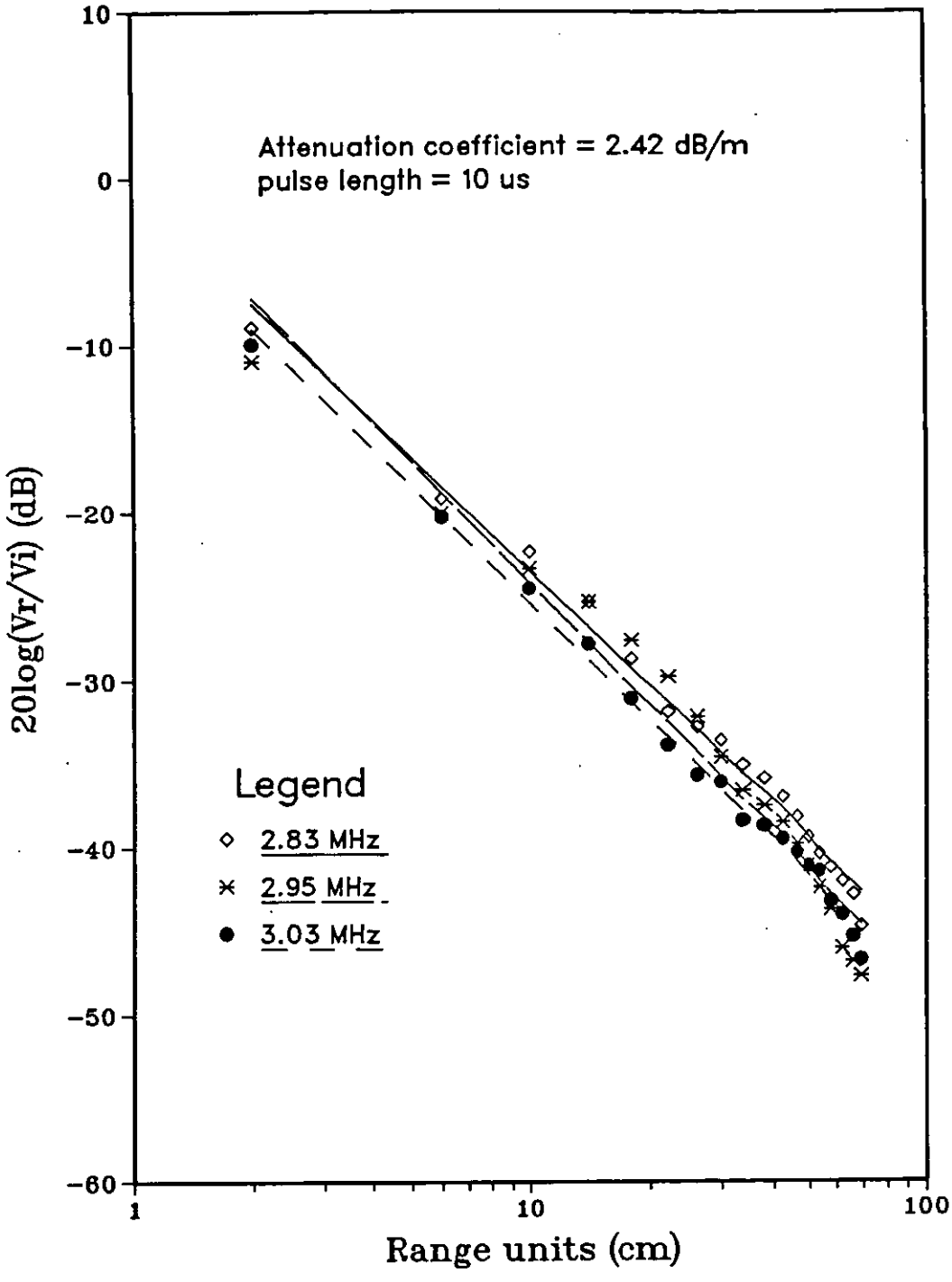

Fig.7.6a Measurement of TS for copper sphere.

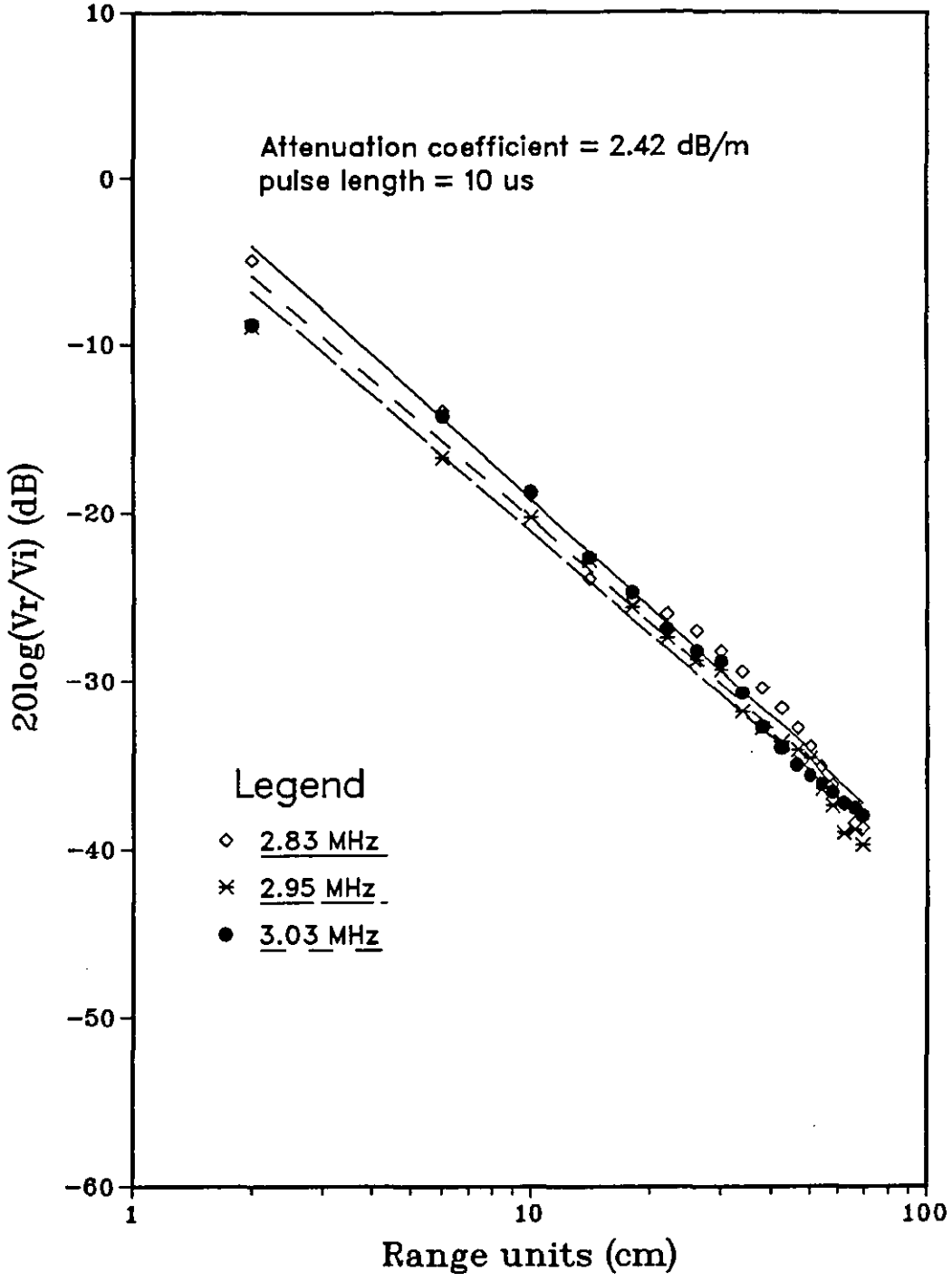

Fig.7.6b Measurement of TS for tungsten sphere.

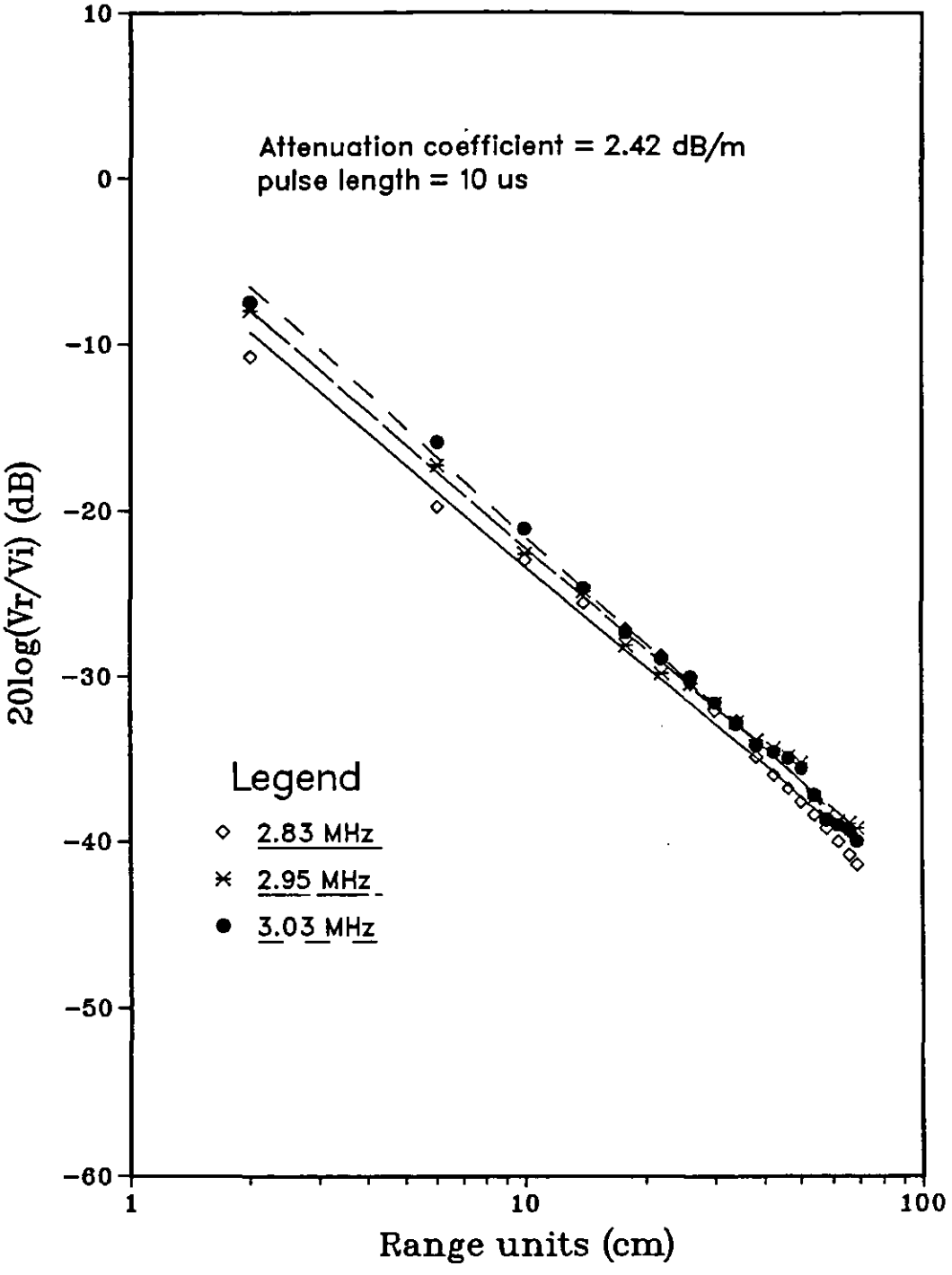

Fig.7.6c Measurement of TS for table tennis ball.

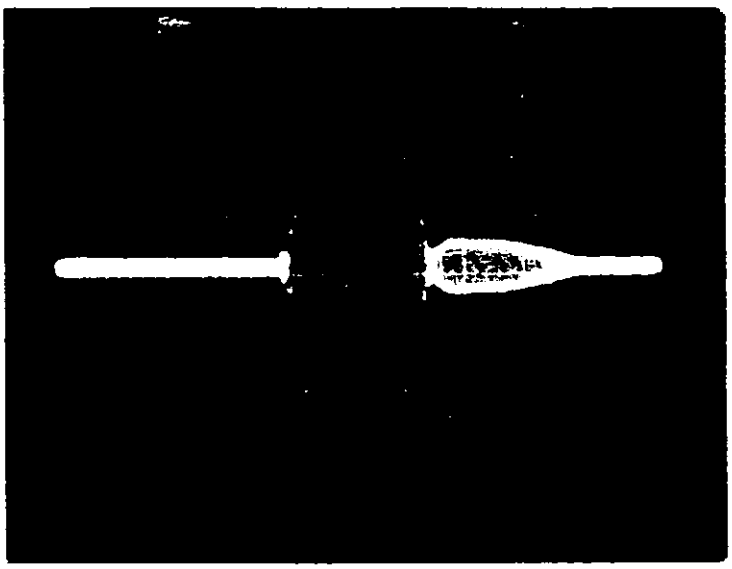

(a). Pulse length of 10 μs.

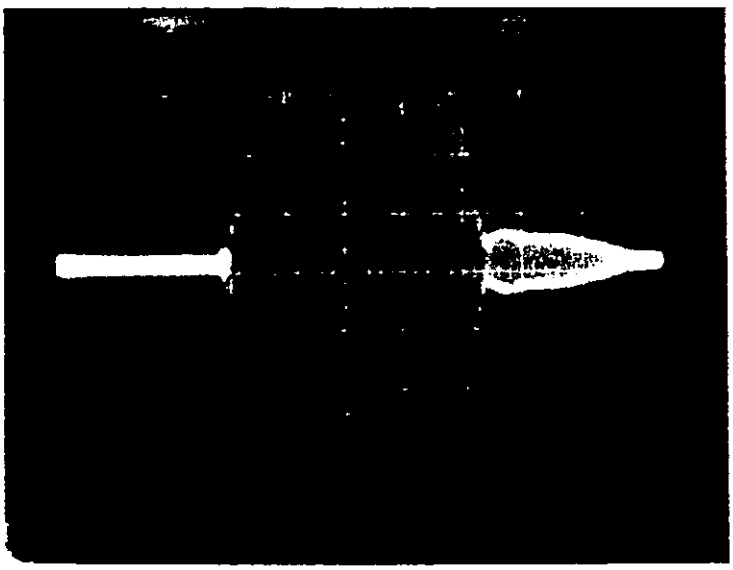

(b). Pulse length of 20 μs.

Fig.7.7 Observed echoes at the receiver output when different pulse lengths are applied to the transmitter input. The vertical scale is 0.2 volts/div..

8. CONCLUSION AND SUGGESTIONS FOR FURTHER WORK

Basic computer modelling of an echo sounder, which was established a few years ago trying to be used in fish abundance measurement, has been modified in this thesis due to the consideration of fish behaviour. This technique employed with the abundance estimation involves energy measurement on the echoes received at the receiver. The effect of the fish behaviour on the abundance measurement was taken into account and investigated.

One of the more important factors of fish behaviour is the orientation of fish, which represents the variation in tilt, roll and pitch direction. The tilt angle variation which is believed to have a significant effect on the target strength was investigated. The average target strength is directly related to the tilt angle distribution which is, in most cases, assumed to be normal distribution. The target strength is very tilt angle dependent and the shape of the target strength function depends on the size of fish and the acoustic frequency. The results obtained from chapter 5 showed that the average target strength of fish is affected by the mean tilt angle and standard deviation of the tilt angle distribution. The absolute value of the tilt angle decreases as the depth increases. In other words, the effect of the tilt angle on the average target strength depends on the depth of the fish, and this effect decreases as the depth increases. The size of fish and the acoustic frequency affect the shape of the target strength function. The shape of the function becomes narrower as the size of fish and/or the acoustic frequency increases and this leads to a decrease in the average target strength when the standard deviation and the mean tilt angle are given.

The swimbladder of fish was assumed to be cylinder of 0.05 fish length in diameter and 0.25 fish length in length. The maximum target strength occured with insonification directed perpendicular to the axis of the swimbladder, and is shifted about a perpendicular plane to the axis of the fish body by the value of the inclination angle of the swimbladder. The inclination angle of the swimbladder depends on the species of fish. A transducer's beam pattern was used in place of the model of backscattering cross section of any object. The results obtained from both of the models seem to be identical under certain conditions, and show that the theoretical diagrams are in general very similar to the experimental ones.

The probability density distribution of the target strength of fish was derived from the target strength function and the tilt angle distribution. It was observed from chapter 4 that the probability density distribution of target strength is not normal as assumed in the previous work [21,22]. The shape of the target strength distribution varies with the mean tilt angle of the tilt angle distribution and tends to be bi-modal after a certain mean value of tilt angle. This initial finding could be useful in determining the threshold of a sonar receiver.

The computer simulation was made to examine the effect of fish behaviour on fish estimation. The variation of the tilt angle of the fish indirectly affects the estimate of fish abundance by the probability density distribution of the target strength of the fish. The average echo energy from a single target varies with depth due to the mean tilt angle being depth dependent. On scaling the total echo energy from multi-targets by the average echo energy of the single target, the number of the targets insonified could be estimated by a number of trials. The

results obtained fron the simulation are satisfactory, but sometimes it is misleading for only one trial.

The target strength of some spheres were measured in the practical work. The target strengths of the table tennis ball, the tungsten sphere and the copper sphere at the frequency of 3 MHz were obtained by using graphic solution. The obtained results are promising, and in general they are consistent with the expected ones, but slightly lower than the results at low frequency (e.g. 40 KHz).

All the results obtained in this thesis are basically satisfactory but the study needs more investigation for further work. The many assumptions and restrictions made in the computer model and in the practical work are not realistic. The positions of fish in the water and the different tilt angle probability density distribution varying with depth for different fish species need more validation before the computer model is to be used for fish abudance measurement. The fish as a acoustic target could not be treated as a point target when the length of fish is long.

REFERENCES

[1]. MacLennan, D.N. and Forbes, S.T. 1984. Fisheries Acoustics: A Review of General Principles. Rapp.p.-v Reun. Cons. int. Explor. Mer, 184: 7 - 18.

[2]. Hood, C.R., Beach, M.H. and Casey, J. 1986. The English Survey System, Including a Microcomputer for Instant Biomass Assessment. ICES Fisheries Acoustic Science and Technology (FAST) Working Group Meeting, Hull, England.

[3]. Foote, K.G. 1980. Effect of Fish Behaviour on Echo Energy: the Need for Measurements of Orientation Distributions. J. Cons. int. Explor. Mer, 39(2): 193-201.

[4]. Buerkle, U. 1983. First Look at Herring Distributions with a Bottom Referencing Underwater Towed Instrumentation Vehicle "BRUTIV". FAO Fisheries Report No. 300, pp 125-130.

[5]. Olsen, K. 1971. Influence of Vessel Noise on Behaviour of Herring. In Modern Fishing Gear of the World: 3, ed. H. Kristjonsson. London, Fishing News Books for FAO. pp 291-294.

[6]. Midttun, L. 1984. Fish and Other Organisms as Acoustic Targets. Rapp. p.-v. Reun. Cons.int. Explor. Mer, 184: 25-33.

[7]. Nakken, O. and Olsen, K. 1977. Target Strength Measurements of Fish. Rapp. p.-v. Reun. Cons. int. Explor. Mer, 170: 52-69.

[8]. Foote, K.G. 1985. Effect of Swimming on Fish Target Strength. ICES C.M. 1985/B:29.

[9]. Olsen, K. 1981. The Significance of Fish Behaviour in the Evaluation of Hydroacoustic Survey Data. ICES C.M. /b:22.

[10]. Olsen, K. *et al.* 1983. Observed Fish Reactions to a Surveying Vessel with Special Reference to Herring, Cod, Capelin and Polar Cod. FAO Fisheries Rep.(300), pp 131-138.

[11]. Olsen, K. *el al.* 1983. Quantitative Estimations of the Influnce of Fish Behaviour on Acoustically Determed Fish Abundance. FAO Fisheries Rep.(300), pp 139-149.

[12]. Partridge, B.L. *et al.* 1980. The Three-Dimensional Structure of Fish Schools. Behav. Ecol. Sociobiol. 6. 277-288.

[13]. Huang, K. and Clay, C.S. 1980. Backscattering Cross Sections of Live Fish: PDF and Aspect. J. Acoust. Soc. Am., 67(3). 795-802.

[14]. Forbes, S.T., Simmonds, E.J. and Edwards, J.I. 1982. Target Strength Measurements on Live Cadoids. In "Symposium on Fisheries Acoustics, Bergen, Norway, 21-24 June 1982", O. Naken and S. C. Venema - eds.

[15]. Fedotova, T.A. and Shatoba, O.E. 1983. Acoustic Backscattering Cross Section of Cod Averaged by Sizes and Inclination of Fish. FAO Fisheries Rep.(300), pp 63-68.

[16]. Foote, K.G., Aglen, A. and Nakken, O. 1985. *IN SITU* Fish Target Strengths Derived with a Split-beam Echo Sounder. ICES C.M. /B:28.

[17]. Goddard, G.C. and Welsby, V.G. 1986. The Acoustic Target Strength of Live Fish. J. Cons. int. Explor. Me, 42:197-211.

[18]. Love, R.H. 1977. Target Strength of an Individual Fish at Any Aspect. J. Acoust. Soc. Am., 62(6): 1397-1403.

[19]. Ona, E. 1984. Tilt Angle Measurements on Herring. ICES C.M. /B:19.

[20]. Foote, K.G. 1986. A Critique of Goddard and Welsby's Paper " The Acoustic Target Strength of Live Fish ". J. Cons. int. Explor. Mer, 42: 212-220.

[21]. Griffiths, J.W.R. and Smith, J.P. 1978. A Model of an Echo Sounder for Fish Abundance Measurement. Proc. of the Conf. on Acoustics in Fisheries, Institute of Acoustics, Underwater Acoustic Group, Hull, Sept., 1978.

[22]. Chen, N.W.S. 1981. Computer Modelling of Sonar Systems. Loughborough University of Technology. M.Sc. Thesis.

[23]. Urick, R.J. 1975. Principles of Underwater Sound. McGraw-Hill Book Company, Printed in USA.

[24]. Midttun, L. 1971. Acoustic Methods for Estimation of Fish Abundance. In Symposium on Remote Sensing in Marine Biology and Fishery Resource. Texas A. and M. Univ. College Station. Texas pp. 218-226.

[25]. Yudanov, K.L. and Kalikhman, I.L. 1981. Sound Scattering by Marine Animals. In Meeting on Hydroacoustical Methods for the Estimation of Marine Fish Populations, 25-29 June, 1979, 2, pp.53-95. Ed. by J.B.Suomala. The Charles Stark Draper Laboratory, Inc., Cambridge, Massachusetts, USA.964 pp.

[26]. Ehrenberg, J.E. and Lytle, D.W. 1971. Acoustic Techniques for Estimating Fish Abundance, IEEE Trans. Geoscience Electronics, Vol. 10-11, (1972-1973).

[27]. Ehrenberg, J.E. 1980. Echo Counting and Echo Integration with a Sector Scanning Sonar. Journal of Sound and Vibration. Vol. 73, No.3, pp.321-332.

[28]. Moose, P.H., Ehrenberg, J.E. and Green, J.H. 1971. Electronic System and Data Processing Techniques for Estimating Fish Abundance. Proceeding of the IEEE Conference on Eng. in Ocean Enviroment. pp. 33-36.

[29]. Swingler, N. and Hampton, I. 1981. Investigation and Comparison of Current Theories for the Echo Integration Technique of Estimating Fish Abundance, and of Their Verification by Experiment. In Meeting on Hydroacoustical Methods for the Estimation of Marine Fish Populations, 25-29 June, 1979, 2, pp. 97-156. Ed. by J.B. Suomala. The Charles Stark Draper Laboratory Inc., Cambridge, Massachusetts, USA. 964 pp.

[30]. Foote, K.G. 1983. Linearity of Fisheries Acoustics, with Addition Theorems. J. Acoust. Soc. Am. Vol. 73, No.6, June 1983.

[31]. MacLennan, D.N., Magurran, A.E., Pitcher, T.J. and Hollingworth, C.E. 1987. Behavioural Determinants of Fish Target Strength. International Symposium on Fisheries Acoustics, June 22-26, 1987 Seattle, Washington, USA.

[32]. Foote, K.G., 1979. Averaging of Fish Target Strength Functions. J. Acoust. Soc. Am. 67(2), pp.504-515.

[33]. Foote, K.G., 1985. Rather-High Frequency Sound Scattering by Swimbladdered Fish. J. Acoust. Soc. Am. 78(2), pp.688-700.

[34]. Pope, J.G. 1982. User Requirements for Precision and Accuracy of Acoustic Surveys. ICES Symp. Fisheries Acoustics. Bergen. Paper No. 84.

[35]. Gaunaurd, G.C. 1985. Sonar Cross Sections of Bodies Partially Insonified by Finite Sound Beams. IEEE Journal of Oceanic Engineering, Vol. OE-10,No.3. pp.213-230.

[36]. MacLennan, D.N. 1981. The Theory of Solid Spheres as Sonar Calibration Targets. Scottish Fisheries Research Report, No. 22 (1981), ISSN 0308-8022, 17pp.

[37]. Clay, C.S. and Medwin, H. 1977. Acoustical Oceanography. John Wiley & Sons, Inc., USA.

[38]. Szilard, J. 1982. Ultrasonic Testing. John Wiley & Sons, Ltd.

[39]. Foote, K.G. 1983. Maintaining Precision Calibrations with Optional Copper Spheres. The Journal of the Acoustical Society of America. pp.1054-1063.

APPENDIX 1

Let the cylinder's length be 2b, a its radius, and k the wavenumber of the incident wave. The contibution from the curved side of the cylinder is given (3) by :

$$f(\pi) = \pm\frac{ik}{2\pi}\int_{\phi=\frac{-\pi}{2}}^{\phi=\frac{\pi}{2}} d\phi \int_{z=-b}^{b} -\sin\theta\cos\phi \exp(-2ika\sin\theta\cos\phi)\exp(-2ikz\cos\theta)a\,dz$$

where we have used the quantities

$$\hat{k}\cdot\hat{n} = -\sin\theta\cos\phi$$

$$\vec{r'} = a\cos\phi\hat{\varepsilon}_x + a\sin\phi\hat{\varepsilon}_y + z\hat{\varepsilon}_z$$

$$|z| \le b$$

$$\frac{-\pi}{2} \le \phi \le \frac{\pi}{2}$$

$$\vec{k}\cdot\vec{r'} = -k(a\sin\theta\cos\phi + z\cos\theta)$$

The geometry and the incident wave are illustrated in Fig.1. The z-integral yields

$$\int_{-b}^{b}\exp(-2ikz\cos\theta)dz = 2b\frac{\sin(2kb\cos\theta)}{2kb\cos\theta} = 2b\,j_0(2kb\cos\theta)$$

and the ϕ integral can be performed by the following equation, namely,

$$\int_0^{\frac{\pi}{2}} \exp(-iz\cos\theta)\cos\theta d\theta = 1 - \frac{\pi}{2}H_1(z) + iJ_1(z)$$

where H_1 and J_1 are the Struve and Bessel functions of order one, respectively.Thus

$$f_1(\pi) = \mp ikab\sin\theta j_0(2kb\cos\theta)\left\{\frac{2}{\pi} - H_1(2ka\sin\theta) - iJ_1(2ka\sin\theta)\right\}$$

is the exact contribution from the cylinder's curved side.

The contribution from the top flat surface of the cylinder is

$$f(\pi) = \pm\frac{i}{\lambda}\int_{r'=0}^{a}\int_{\phi=0}^{2\pi}(-\cos\theta)\cdot\exp(-2ik(r'\sin\theta\cos\phi + b\cos\theta))r'dr'd\phi$$

where we have used the relations

$$\hat{k}\cdot\hat{n} = -\cos\theta$$

$$\vec{k} = -k\sin\theta\hat{\varepsilon}_x - k\cos\theta\hat{\varepsilon}_y$$

$$r' = r\sin\alpha$$

$$\vec{r'} = (r\sin\alpha)\cos\phi\hat{\varepsilon}_x + (r\sin\alpha)\sin\phi\hat{\varepsilon}_y + b\hat{\varepsilon}_z$$

and

$$\vec{k}\cdot\vec{r'} = -k(r'\sin\theta\cos\phi + b\cos\theta)$$

If we use the known expressions

$$J_0(z) = \frac{1}{2\pi}\int_0^{2\pi}\exp(-iz\cos\phi)d\phi$$

and

$$\int zJ_0(z)dz = zJ_1(z)$$

then the integral in (3) can be evaluated, and the results is

$$f_2(\pi) = \pm ika\left\{\frac{a}{2}\cos\theta\exp(-2ikb\cos\theta)\frac{J_1(2ka\sin\theta)}{ka\sin\theta}\right\}$$

Since the orientation of the fish we are interested in is tilt angle $\theta'(\theta' = 90-\theta)$. The expected equations in which the θ is replaced by the tilt angle θ' are rewqitten as follows,respectively,

$$f_1(\pi) = ikab\cos\theta j_0(2kb\sin\theta')\left\{\frac{2}{\pi} - H_1(2ka\cos\theta') - iJ_1(2ka\cos\theta)\right\}$$

$$f_2(\pi) = iab\left\{\frac{a}{2}\sin\theta'\exp(-i2kb\sin\theta')\frac{J_1(2ka\cos\theta')}{ka\cos\theta'}\right\}$$

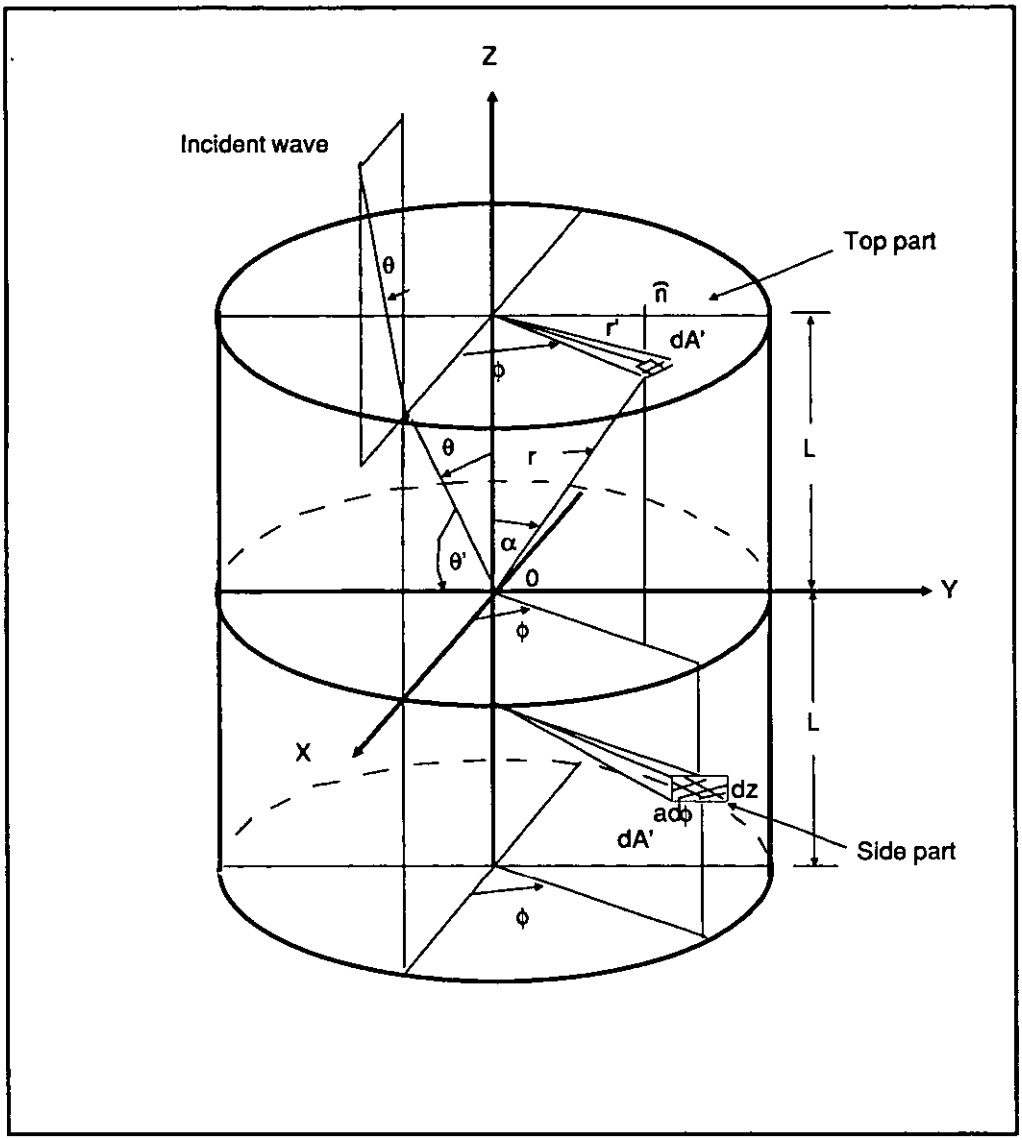

Fig.1 Geometry and coordinates for the insonification of a finite-length cylinder.